Coastal Studies Institute
Louisiana State University
Baton Rouge, Louisiana 70803

Technical Report No. 156

ANALYSIS OF MAJOR RIVER SYSTEMS AND THEIR DELTAS: MORPHOLOGIC AND PROCESS COMPARISONS

By L. D. Wright, J. M. Coleman, and M. W. Erickson

Unclassified
Security Classification

AD-776258

DOCUMENT CONTROL DATA - R & D

(Security classification of title, body of abstract and indexing annotation must be entered when the overall report is classified)

1. ORIGINATING ACTIVITY (Corporate author)	2a. REPORT SECURITY CLASSIFICATION
Coastal Studies Institute Louisiana State University Baton Rouge, Louisiana 70803	Unclassified 2b. GROUP Unclassified

3. REPORT TITLE

ANALYSIS OF MAJOR RIVER SYSTEMS AND THEIR DELTAS: MORPHOLOGIC AND PROCESS COMPARISONS

4. DESCRIPTIVE NOTES (Type of report and inclusive dates)

5. AUTHOR(S) (First name, middle initial, last name)

Lynn D. Wright, James M. Coleman, and Mary W. Erickson

6. REPORT DATE	7a. TOTAL NO. OF PAGES	7b. NO. OF REFS
January 1974	125	28

8a. CONTRACT OR GRANT NO.	9a. ORIGINATOR'S REPORT NUMBER(S)
N00014-69-A-0211-0003 b. PROJECT NO NR 388 002 c. d.	Technical Report No. 156 9b. OTHER REPORT NO(S) (Any other numbers that may be assigned this report)

10. DISTRIBUTION STATEMENT

Approved for public release; distribution unlimited.

11. SUPPLEMENTARY NOTES	12. SPONSORING MILITARY ACTIVITY
	Geography Programs Office of Naval Research Arlington, Virginia 22217

13. ABSTRACT

Thirty-four major river systems were compared in terms of the morphology and process environments of their drainage basins, alluvial valleys, receiving basins, and delta plains. Data for a multitude of variables, as previously defined by Coleman and Wright (1971), were generated and compiled for each of the 34 systems. These data were stored in a systematic hierarchical arrangement in a comprehensive information storage and retrieval computer system. (U)

For purposes of comparisons between river and delta systems, optimum combinations of salient variables were selected and were subjected to multivariate statistical procedures, including factor analysis, cluster analysis, and discriminant analysis. The procedures established the existence of some discrete groups of river systems and facilitated quantitative assessment of the degrees of mutual similarity or dissimilarity between individual river systems and between groups of two or more systems. Separate comparisons were made in terms of (1) drainage-basin morphology, (2) drainage-basin climate, (3) factor scores of combined drainage-basin properties, (4) alluvial-valley morphology, (5) alluvial-valley discharge regime, (6) receiving-basin bottom morphology, (7) receiving-basin energy regime, (8) factor scores of combined receiving-basin properties, (9) delta-component ratios, (10) delta-plain morphometry, (11) delta-plain landform suites, (12) delta-plain distributary network patterns, (13) river-mouth morphology, and (14) factor scores of combined delta-plain morphologic properties. (U)

The comparisons revealed that, with respect to single sets of related morphologic or environmental characteristics (such as river-mouth morphology or receiving-basin energy), the systems tended to cluster into multiple relatively discrete groups. However, these clusters most commonly exhibited very little coincidence between sets of parameters. (U)

DD FORM 1 NOV 65 1473 (PAGE 1)
S/N 0101-807-6811

Unclassified
Security Classification

A-31408

PRICES SUBJECT TO CHANGE

14 KEY WORDS	LINK A		LINK B		LINK C	
	ROLE	WT	ROLE	WT	ROLE	WT
Comparisons, morphologic and process						
Drainage basin						
Alluvial valley						
Receiving basin						
Delta plain						
Factor analysis						
Cluster analysis						
Discriminant analysis						
Delta variability						
Delta models						
Information systems						

ABSTRACT

Thirty-four major river systems were compared in terms of the morphology and process environments of their drainage basins, alluvial valleys, receiving basins, and delta plains. Data for a multitude of variables, as previously defined by Coleman and Wright (1971), were generated and compiled for each of the 34 systems. These data were stored in a systematic hierarchical arrangement in a comprehensive information-storage-and-retrieval computer system.

For purposes of comparisons between river and delta systems, optimum combinations of salient variables were selected and were subjected to multivariate statistical procedures, including factor analysis, cluster analysis, and discriminant analysis. The procedures established the existence of some discrete groups of river systems and facilitated quantitative assessment of the degrees of mutual similarity or dissimilarity between individual river systems and between groups of two or more systems. Separate comparisons were made in terms of (1) drainage-basin morphology, (2) drainage-basin climate, (3) factor scores of combined drainage-basin properties, (4) alluvial-valley morphology, (5) alluvial-valley discharge regime, (6) receiving-basin bottom morphology, (7) receiving-basin energy regime, (8) factor scores of combined receiving-basin properties, (9) delta-component ratios, (10) delta-plain morphometry; (11) delta-plain landform suites; (12) delta-plain distributary network patterns, (13) river-mouth morphology, and (14) factor scores of combined delta-plain morphologic properties.

The comparisons revealed that, with respect to single sets of related morphologic or environmental characteristics (such as river-mouth morphology or receiving-basin energy), the systems tended to cluster into multiple relatively discrete groups. However, these clusters most commonly exhibited very little coincidence between sets of parameters. Owing to the natural complexities and uniquenesses of the systems, cluster analyses based on combinations of two or more parameter sets yielded progressions of dissimilarities rather than well-defined clusters.

ACKNOWLEDGMENTS

This research was supported by the Geography Programs, Office of Naval Research, under Contract N00014-69-A-0211-0003, Project NR 388 002, with the Coastal Studies Institute, Louisiana State University. Mr. Brad Gane and Ms. Barbara Julien assisted with the data compilation and analysis. Ms. Gerry Dunn performed all cartographic work.

CONTENTS

LIST OF FIGURES

LIST OF TABLES

INTRODUCTION

Deltas vary because of variations in associated process environment. Understanding delta variability involves (1) understanding the causal links between process environment and morphologic response (deterministic studies) and (2) knowledge of the actual process environments and responses and their global associations. In order to understand the reasons for the existence of deltaic forms, the details of deterministic associations between process and form and the conditions which exist in different parts of the world must be examined simultaneously. The study of deterministic associations can lead to establishment of universal cause-effect relationships and development of theoretical models. Investigation of global variability of process environments and delta forms permits evaluation of variations in intensity of forcing agents and morphologic responses and determination of the realistic spectrum of probable process-form models.

The purpose of this report is to present the results of a comparison of delta forms and their associated process environments, to identify the natural groupings of deltas into spectra of morphology and process types, to evaluate the differences and similarities between these delta types, and to identify the process-form associations which are most significant and which require more intensive future investigation.

Previous Results

The Coastal Information Program on major river deltas was initiated by the Coastal Studies Institute, Louisiana State University, in 1966 to facilitate evaluation of the macroscale relationships between delta morphology and secular process environments. The Coastal Information Program is a practical system which provides mechanisms for generating, structuring, and comparing large volumes of meaningful information. Interpretation and synthesis of the results of these comparisons involve application and development of deterministic theory and lie in the realm of systematic morphodynamics.

The purpose and structure of the delta study were stated in detail in the initial report on the project by Coleman and Wright (1971). In that report, procedures of parameter determination were described, rationale for parameter selection was discussed, and data categories and parameters were rigidly defined.

As information was progressively assembled during the study, causal associations between delta forms and process environments became evident and pointed to the need for more systematic investigations of certain process-form relationships. Comparisons showed that the forms of river mouths which debouch into low-tide-range seas and which experience salt-wedge intrusion are very similar. Through detailed field studies in one example of this type of river mouth, the Mississippi, better understanding was gained of the deterministic relationships characteristic of this river-mouth type and general morphodynamic models were suggested to explain the observed associations. Findings to date have been reported in several articles (Wright, 1970, 1971; Wright and Coleman, 1971a; Wright, Coleman, and Suhayda, 1973; Waldrop, 1973). A more comprehensive paper dealing with relationships between the dynamics of stratified effluents and river-mouth bar development has recently been

completed (Wright and Coleman, in press).

The comparisons also revealed that many of the world's river mouths, particularly those in high-tide-range environments, could not be explained in terms of the model developed for the mouths of the Mississippi. In order to better understand the causal relationships typical of tide-dominated deltas and river mouths, a systematic field study of delta and channel morphodynamics was conducted in the Ord Delta region of northwestern Australia in 1971. This region experiences a tide range of 8 meters and an arid tropical monsoon climate. The study led to development of a morphodynamic model relating funnel-shaped river mouths to tidal modification (Wright, Coleman, and Thom, 1973) and also to more adequate understanding of tidal-flat evolution in high-tide-range deltas (Wright, Coleman, and Thom, 1972).

One of the most conspicuous process-form associations revealed through the comparisons was the close contingency between gross deltaic geometry, landform suites, and discharge/wave-power climate. By application of morphometric analyses and a comprehensive wave-climate program developed in the Coastal Information Program, it was possible to explain much of the variability exhibited by delta shorelines (Wright and Coleman, 1971b, 1972, 1973).

All these systematic studies, developed out of the more general Coastal Information Program, were conducted simultaneously with the information generation and comparison aspect of that program and, upon their completion, have provided improvement of the program by suggesting more meaningful parameters and associations.

This report is concerned with the final analyses of the variability of delta systems based on the information compiled, structured, and compared in the Coastal Information Program. Since the completion of the first report (Coleman and Wright, 1971), many techniques have been refined; a few new parameters have been added, and some others have been found to contain minimal useful information and have been dropped for purposes of the comparisons reported herein. Initially, 55 major deltas were chosen for the analyses. Of these, the information sets described in Coleman and Wright (1971) were completely available for fewer than 30. However, 34 river and delta systems had sufficient data available to permit reasonably detailed comparisons; these 34 deltas (Fig. 1, Table 1) and their common associations are the subjects of this report.

METHODOLOGY

Although the systematic phases of the study involve field work using a variety of techniques, the macroscale information compilation, generation, and comparisons phase with which this report is concerned is based entirely on data from maps, photos, atlases, and published reports. By means of standardized and rigidly defined sets of procedures and computer programs, these data, once assembled, are digested into macrostates of causally meaningful information and compiled into a hierarchical structure. Once all the information has been compiled, it can be retrieved either in entire sets or in smaller subsets to be compared and grouped statistically, qualitatively, or deterministically. Figure 2 illustrates the general sequence of procedures followed in this program.

Data Selection, Definition, and Acquisition

In the initial phase, preliminary decisions were made, on the basis of previous field experiences and field reconnaissances, as to the types of data required to adequately and meaningfully describe river and delta systems. The next step involved inventorying available data, including resolution levels, and available maps

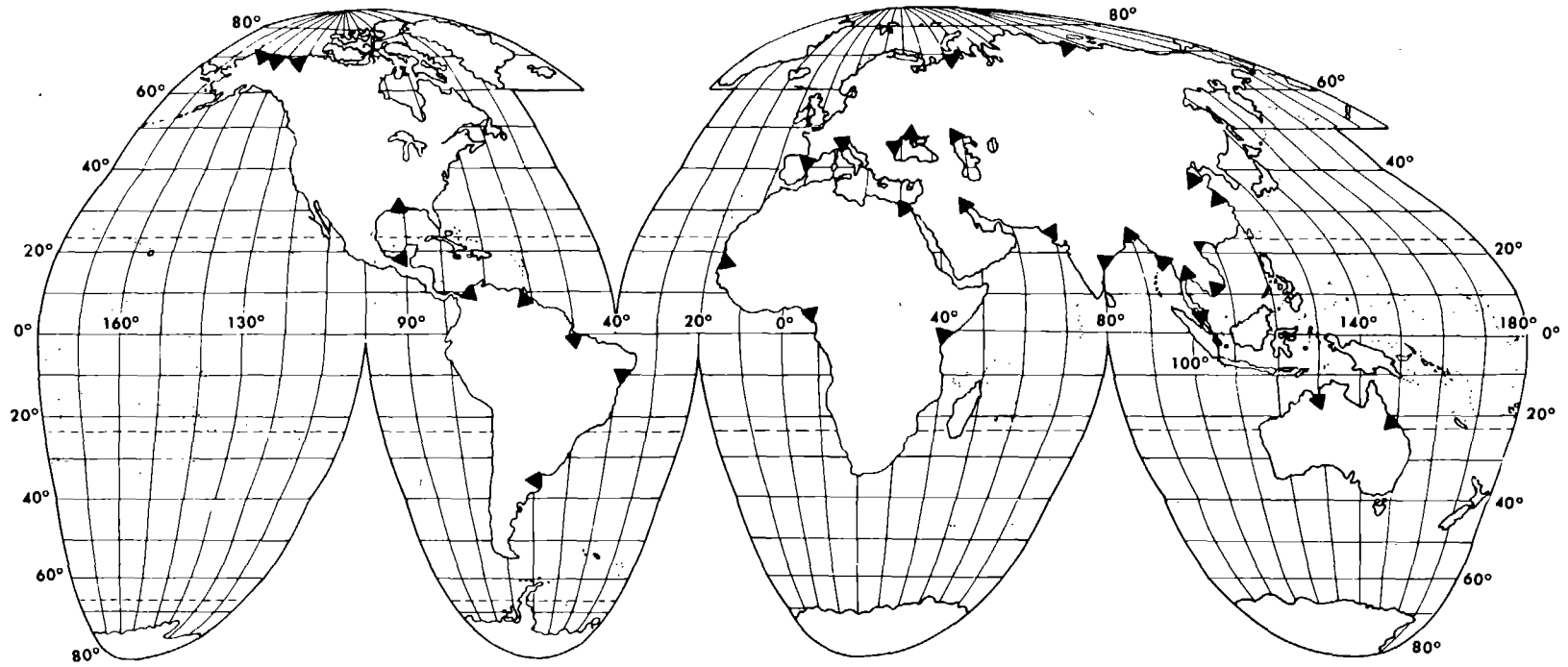

Figure 1. Global distribution of river systems studied.

Table 1

List of Deltas Studied and Their Locations

River	Continent	Receiving Body of Water	Coordinates	
			Latitude	Longitude
Amazon	South America	Atlantic Ocean	0	52°W
Burdekin	Australia	Coral Sea	19°S	147°E
Chao Phraya	Asia	Gulf of Siam	13°N	101°E
Colville	North America	Beaufort Sea	71°N	151°W
Danube	Europe	Black Sea	43°N	28°E
Dneiper	Asia	Black Sea	47°N	32°E
Ebro	Europe	Mediterranean Sea	41°N	02°E
Ganges-Brahmaputra	Asia	Bay of Bengal	32°N	90°E
Grijalva	North America	Gulf of Mexico	18°N	93°W
Hwang Ho	Asia	Yellow Sea	37°N	118°E
Indus	Asia	Arabian Sea	24°N	67°E
Irrawaddy	Asia	Bay of Bengal	16°N	94°E
Klang	Asia	Straits of Malacca	3°N	101°E
Lena	Asia	Laptev Sea	73°N	125°E
Magdalena	South America	Caribbean Sea	12°N	69°W
Mackenzie	North America	Beaufort Sea	68°N	139°W
Mekong	Asia	South China Sea	10°N	107°E
Mississippi	North America	Gulf of Mexico	30°N	90°W
Niger	Africa	Gulf of Guinea	4°N	7°E
Nile	Africa	Mediterranean Sea	32°N	31°E
Ord	Australia	Timor Sea	16°S	120°E
Orinoco	South America	Atlantic Ocean	8°N	62°W
Po	Europe	Adriatic Sea	44°N	12°E
Parana	South America	Atlantic Ocean	33°S	58°W
Pechora	Europe	Barents Sea	68°N	54°E
Red	Asia	Gulf of Tonkin	21°N	107°E
Sagavanirktok	North America	Beaufort Sea	70°N	148°W
Sao Francisco	South America	Atlantic Ocean	11°S	37°W
Senegal	Africa	Atlantic Ocean	17°N	16°W
Shatt-al-Arab	Asia	Persian Gulf	30°N	49°E
Tana	Africa	Indian Ocean	2°S	42°E
Volga	Europe	Caspian Sea	47°N	48°E
Yangtze-Kiang	Asia	East China Sea	32°N	122°E

and their scales for each river system.

To standardize data compilation, variables were rigidly defined, working map scales were optimized and selected, and data categories were defined. For each river system, approximately 900 qualitative and quantitative parameters were selected on the basis of causal connections indicated by experience and by published literature. These parameters and the methods of their determination were defined by Coleman and Wright (1971). Map scale selection depended on map availability and required resolution. In the analyses of drainage basins, 1:1,000,000 scale maps were used; scales of 1:250,000 and larger were used in morphometric analyses and landform determinations of the alluvial valleys, delta plains, and receiving basins.

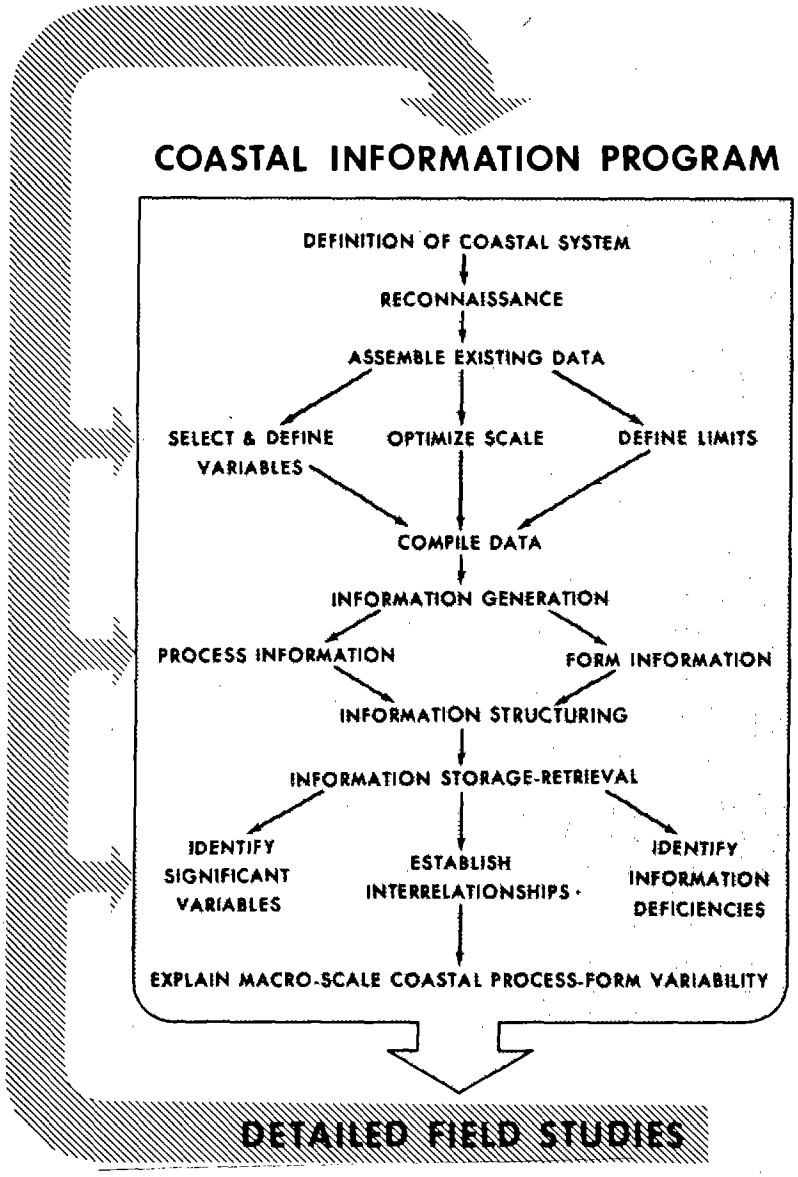

Figure 2. Sequence of procedures followed in the Coastal Information Program.

Information Generation

Following compilation, data were transformed into meaningful information macrostates by means of various computer programs, morphometric analyses, and grouping procedures. In this information generation stage, large volumes of raw data were converted into a few diagnostic process and form parameters. Selection of these parameters and development of procedures for their determination followed considerable experimentation. By means of a CALMA model 303 electronic digitizer, elevation and bathymetric contours were stored on magnetic tape and input to various Fortran IV computer programs written for the IBM 360-65, which converts these data into single parameters such as hypsometric integral, delta bulge volume distribution,

basin relief, etc. Numerous other calculations were performed on Wang 700 programmable calculators. Definitions and calculation procedures for all parameters are presented by Coleman and Wright (1971); salient parameters used in final comparisons are defined elsewhere in this report.

Information Structuring

After information was generated and transformed, it was structured into the hierarchical arrangement illustrated in Figure 3. Each total river system (level I in the hierarchy) is subdivided, for purposes of information grouping, into its natural subsystems (level II). Each of these is, in turn, further subdivided into information categories (level III), which are finally broken down into the individual parameters (level IV) and subparameters (level V). (For example, river discharge is considered a parameter, whereas monthly values of discharge, discharge mean, standard deviation, etc., are subparameters.)

Information Storage and Retrieval

Information in this hierarchical form was then entered as input into a comprehensive computer program referred to as the Information Compilation and Comparison System (ICCS) (Dooley, 1970). Originally designed to contain information on space vehicles and aircraft performance characteristics, this program was revised to handle the information on major river systems. The program allows a masterfile containing information in the various categories to be updated at any time, as new information is generated, without destroying information already contained in the masterfile. The masterfile can be recalled for review of available information, or a search for information on specific river systems can be run. More important, the SEARCH routine allows comparisons between river systems on the basis of individual parameters or combinations of up to 50 parameters. Each parameter may be assigned a weighting factor between 1 and 999, depending on its relative importance. The output ranks the deltas on the basis of number of conditions satisfied by the search.

All information so far collected on river systems is filed in this program and is readily accessible. The program has proved valuable for retrieving organized information in the various categories for comparisons.

Statistical Comparisons

The primary purpose of the comparisons of river systems in this study was to establish the degree and range of similarity or dissimilarity between deltas and their subsystems and to relate this variability to corresponding similarities and dissimilarities between process environments. Several statistical techniques have been employed. Because of the small sample size of only 34 deltas and the large number of variables, it was not feasible to perform inferential analyses, such as multiple regression, to evaluate causal relationships between variables. Instead, the approach has been to examine the affinities and differences between deltas in terms of several variables by using a combination of multivariate analyses, including cluster analysis, factor analysis, and discriminant analysis.

Cluster analyses were performed by means of the CLUSTAN computer procedures developed by Wishart (1969). Detailed discussions of the concepts and procedures of cluster analysis can be found in Sokal and Sneath (1963), Kendall (1966), Mather (1972), and Cooley and Lohnes (1971). McCammon (1968a and b) and McCammon and Wenninger (1970) have applied clustering techniques to geologic data. Somewhat similar numerical classifications have been applied to coastal classifications by Resio et al. (1973) and Biscoe et al. (1973).

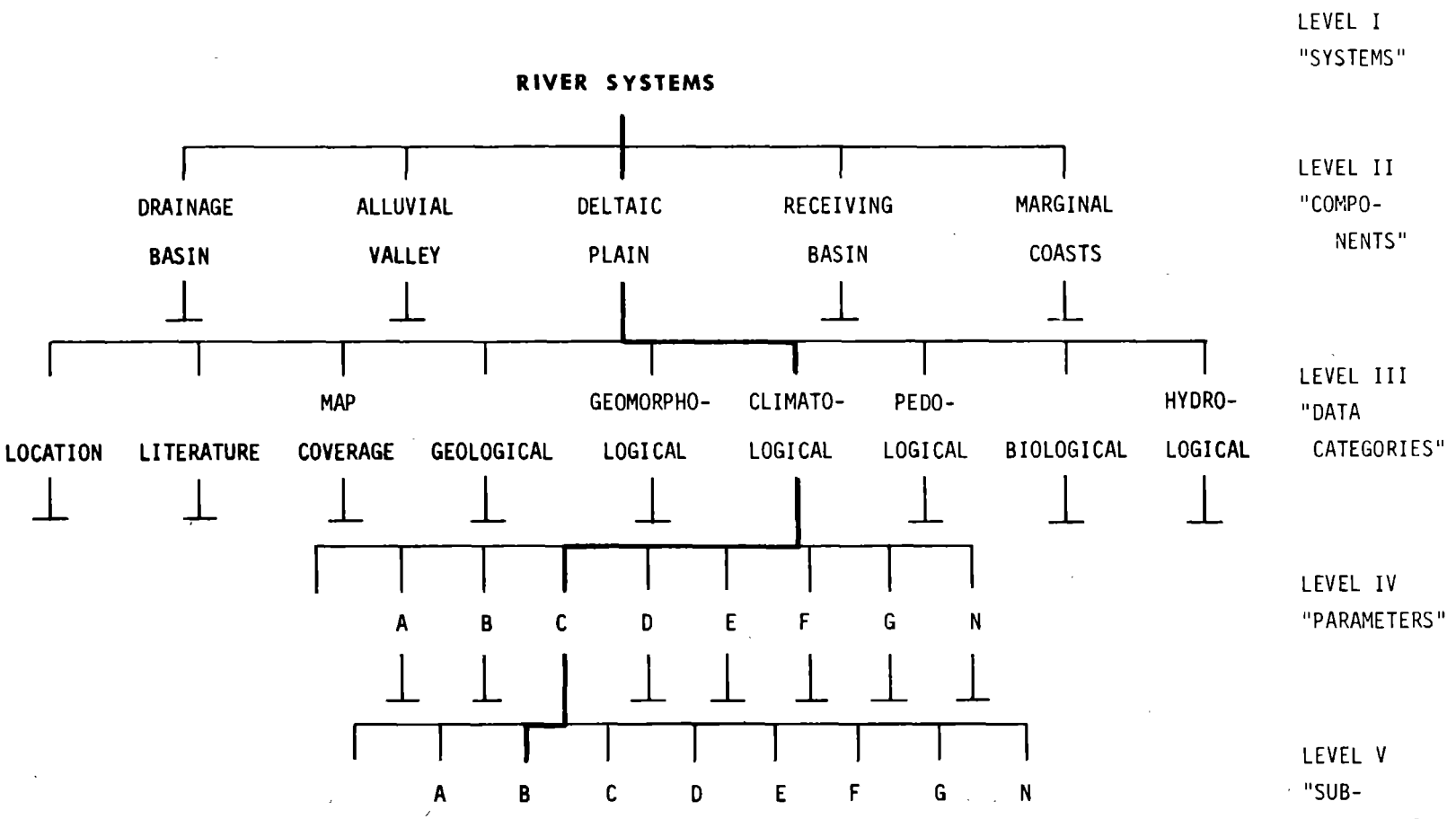

Figure 3. Hierarchy for structuring river system information.

Clustering techniques employed in this study involved Q-mode analyses of the associations between operational taxonomic units (OTUs), which, in this case, were the individual river systems. Q-mode analysis contrasts with R-mode analysis in the sense that the latter is concerned with associations between variables. Clustering is based on computation of coefficients of similarity or dissimilarity between all possible pairs of OTUs. In the present case, the multidimensional Euclidian distance coefficient d_{jk} was used to index the degree of dissimilarity between any two OTUs designated by the subscripts j and k. The coefficient d_{jk} is calculated from the relationship

$$d_{jk} = \left[\sum_{i=1}^{M} (X_{ij} - X_{ik})^2 \right]^{1/2}$$

where X_{ij} indicates the value of the ith variable for the jth observation (OTU) and M is the total number of variables. In order to avoid biasing the analysis toward variables of large magnitude, the distance coefficients are computed from the matrix of standard scores X_{ij}* rather than from raw data. The standard score X_{ij}* of the jth observation of variable i is defined as

$$X_{ij}^* = (X_{ij} - \bar{X}_i)/s_i$$

where $\bar{X}_i$ and s_i are respectively the mean and standard deviation of variable i. Input data may be in numeric, binary, or multistate forms. An example of the last form includes semidiscrete categories such as absent, rare, common, and abundant.

Once distance coefficients have been computed, the OTUs (river or delta systems) are grouped into clusters, within which the members are regarded as similar at some given affinity (Euclidian distance) level. Initially, only those OTUs which are absolutely identical ($d_{jk} = 0$) are grouped. As clustering proceeds, group means (multidimensional) of the protoclusters are computed and distances (d_{jk}) from the means to remaining OTUs are calculated. New members are successively added to clusters by lowering the requirements for admission (i.e., by increasing d_{jk}). From the results of clustering, a dendrogram or linkage tree can be constructed to illustrate the hierarchy of clustering whereby the number of clusters decreases as distance (d_{jk}) increases. The optimum number of clusters to be finally compared depends on selection of an upper cutoff limit for d_{jk}. Because the values of the distance coefficient will vary between analyses, depending on the particular variable combinations used, it is meaningless to select a constant d_{jk} value for all analyses. Instead, the cutoff point is selected for each analysis by plotting the number of clusters against d_{jk} and letting the distance value corresponding to the first significant break in the curve serve as the cutoff point.

Cluster analyses were supplemented by discriminant analyses, using the Statistical Analysis Systems (SAS) program on the LSU IBM 360-65 computer, in order to determine more quantitatively the degrees of within-cluster similarity and between-cluster dissimilarity. By means of the discriminant analysis procedure, tables were constructed to indicate the multidimensional separation between clusters and between each individual OTU and each cluster. This procedure permits determination of the positions of transitional or unique river systems (i.e., those systems which do not cluster at the selected cutoff distances) relative to previously constructed clusters. Determination of contrasts and similarities between clusters using this procedure is not restricted to the variables on which the clusters were

originally constructed but may involve any other variables or variable combinations.

In most instances, clustering in this study was based on a few variables which are similar in dimension and function and are derived from the same subsystem (i.e., one cluster set for abundance of various landforms in the delta plain, another set for the morphometric properties of river mouths, etc.). This was done to avoid constructing meaningless and uninterpretable associations. In a few cases, however, it was desired to calculate major clusters in which numerous variables of several different types were considered. In these cases, large numbers of variables were reduced to a few factors by the procedure of factor analysis, again using the routines of the SAS program. Cluster analyses were then performed on the individual factor scores (obtained for each OTU) rather than on the original data. Factor analysis combines several variables into one or more macrovariables or factors and computes the contribution of each variable to the total variance of each factor.

MAJOR RIVER SYSTEMS AND THEIR SUBSYSTEM COMPONENTS

This report is concerned primarily with river deltas and their variability. However, a delta is an integral part of a larger total river system and, to be adequately understood, must be considered in that context. Each component subsystem of a river system contributes in varying degrees to the characteristics of the delta. Because of the numerous interactions which take place between subsystems, the river system as a whole is more than the sum of its parts.

Figure 4 diagrammatically illustrates the spatial relationships between the basic river subsystems. A river system consists of at least four subsystems: (1) the drainage basin; (2) the alluvial valley; (3) the receiving basin; and (4) the delta plain. Within each of these subsystems, climatic, geologic, geomorphic, hydrologic, and biologic events mutually interact. Some of these interactions are illustrated in Figure 5. The drainage basin supplies water and sediment to the remainder of the river system and is characterized by net erosion; the alluvial valley is a graded conduit which, over the long term, experiences neither significant erosion nor deposition and through which water and sediment are transported en route from the drainage basin to the sea. The receiving basin serves as a sink for the water and sediment discharged by the river and supplies energy, which opposes the seaward-directed riverine energy.

The delta itself is, for the purposes of this study, regarded as the response to these various subsystem contributions. The delta is characterized by sediment dispersal and accumulation and results from the interactions between riverine and marine forces.

In the discussions that follow, each of the contributing subsystems will be considered separately in terms of its salient morphologic and dynamic characteristics. The delta plain will receive the most detailed treatment.

THE DRAINAGE BASIN

The drainage basin, or catchment, is the source of the water and sediment ultimately supplied to the delta. The amount and temporal distribution of river discharge are of paramount importance to deltaic sedimentation and are functions of basin climate, area, and shape. The sediment yield of a basin is affected by these same factors, as well as by basin geology, relief, and hypsometry.

A total of 42 different geologic, geomorphologic, biologic, climatologic, and hydrologic variables, as defined by Coleman and Wright (1971) were measured and

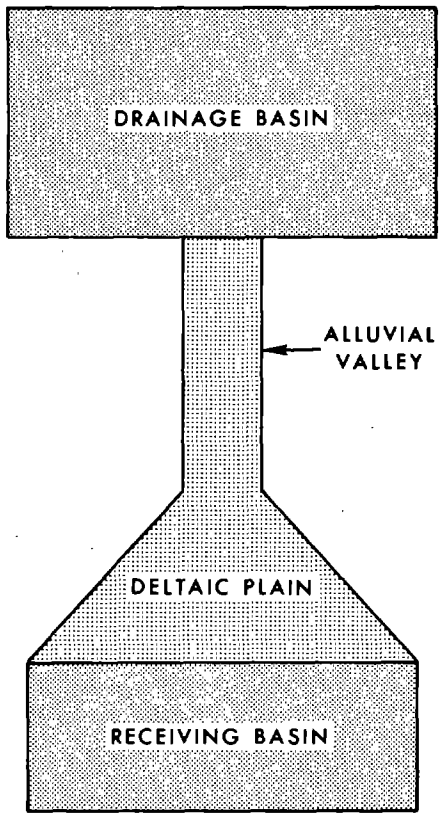

Figure 4. River system components.

recorded for drainage basins; this information is presently stored for 34 rivers in the ICCS retrieval program. For purposes of statistical comparisons, only a few of the more fundamental variables were selected for inclusion in the cluster analyses. Cluster analyses were performed separately on three different subsets of basin data. The first cluster set was concerned with the absolute dimensions of the basins; the variables involved were basin area, basin perimeter length, mean relief, and mean elevation. The second cluster set is also geomorphic but is based on dimensionless morphometric parameters, the values of which are independent of absolute dimensions. In this case, clusters are determined on the basis of drainage density, the relief ratios of Shumm (1956) and Melton (1957), basin hypsometric integral, and the high relief fraction of the hypsometric curve. Climatic and hydrologic variables, including mean annual precipitation, the coefficient of variability of precipitation, the difference between precipitation and actual evapotranspiration (P-AE), mean annual discharge of the trunk stream at the lower end of the basin, and duration of freeze were combined to produce the third set of clusters. Finally, all the above-mentioned variables were reduced to factors by factor analysis, and the resulting factor scores were used to construct a fourth set of clusters.

The results of clustering based on absolute basin dimensions are presented in Figure 6 as a dendrogram. This diagram shows individual drainage basins (OTUs) arranged on the X axis in such a way that the most similar members are closest together and the most dissimilar are farthest apart. It should be noted that this axis possesses no constant scale and is not referenced to an origin. The arrangement

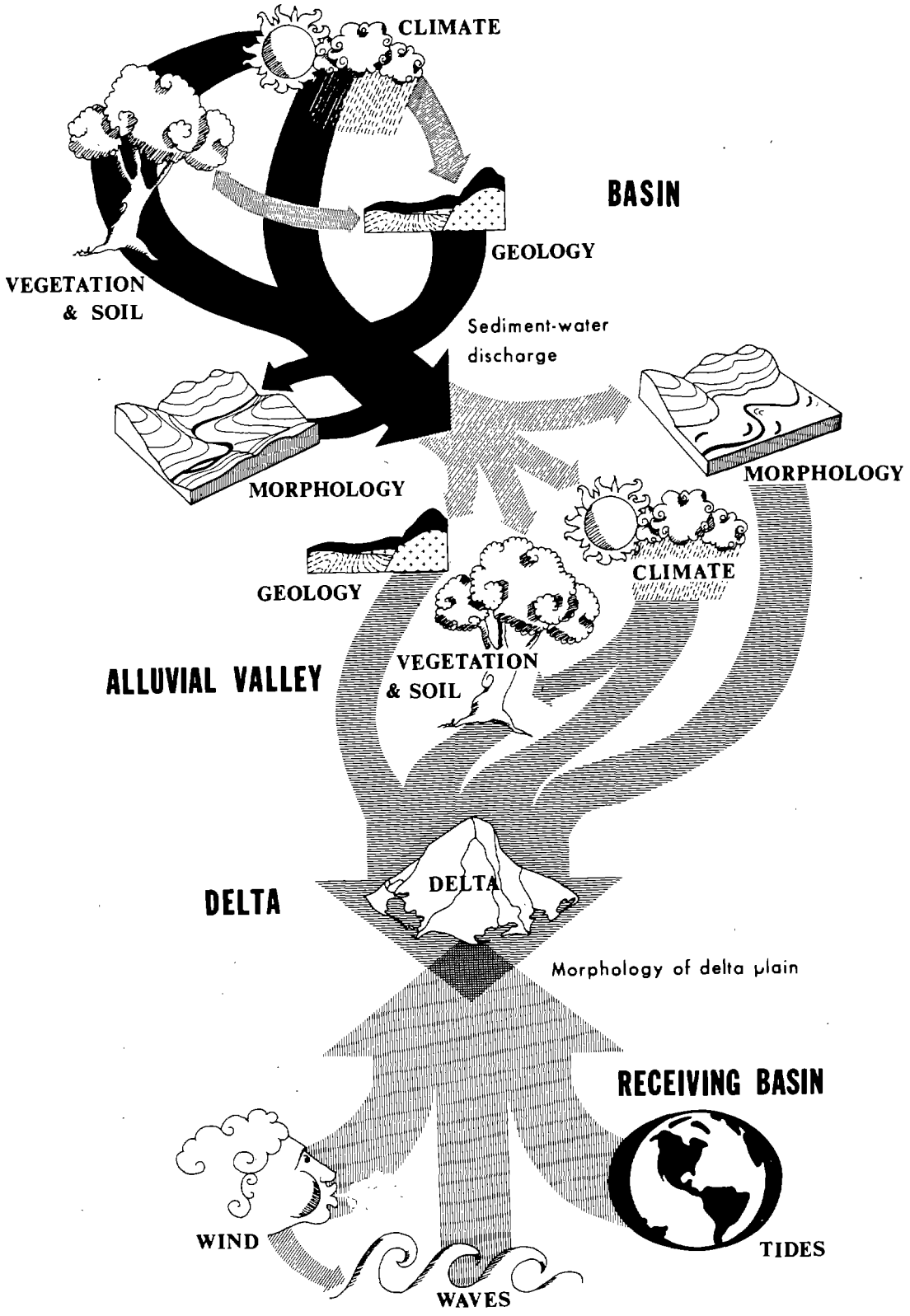

Figure 5. Diagram of process interactions in a river system.

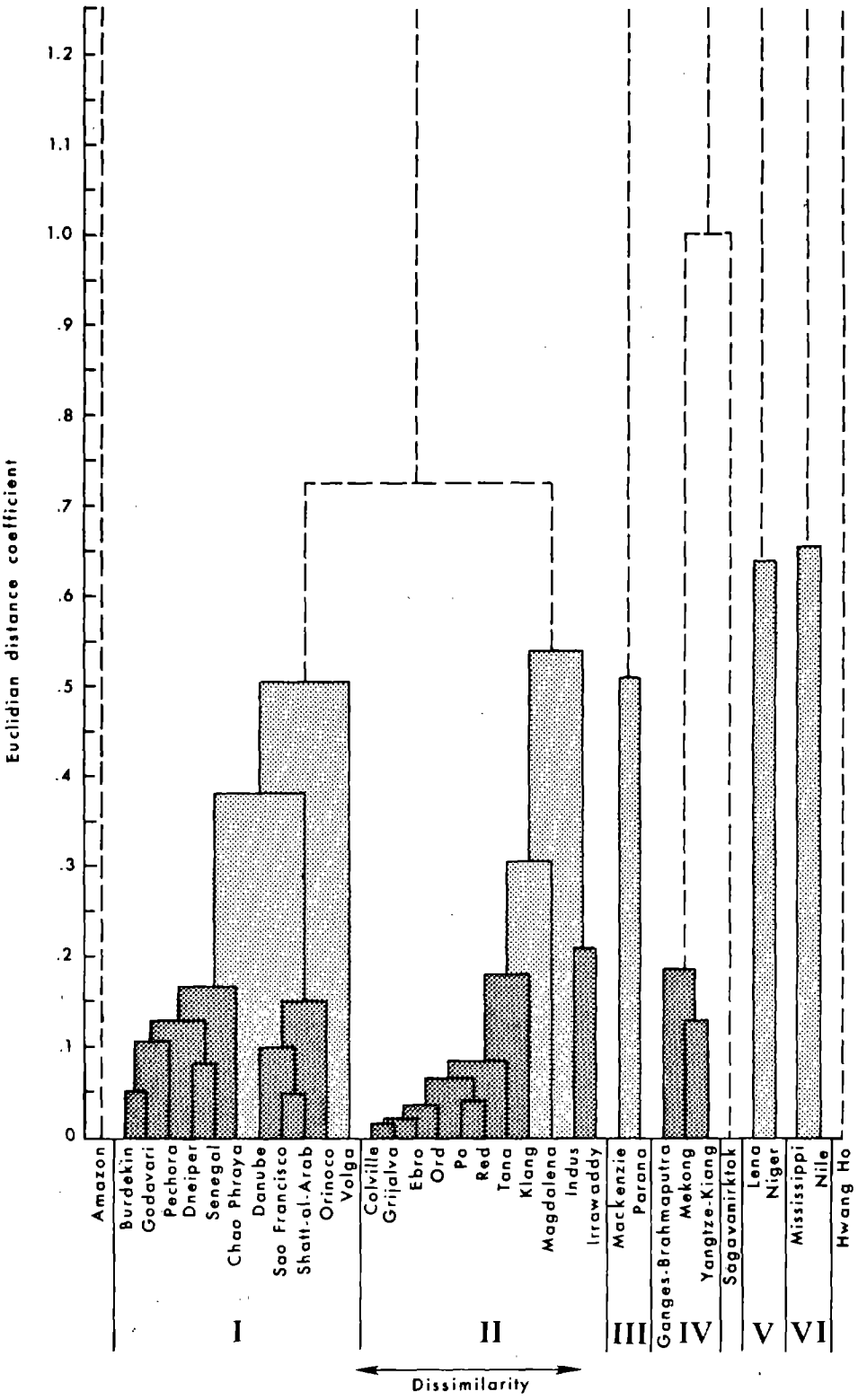

Figure 6. Cluster analysis dendrogram for drainage basins based on absolute dimensions.

simply shows as adjacent neighbors basins which are most mutually similar; however, the absolute distances (d_{jk}) between different adjacent neighbors may vary considerably. The actual values of the dissimilarity or distance coefficient (d_{jk}, calculated from standard scores) are shown on the Y axis. The linkage trees indicate the distance level at which individual basins or basin subclusters can be regarded as resembling one another. Maximum similarities are indicated by linkages at low d_{jk} values, whereas linkages at high values suggest lower similarities. For example, Figure 6 shows that no two basins are perfectly identical in terms of the parameters considered because such an identity would be indicated by a linkage at $d_{jk} = 0.0$. However, several groups of deltas (the Colville, Grijalva, Ebro, and Ord; the Burdekin and Godavari; the Sao Francisco and Shatt-al-Arab; and the Po and Red) link below the 0.05 level, indicating very close similarity. On the other hand, although the Mackenzie is more similar to the Parana than to any of the other basins, the linkage between these two basins occurs at a distance level of 0.51, suggesting that the similarity is less pronounced.

As the distance levels increase, subclusters combine into progressively fewer high-order clusters; however, the variance within these clusters increases. The choice of a maximum distance value at which to accept linkages depends on the desired resolution for the resulting clusters, and maximum d_{jk} cutoff values may be selected to suit individual requirements. For purposes of cluster comparisons presented herein, optimal cutoff values have been selected for each cluster set according to the criteria described in the methodology section. In the case of the cluster set (clusters I-VI) displayed in Figure 6, clusters were accepted on the basis of linkages occurring at d_{jk} values less than 0.70.

Because the absolute basin dimensions vary appreciably, Figure 6 displays linkages over a broad range of d_{jk} values. For the given maximum distance of 0.70, two major clusters (I and II), four small clusters (III-VI) containing only two or three members, and three unique or unclustered individuals result. The values for each river system, arranged and grouped as in Figure 6, are presented in Table 2, together with cluster means and coefficients of variability. The two major clusters differ appreciably from each other in terms of the magnitudes of horizontal dimensions: the area, perimeter, stream length, and length of long axis of cluster I are more than twice as great as the corresponding values for cluster II, though mean elevation and relief values are comparable between the two clusters. Cluster III is distinguished by relatively large horizontal dimensions, together with significantly higher elevation and relief, whereas the three basins comprising cluster IV, the Ganges-Brahmaputra, Mekong, and Yangtze-Kiang, are characterized by large areas, perimeters, stream lengths, and long-axis lengths. The remaining individual basins are isolated (at the given distance level) because of the unique combinations of dimensions indicated in Table 2.

Discriminant analysis results, as presented in Table 3, show a high degree of discretion between clusters but relatively tight homogeneity within clusters, as indicated by the distance-squared coefficients between clusters and their individual members. The isolated basins exhibit large squared distances from all clusters.

The dimensionless morphometric parameters (drainage density, Shumm's and Melton's relief ratios, hypsometric integral, and the ratio of the hypsometric integral above the break in slope to the total hypsometric integral) were used to produce the cluster analysis results presented in Figure 7. The dendrogram and Table 4 indicate a considerable range of variability in these parameters. In this case, clusters were defined on the basis of linkages occurring at or below distance coefficients of 0.5. Four clusters resulted, and eight basins remained unique. Discriminant analysis (Table 5) performed on the clusters suggested that they were

Table 2

Drainage-Basin Absolute Dimensions

	Delta	Relief (m)	Area x 10^3 (km^2 x 10^3)	Perimeter x 10^3 (km x 10^3)	Stream Length (km)	Long Axis (km)	Elevation (m)
	Amazon	2,050.00	5,877.49	11.70	5,259.80	3,101.70	2,250.00
Cluster I	Burdekin	338.70	266.70	4.03	612.96	711.04	732.10
	Godavari	190.60	305.30	3.39	967.65	998.90	668.50
	Pechora	147.30	300.70	4.97	1,512.90	822.90	282.00
	Dneiper	44.53	801.30	3.42	1,222.80	1,069.90	232.40
	Senegal	39.74	196.42	2.61	1,190.00	647.60	94.50
	Chao Phraya	176.49	922.00	2.17	866.34	599.30	1,032.60
	Danube	291.74	742.60	5.59	2,535.80	1,544.60	950.00
	Sao Francisco	62.80	602.30	5.72	2,227.00	1,854.00	563.00
	Shatt-al-Arab	111.60	461.80	6.88	2,658.40	1,669.20	435.20
	Orinoco	243.18	951.30	4.54	1,530.60	1,523.00	683.60
	Volga	31.96	1,614.40	1.44	2,365.00	1,737.00	240.90
	Mean	152.60	651.35	4.07	1,608.13	1,197.95	537.71
	CV	0.66	0.61	0.39	0.44	0.38	0.55
Cluster II	Colville	468.67	59.40	1.42	567.02	390.40	1,256.40
	Grijalva	351.08	112.00	1.59	656.08	376.50	1,243.90
	Ebro	402.14	89.80	1.59	623.60	502.80	1,632.40
	Ord	297.33	46.57	1.01	405.50	302.50	1,610.70
	Po	480.35	71.72	1.28	381.80	368.30	2,101.80
	Red	420.37	143.90	2.10	760.00	710.00	1,984.00
	Tana	554.87	63.50	1.10	522.00	864.80	1,319.00
	Klang	446.28	0.90	0.14	55.90	50.80	690.70
	Magdalena	786.50	251.71	2.41	1,081.00	1,075.00	1,957.50
	Indus	605.55	887.70	4.75	1,486.80	1,244.30	3,271.60
	Irrawaddy	352.80	341.80	2.59	1,295.00	1,074.00	2,746.40
	Mean	469.63	188.09	1.82	712.25	632.67	1,801.38
	CV	0.28	1.28	0.63	0.56	0.58	0.39
Cluster III	Mackenzie	730.00	1,448.40	6.34	1,470.00	1,909.00	1,275.00
	Parana	1,110.00	2,871.80	8.00	1,168.00	1,219.00	1,475.00
	Mean	920.00	2,160.10	7.17	1,319.00	1,564.00	1,375.00
	CV	0.21	0.33	0.12	0.11	0.22	0.07
Cluster IV	Ganges-Brahmaputra	681.98	1,579.20	7.17	3,901.80	2,418.30	2,580.10
	Mekong	439.97	517.50	6.47	4,350.00	2,603.00	2,573.20
	Yangtze-Kiang	567.40	1,354.20	6.71	3,807.00	2,686.20	3,085.40
	Mean	496.45	1,150.30	6.78	4,019.60	2,569.17	2,746.23
	CV	0.27	0.40	0.04	0.06	0.04	0.87
	Sagavanirktok	324.15	11.83	0.51	2,795.00	2,735.00	2,122.00
Cluster V	Lena	222.92	2,421.40	7.67	4,318.55	4,842.00	1,204.20
	Niger	93.00	1,112.70	10.10	4,461.60	3,465.80	413.00
	Mean	157.96	1,767.05	8.89	4,390.07	4,153.90	808.60
	CV	0.41	0.37	0.14	0.02	0.17	0.49
Cluster VI	Mississippi	915.00	3,344.60	9.08	6,210.70	2,703.10	1,200.00
	Nile	1,007.40	2,715.60	12.90	3,877.70	2,651.20	2,262.40
	Mean	961.20	3,030.10	10.99	5,044.20	2,677.15	2,131.20
	CV	0.05	0.10	0.17	0.23	0.01	0.06
	Hwang Ho	514.16	865.10	4.93	2,791.60	1,674.90	7,521.29
	Overall Mean	450.02	980.99	4.60	2,056.94	1,533.71	1.579.14
	Overall CV	0.88	1.26	0.71	0.78	0.71	0.86

Table 3

Drainage-Basin Absolute Dimensions Discriminant Analysis--d^2 Values

Cluster	I	II	III	IV	V	VI
I	0.00	37.68	38.95	38.34	61.72	86.07
II	37.68	0.00	70.94	34.27	161.84	136.17
III	38.95	70.94	0.00	61.21	83.13	41.10
IV	38.34	34.27	61.21	0.00	90.42	62.24
V	61.72	161.84	83.13	90.42	0.00	91.93
VI	86.07	136.17	41.10	62.24	91.93	0.00

	Cluster					
Delta	I	II	III	IV	V	VI
Amazon	318.62	367.70	159.07	277.88	297.46	98.85
Burdekin	5.80	20.49	34.76	39.94	91.26	98.77
Godavari	2.69	24.12	43.79	38.80	79.12	105.68
Pechora	1.91	43.01	42.12	44.17	69.78	85.88
Dneiper	2.48	59.90	45.35	57.80	61.58	100.76
Senegal	2.69	34.42	55.47	48.42	83.94	110.42
Chao Phraya	7.76	23.04	46.73	43.58	104.93	105.26
Danube	4.26	35.69	34.27	20.64	58.54	60.56
Sao Francisco	4.59	60.68	48.30	43.94	36.64	87.41
Shatt-al-Arab	7.14	65.69	47.53	41.28	40.59	72.11
Orinoco	1.71	43.33	29.42	40.70	50.58	79.92
Volga	10.17	62.35	51.90	53.62	53.20	91.22
Colville	33.29	1.24	65.75	38.28	158.09	132.44
Grijalva	25.01	2.36	64.81	36.42	147.13	129.23
Ebro	34.41	0.36	73.01	36.48	160.59	139.76
Ord	35.34	2.41	82.47	43.65	169.16	153.40
Po	53.99	1.85	90.14	45.62	196.10	160.89
Red	37.66	0.41	75.43	33.31	161.02	140.45
Tana	41.76	4.25	68.75	41.46	154.26	143.32
Klang	34.20	5.28	67.15	52.50	164.99	144.06
Magdalena	62.36	9.04	73.21	37.45	176.71	133.01
Indus	50.87	9.65	69.15	23.86	164.61	114.68
Irrawaddy	48.07	5.59	92.96	30.35	170.04	149.10
Mackenzie	21.71	47.72	7.31	40.19	61.29	55.83
Parana	70.80	108.79	7.31	96.85	119.59	40.99
Ganges-Brahmaputra	39.37	39.40	41.30	3.78	89.47	39.18
Mekong	52.09	38.07	88.42	3.96	108.05	86.31
Yangtze-Kiang	34.41	36.20	64.78	3.12	84.59	72.09
Sagavanirktok	85.25	40.11	142.48	46.44	157.61	193.82
Lena	83.58	180.58	96.19	109.26	6.57	115.47
Niger	53.01	156.25	83.22	84.73	6.57	81.54
Mississippi	110.58	152.79	73.16	70.46	123.97	8.86
Nile	79.29	137.29	26.77	71.75	77.61	8.86
Hwang Ho	301.81	166.72	356.27	182.75	486.11	377.90

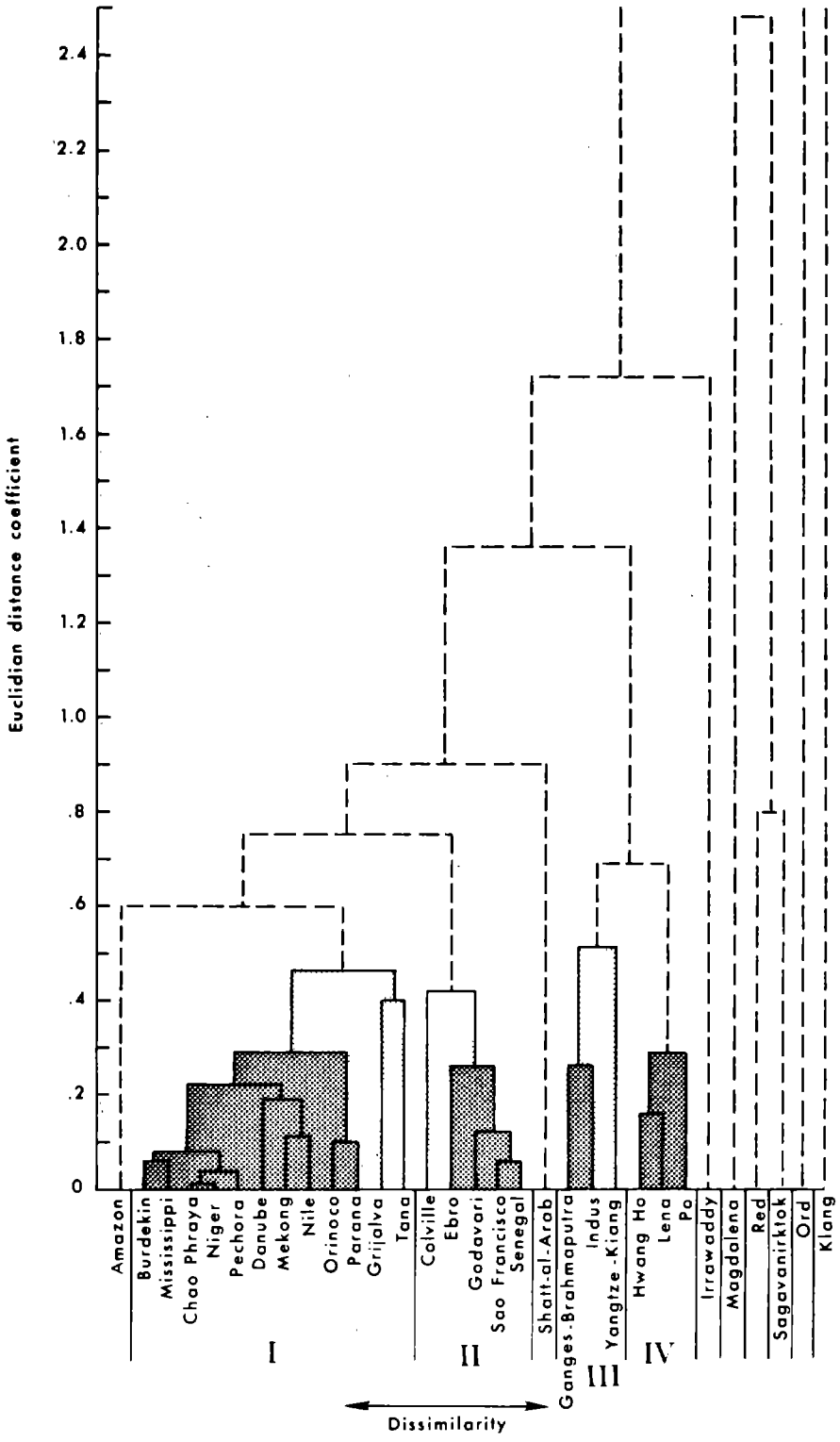

Figure 7. Cluster analysis dendrogram for drainage basins based on dimensionless morphology.

Table 4

Drainage-Basin Dimensionless Morphology Data

	Delta	Drainage Density	Relief Ratio (Shumm)	Relief Ratio (Melton)	Hypso-metric Integral	HI_a/HI^*
	Amazon	0.14	0.0017	0.0660	0.0829	0.3614
Cluster I	Burdekin	0.22	0.0012	0.0803	0.2553	0.0710
	Mississippi	0.19	0.0016	0.0741	0.2415	0.1717
	Chao Phraya	0.19	0.0024	0.0638	0.1975	0.0678
	Niger	0.20	0.0008	0.0247	0.2120	0.0381
	Pechora	0.21	0.0003	0.0004	0.1711	0.0936
	Danube	0.30	0.0013	0.0321	0.2145	0.1890
	Mekong	0.23	0.0047	0.0168	0.2128	0.3325
	Nile	0.20	0.0012	0.0016	0.1686	0.2059
	Orinoco	0.23	0.0004	0.1198	0.0954	0.1865
	Parana	0.30	0.0038	0.0749	0.1005	0.2030
	Grijalva	0.18	0.0649	0.1426	0.2206	0.0201
	Tana	0.24	0.0044	0.3383	0.1428	0.0091
	Mean	0.22	0.0072	0.0808	0.1861	0.1324
	CV	0.17	2.431	1.100	0.266	0.705
Cluster II	Colville	0.31	0.0065	0.1757	0.3236	0.0976
	Ebro	0.15	0.0101	0.1910	0.3167	0.0843
	Godavari	0.22	0.0083	0.0444	0.3613	0.0397
	Sao Francisco	0.19	0.0009	0.0272	0.4518	0.0091
	Senegal	0.16	0.0005	0.0105	0.4306	0.0990
	Mean	0.21	0.0052	0.0898	0.3768	0.0659
	CV	0.27	0.8000	0.862	0.142	0.518
	Shatt-al-Arab	0.01	0.0005	0.0100	0.2600	0.0170
Cluster III	Ganges	0.24	0.0020	0.0649	0.2276	0.6685
	Indus	0.37	0.0016	0.0384	0.2758	0.7510
	Yangtze-Kiang	0.36	0.0013	0.0455	0.3974	0.5269
	Mean	0.32	0.0016	0.0496	0.3002	0.648
	CV	0.22	0.219	0.276	0.291	0.175
Cluster IV	Hwang Ho	0.23	0.0006	0.0118	0.3873	0.4449
	Lena	0.19	0.0007	0.0166	0.3091	0.3209
	Po	0.26	0.0436	0.1159	0.2578	0.3988
	Mean	0.22	0.0150	0.0481	0.3181	0.3881
	CV	0.13	1.353	1.000	0.1676	0.1324
	Irrawaddy	0.21	0.0164	0.6751	0.1630	0.1709
	Magdalena	0.67	0.0317	0.2038	0.2551	0.0014
	Red	0.31	0.0206	0.7034	0.5713	0.0000
	Sagavanirktok	0.45	0.0302	0.4729	0.4042	0.0914
	Ord	0.11	0.0147	0.2818	0.6621	0.6228
	Klang	0.01	0.3848	1.0870	0.1457	0.3510
	Overall Mean	0.23	0.0213	0.1681	0.2747	0.2137
	Overall CV	0.49	3.19	1.461	0.482	0.973

*Ratio of dimensionless volume of basin above the break in slope of the hypsometric curve to total dimensionless volume.

Table 5

Drainage-Basin Dimensionless Morphology Discriminant Analysis--d^2 Values

Cluster	I	II	III	IV
I	0.00	15.46	62.80	27.43
II	15.46	0.00	71.85	22.19
III	62.80	71.85	0.00	15.44
IV	27.43	22.19	15.44	0.00

	Cluster			
Delta	I	II	III	IV
Amazon	21.67	54.63	36.98	32.93
Burdekin	2.60	6.67	72.62	28.22
Mississippi	2.89	9.80	48.92	16.63
Chao Phraya	1.00	15.01	76.58	35.18
Niger	2.76	16.38	87.94	41.78
Pechora	2.74	24.35	83.43	43.39
Danube	2.87	16.65	63.43	27.58
Mekong	7.41	22.75	28.99	10.92
Nile	2.43	24.81	56.00	28.24
Orinoco	3.55	31.21	60.65	35.72
Parana	5.00	34.65	69.34	41.12
Grijalva	13.71	22.09	80.54	35.41
Tana	12.20	20.34	84.38	44.17
Colville	15.65	4.53	72.30	25.38
Ebro	16.37	5.13	58.64	18.66
Godavari	12.11	1.52	80.87	27.68
Sao Francisco	27.01	2.58	93.76	34.20
Senegal	21.93	2.00	69.42	20.77
Shatt-al-Arab	15.58	21.77	84.14	41.82
Ganges-Brahmaputra	59.75	71.54	1.50	16.97
Indus	68.87	75.15	1.50	16.91
Yangtze-Kiang	47.78	33.60	17.96	5.57
Hwang Ho	36.76	25.19	16.47	1.75
Lena	14.71	14.58	26.20	4.34
Po	27.57	32.46	18.20	5.42
Irrawaddy	86.37	74.61	83.11	67.85
Magdalena	101.20	101.00	214.72	145.52
Red	203.10	125.30	204.20	149.21
Sagavanirktok	83.88	45.69	115.08	64.93
Ord	253.81	185.65	126.74	129.35
Klang	787.22	770.65	640.08	659.13

only moderately discrete.

Cluster I contains twelve (39 percent) of the basins examined and exhibits intermediate values for all variables. The basins of this group are characterized by a tendency for high altitudes to be confined to a relatively small fraction of the total basin area. According to Strahler's (1952) interpretation, the low hypsometric integral values ($\overline{HI}$ = 0.186) can be considered to indicate the monadnock stage of basin evolution as a whole. The second basin cluster is distinguished from cluster I primarily by a pronounced increase in the hypsometric integral, whereas high drainage density sets apart the basins of cluster III. Relatively high values for all parameters characterize cluster IV.

In terms of the climatic parameters (number of days of freeze, mean precipitation, coefficient of variability for precipitation, and the difference between precipitation and actual evapotranspiration; Table 6), 31 drainage basins fall into 9 clusters which link at distances less than 0.5 (Fig. 8). Two basins (Burdekin and Hwang Ho) fail to link at the cutoff level. Discriminant analysis of cluster results (Table 7) indicates that the clusters are comparatively discrete and internally fairly tight.

Four humid tropical drainage basins comprise cluster I. Precipitation is abundant, variability is relatively low, as exemplified by the precipitation curve for the Amazon (Fig. 9A), and there is no freezing. The two basins of cluster II also experience abundant rainfall and large water surplus, but there is appreciable annual variability, as illustrated by the curve for the Senegal basin (Fig. 9B).

Except for a moderate decrease in P-AE, the precipitation characteristics of cluster III are similar to those of cluster II; however, at least one station in the three basins of this cluster has temperatures below freezing 3-4 months of the year (although the average temperature for all stations combined may be substantially warmer). The average climatic characteristics of the Mekong basin (Fig. 9C) are typical of this type.

The seven basins of cluster IV receive abundant rainfall, and annual variability is appreciable. However, actual evapotranspiration is much higher, so that P-AE is a great deal lower than in the basins of clusters I, II, and III. Temperatures remain above freezing year-round. The average basin climate of the Niger River (Fig. 9D) offers an ideal example of this type.

Cluster V consists of the semiarid basins of the Ord and Shatt-al-Arab Rivers. Total precipitation is substantially reduced, as compared with the previously described clusters, and exhibits appreciable annual variability owing to the existence of a peaked wet season. There is an annual water-balance deficit. Figure 9E summarizes the climatic characteristics of the Ord basin.

The five basins of cluster VI, typified by the Colville (Fig. 9F), are situated in arctic or subarctic environments, where below-freezing temperatures prevail for at least half the year. Total precipitation is relatively low, and the differences between precipitation and actual evapotranspiration are very small.

Mid-latitude climates and subfreezing winters distinguish the basins of cluster VII. Precipitation is moderate but varies considerably between the individual basins. The climate of the Mississippi catchment (Fig. 9G) is representative.

The basins of the Parana and Po Rivers (Fig. 9H), the two members of cluster VIII, are hydrologically similar to those of cluster IV, except that discharge

Table 6

Drainage-Basin Climate Data

	River	Days of Freeze	CV (Precipitation)	Mean Precipitation (mm)	P-AE (mm)
Cluster I	Amazon	0.000	0.36	1,701.00	502.00
	Magdalena	0.000	0.46	1,777.00	557.00
	Grijalva	0.000	0.60	1,585.36	562.00
	Klang	0.000	0.21	2,135.20	425.40
	Mean	0.000	0.41	1,799.64	511.60
	CV	0.000	0.35	0.11	0.11
	Burdekin	0.000	0.80	662.00	606.80
Cluster II	Godavari	0.000	1.14	1,512.50	640.50
	Senegal	0.000	1.00	1,381.00	533.00
	Mean	0.000	1.07	1,446.75	586.75
	CV	0.000	0.07	0.04	0.09
Cluster III	Indus	105.00	1.05	720.60	403.74
	Mekong	120.00	0.81	1,530.30	346.97
	Yangtze-Kiang	120.00	0.97	1,214,86	456.43
	Mean	115.00	0.94	1,155.25	402.38
	CV	0.06	0.10	0.29	0.11
Cluster IV	Chao Phraya	0.000	0.81	1,317.00	32.00
	Orinoco	0.000	0.78	1,434.00	184.85
	Red	0.000	0.82	1,282.50	362.28
	Sao Francisco	0.000	0.71	1,222.76	329.72
	Niger	0.000	1.02	1,062.23	172.23
	Nile	0.000	0.54	870.48	157.23
	Tana	0.000	0.74	733.00	59.17
	Mean	0.000	0.77	1,131.67	185.55
	CV	0.000	0.17	0.21	0.62
Cluster V	Ord	0.000	1.14	528.00	0.00
	Shatt-al-Arab	0.000	0.95	148.60	- 1.80
	Mean	0.000	1.05	338.30	- 0.90
	CV	0.000	0.09	0.56	- 1.41
Cluster VI	Colville	305.00	0.78	116.00	0.00
	Lena	285.00	0.60	253.20	- 0.40
	Mackenzie	300.00	0.46	257.00	0.00
	Pechora	285.00	0.46	446.50	85.00
	Volga	240.00	0.47	527.50	101.50
	Mean	283.00	0.56	320.04	37.22
	CV	0.08	0.24	0.46	1.24
	Hwang Ho	180.00	0.95	431.55	20.45
Cluster VII	Danube	180.00	0.25	791.89	197.98
	Mississippi	120.00	0.81	1,530.30	346.97
	Dneiper	165.00	0.33	489.25	3.00
	Ebro	120.00	0.22	583.50	82.00
	Mean	146.25	0.40	848.74	135.78
	CV	0.18	0.68	0.56	0.74
Cluster VIII	Parana	0.000	0.42	1,205.50	262.75
	Po	0.000	0.23	846.75	105.87
	Mean	0.000	0.32	1,026.12	184.31
	CV	0.000	0.30	0.17	0.42
Cluster IX	Ganges-Brahmaputra	0.000	1.11	1,814.52	959.54
	Irrawaddy	0.000	1.07	2,192.17	1,104.84
	Mean	0.000	1.09	2,003.34	1,032.19
	CV	0.000	0.19	0.09	0.07
	Overall Mean	76.52	0.68	1,023.97	288.25
	Overall CV	1.38	0.45	0.55	0.96

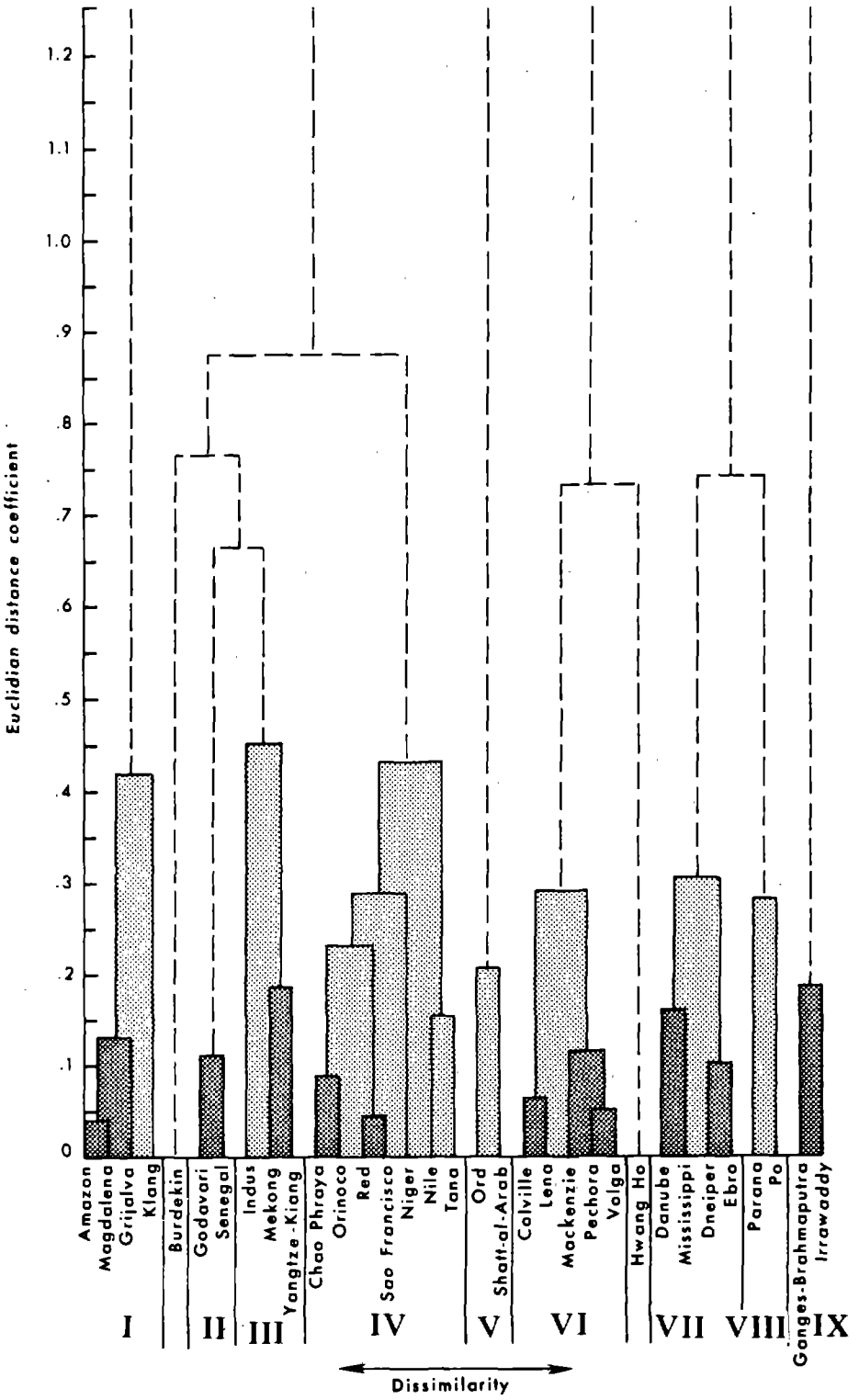

Figure 8. Cluster analysis dendrogram for drainage basins based on salient climatic properties.

Table 7

Drainage-Basin Climate Discriminant Analysis d^2 Values

Cluster	I	II	III	IV	V	VI	VII	VIII	IX
I	0.00	26.33	58.92	23.88	71.10	334.00	108.50	17.66	53.96
II	26.33	0.00	58.45	22.72	47.47	385.50	166.92	50.37	24.38
III	58.92	58.45	0.00	66.76	98.86	146.08	46.88	75.30	86.87
IV	23.88	22.72	66.76	0.00	14.20	357.55	131.58	14.31	88.93
V	71.10	47.47	98.86	14.20	0.00	395.05	170.60	38.88	137.87
VI	334.00	385.50	146.08	357.55	395.05	0.00	73.67	323.03	430.77
VII	108.05	166.92	46.88	131.58	170.60	73.67	0.00	94.28	217.55
VIII	17.66	50.37	75.30	14.31	38.88	323.03	94.28	0.00	115.15
IX	53.96	24.38	86.87	88.93	137.87	430.76	217.55	115.15	0.00

Delta	I	II	III	IV	V	VI	VII	VIII	IX
Amazon	0.39	30.04	60.19	25.14	71.51	328.61	102.96	14.94	58.91
Magdalena	0.40	22.31	56.98	25.38	72.21	336.39	112.04	20.96	45.55
Grijalva	2.93	13.24	52.86	20.43	59.94	340.57	117.90	21.95	37.46
Klang	5.02	48.46	74.40	33.32	89.47	339.15	109.85	21.50	82.66
Burdekin	31.30	22.20	65.79	37.17	55.29	350.28	132.70	37.73	46.84
Godavari	32.85	0.65	62.55	30.49	56.16	398.08	180.64	62.30	19.47
Senegal	21.11	0.65	55.65	16.24	40.08	374.22	154.49	39.74	30.58
Indus	62.47	51.03	4.34	60.91	80.75	163.62	55.94	70.96	83.12
Mekong	58.88	71.14	4.16	71.77	113.41	139.79	42.90	77.97	102.34
Yangtze-Kiang	64.48	62.22	0.54	76.64	111.45	143.85	50.83	86.02	84.18
Chao Phraya	42.38	40.73	86.86	5.63	17.44	384.34	155.58	27.85	122.20
Orinoco	24.34	23.73	69.56	1.89	21.50	368.19	141.29	20.70	88.67
Red	14.58	8.95	55.83	3.79	25.24	355.10	131.75	18.91	56.28
Sao Francisco	11.63	14.67	56.55	3.18	25.58	344.06	119.61	11.39	65.16
Niger	41.16	20.76	74.80	3.95	9.54	386.50	162.27	32.79	89.76
Nile	22.39	38.39	71.41	5.75	20.64	334.70	107.51	2.98	107.65
Tana	38.48	39.57	80.07	3.60	7.26	357.74	130.82	13.31	120.55
Ord	74.82	44.88	101.00	14.79	1.62	409.99	185.58	47.56	134.74
Shatt-al-Arab	70.62	53.31	99.96	16.85	1.62	383.35	158.86	33.44	144.25
Colville	381.35	418.90	166.34	394.64	424.09	3.87	102.46	369.12	466.88
Lena	335.97	380.58	142.80	351.96	384.65	0.74	76.81	322.94	430.21
Mackenzie	382.58	445.20	184.43	411.41	451.93	2.48	93.05	368.24	491.76
Pechora	341.23	400.79	155.94	374.60	419.05	1.10	76.54	334.35	439.78
Volga	244.42	297.62	96.44	270.71	311.10	7.37	35.02	236.04	340.77
Hwang Ho	145.75	154.42	29.97	130.55	145.35	66.17	32.39	131.68	216.87
Danube	150.27	212.24	60.75	184.84	231.39	42.92	5.95	144.29	251.46
Mississippi	77.56	139.30	42.24	111.72	159.30	105.41	4.23	72.80	178.88
Dneiper	136.26	190.48	55.03	146.41	176.79	57.71	3.26	112.70	253.79
Ebro	87.24	142.96	46.79	100.64	132.24	105.93	3.87	64.64	203.38
Parana	9.90	35.30	65.16	9.47	37.28	326.11	96.69	1.59	91.54
Po	28.59	68.61	88.62	22.32	43.66	323.12	93.05	1.59	141.94
Ganges-Brahmaputra	48.05	16.80	79.14	75.00	117.50	420.14	206.53	101.60	0.92
Irrawaddy	61.71	33.80	96.44	104.71	160.09	443.23	230.41	130.55	0.92

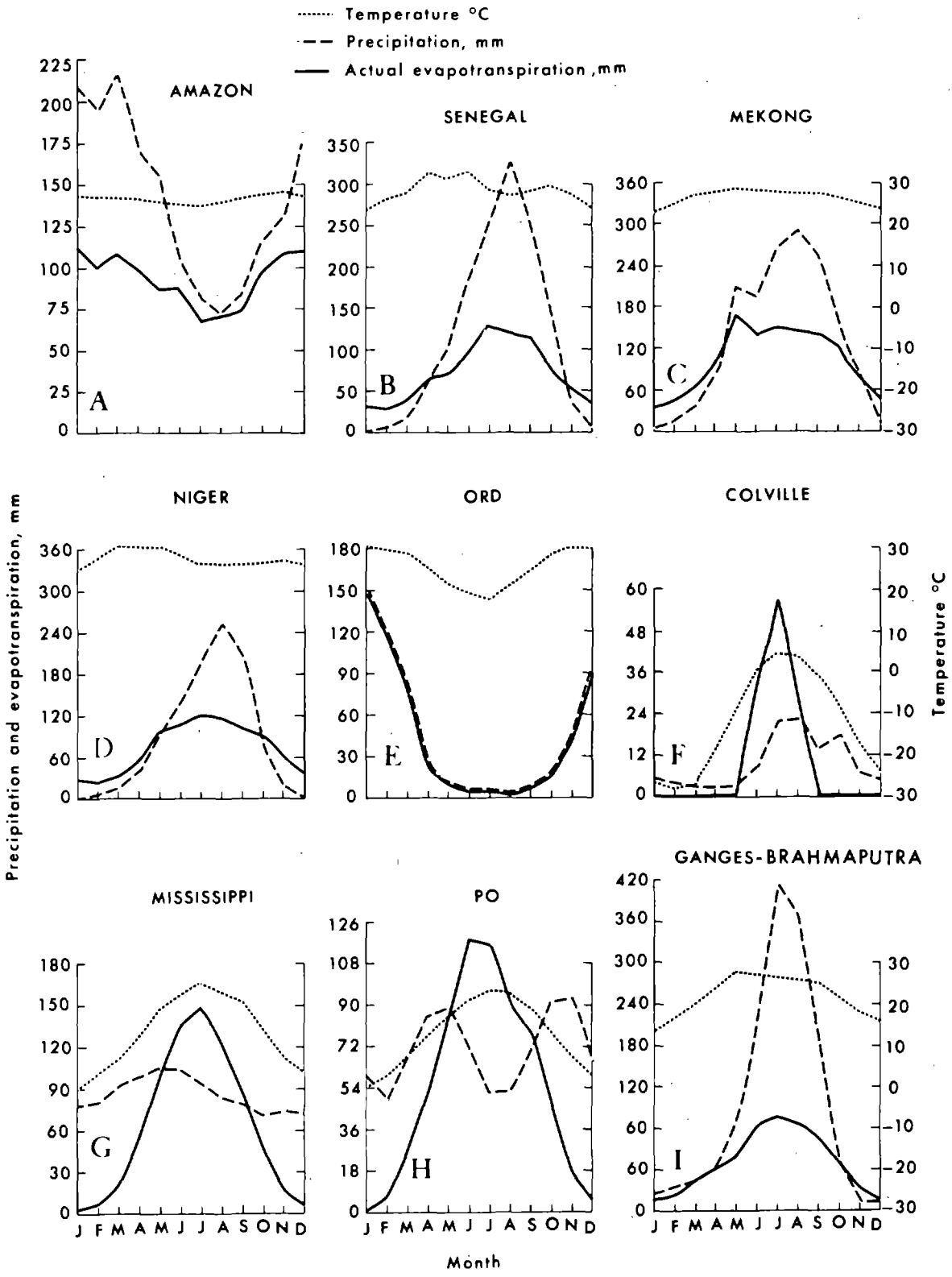

Figure 9, A-I. Representative examples of drainage basin climate types.

exhibits low annual variability.

Cluster IX is composed of the basins of the Ganges-Brahmaputra and Irrawaddy Rivers. Extremely abundant precipitation and relatively low actual evapotranspiration make these basins the wettest of those examined. This situation is attributable to the monsoon climate, which causes the dry season to coincide with cool temperatures, thereby reducing the difference between precipitation and evapotranspiration. The monsoon climate is also responsible for producing annual precipitation coefficients of variability in excess of 1.0. Mean climatic characteristics of the Ganges-Brahmaputra basin are illustrated by Figure 9I.

The unique combinations of all the drainage basin properties, including absolute dimensions, dimensionless forms, and hydrology, are also important to deltaic development. The particular basin signatures which result from the combination of all these variables are unique to each basin. In order to compare drainage basins in terms of the composite of all the morphologic and hydrologic properties previously described, each of the three drainage basin variable subsets (i.e., absolute dimensions, dimensionless form, and hydrology) was subjected to factor analysis. This procedure allowed the original 15 parameters to be reduced to a total of six factors. Cluster analysis was then performed, using the individual factor scores for each basin, on each of the six factors. The results of the three factor analyses are presented in Table 8. In these tables the eigenvalues corresponding to each significant factor are given. Only those factors with eigenvalues greater than 1.0 are accepted as making a significant contribution to the overall basin variability. The unrotated and rotated matrices of factor loadings are also presented. The values of the factor loadings are equivalent to the square roots of the fraction of the variance of each variable that is accounted for by each factor. For example, the factor analysis on the six variables describing absolute basin dimensions indicates that only the first two eigenvalues exceed 1.0, hence most of the variance of the data can be described in terms of two factors. From the factor matrices for drainage basin absolute dimensions it is seen that most of the variance of basin area, perimeter length, stream length, and long axis length is contained in the first factor, whereas elevation contributes largely to the second factor and both factors reflect the variance of relief. Similarly, three factors are required to explain the variance of the five morphometric variables. In the case of the four climatic variables, only the first eigenvalue was greater than 1.0.

The results of cluster analysis performed on the scores of these six factors are presented in the dendrogram shown in Figure 10. The dendrogram indicates that there is a progressive hierarchy of linkages at steadily increasing distance levels and that there is a well-defined cutoff distance. This pattern suggests that, although there are small groups of mutually similar basins [notably (1) the Burdekin, Chao Phraya, Orinoco, Grijalva, and Tana; (2) the Colville, Ebro, and Po; (3) the Danube, Pechora, and Shatt-al-Arab; and (4) the Mekong, Mississippi, Nile, and Parana], objectively discrete clusters are not very prominent. Rather, there appears to be a spectrum of similarities or dissimilarities between individual basins, and these similarities can be generally discerned from the arrangement of basins on the dendrogram. Table 9 is a similarity matrix indicating the Euclidian distance values separating all possible pairs of basins. From this table, the nearest analogy or most opposite counterpart to any individual basin can be determined by searching for, respectively, the lowest or largest distance coefficient corresponding to the basin of interest.

Table 8

Drainage Basin Factor Analysis

Basin Dimensions

Variable	Absolute Dimensions: Mean	Absolute Dimensions: Standard Deviation	Correlation Matrix: Area	Perimeter	Stream Length	Long Axis	Elevation	Absolute Relief	Factor Matrices: Unrotated Factor 1	Unrotated Factor 2	Rotated Factor 1	Rotated Factor 2
Basin Area (x 10^3)	980.99	1,238.59	1.00	0.77	0.70	0.61	0.13	0.75	0.90	0.08	0.79	0.43
Basin Perimeter "	4.60	3.28	0.77	1.00	0.79	0.72	0.13	0.50	0.90	-0.17	0.89	0.21
Stream Length	2,056.94	1,602.68	0.70	0.79	1.00	0.88	0.24	0.35	0.90	-0.24	0.92	0.14
Long Axis	1,533.71	1.081.91	0.61	0.72	0.88	1.00	0.16	0.23	0.83	-0.37	0.91	0.01
Elevation	1,579.14	1,362.95	0.13	0.13	0.24	0.16	1.00	0.36	0.31	0.73	0.01	0.79
Absolute Relief	450.02	394.73	0.75	0.50	0.35	0.23	0.36	1.00	0.66	0.59	0.36	0.80

Factor	1	2	3	4	5	6
Eigenvalue	3.64	1.11	0.83	0.21	0.11	0.10

Basin Morphometry

Variable	Dimensionless Morphometry: Mean	Dimensionless Morphometry: Standard Deviation	Correlation Matrix: Drainage Density	Relief Ratio (Shumm)	Relief Ratio (Melton)	Hypsometric Integral	HI_a/HI	Factor Matrices: Unrotated Factor 1	Unrotated Factor 2	Unrotated Factor 3	Rotated Factor 1	Rotated Factor 2	Rotated Factor 3
Drainage Density	0.23	0.12	1.00	-0.27	-0.06	0.08	-0.02	0.40	0.26	-0.62	0.21	0.66	-0.35
Relief Ratio (Shumm)	0.02	0.06	-0.27	1.00	0.72	-0.15	0.06	-0.94	0.03	0.03	0.90	-0.26	0.08
Relief Ratio (Melton)	0.17	0.25	-0.06	0.72	1.00	0.08	-0.08	-0.86	0.22	-0.34	-0.94	0.12	-0.09
Hypsometric Integral	0.28	0.13	0.08	-0.15	0.08	1.00	0.11	0.13	0.82	-0.20	0.08	0.78	0.33
HI_a/HI	0.21	0.21	-0.02	0.06	-0.08	0.11	1.00	0.01	0.57	0.70	0.04	0.04	0.90

Factor	1	2	3	4	5
Eigenvalue	1.80	1.12	1.03	0.85	0.20

Basin Climate

Variable	Hydrology: Mean	Hydrology: Standard Deviation	Correlation Matrix: Number of Days of Freeze	CV	Mean Annual Precipitation	P-AE	Factor Matrices: Unrotated	Rotated
No. Days Freeze	76.52	112.68	1.00	-0.26	-0.63	-0.47	0.79	Only 1 factor retained. No rotation made.
CV	0.68	0.31	-0.26	1.00	0.09	0.32	-0.41	
Mean Annual Precipitation	1,023.98	571.87	-0.63	0.09	1.00	0.78	-0.90	
P-AE	288.25	282.71	-0.47	0.32	0.78	1.00	-0.88	

Factor	1	2	3	4
Eigenvalue	2.37	0.94	0.54	0.14

Table 9

Similarity Matrix (Euclidian Distance Coefficient d_{jk}) from Factor Scores for Drainage Basins
(All Parameters)

River	Amazon	Burdekin	Chao Phraya	Orinoco	Grijalva	Tana	Godavari	Senegal	Sao Francisco	Colville	Ebro	Po	Danube	Pechora	Shatt-al-Arab	Mackenzie
Amazon	0.0															
Burdekin	3.292	0.0														
Chao Phraya	3.232	0.052	0.0													
Orinoco	2.848	0.180	0.128	0.0												
Grijalva	3.373	0.178	0.208	0.391	0.0											
Tana	3.575	0.298	0.219	0.557	0.274	0.0										
Godavari	3.744	0.171	0.391	0.434	2.902	0.797	0.0									
Senegal	4.209	0.277	0.492	0.510	0.608	1.059	0.103	0.0								
Sao Francisco	3.894	0.395	0.606	0.518	0.927	1.087	0.288	0.209	0.0							
Colville	4.765	0.925	0.889	1.457	1.350	0.620	1.550	1.499	1.308	0.0						
Ebro	3.666	0.461	0.379	0.784	0.662	0.285	1.042	1.022	1.062	0.215	0.0					
Po	3.301	0.622	0.625	1.040	0.757	0.714	1.048	0.961	1.277	0.649	0.224	0.0				
Danube	3.280	0.412	0.375	0.411	0.989	0.650	0.824	0.740	0.406	0.604	0.466	0.862	0.0			
Pechora	4.157	0.704	0.491	0.568	1.238	0.719	1.379	1.240	0.961	0.725	0.529	1.155	1.99	0.0		
Shatt-al-Arab	3.310	0.684	0.511	0.268	1.131	1.033	1.152	1.010	0.777	1.532	0.958	1.398	0.333	0.273	0.0	
Mackenzie	2.785	1.374	1.180	1.256	1.773	1.330	2.145	1.905	1.659	1.009	0.614	0.743	0.698	0.774	0.843	0.0
Mekong	1.728	0.498	0.545	0.355	0.892	1.102	0.677	0.666	0.556	1.592	0.947	0.869	0.467	0.988	0.560	0.879
Mississippi	1.208	1.318	1.292	1.019	1.846	1.601	1.741	1.854	1.225	1.895	1.467	1.695	0.725	1.294	0.952	0.911
Nile	0.838	1.193	1.127	0.878	1.589	1.463	1.646	1.841	1.397	2.049	1.444	1.567	0.852	1.374	0.981	1.021
Parana	1.363	0.593	0.551	0.655	0.722	0.598	1.048	1.389	1.280	1.304	0.768	0.859	0.780	1.224	1.179	1.173
Lena	3.623	2.199	2.150	1.711	3.226	2.847	2.604	2.195	1.365	2.339	2.159	2.569	0.893	1.226	0.909	1.085
Niger	3.534	1.261	1.293	0.721	1.589	2.014	1.306	1.284	0.688	2.780	2.280	2.851	0.862	1.212	0.576	2.174
Ganges-Brahm.	1.813	1.685	1.948	1.644	1.909	2.861	1.424	1.389	1.698	3.658	2.570	1.735	2.228	3.525	2.295	2.391
Indus	2.747	1.528	1.697	1.977	1.919	2.152	1.707	1.499	1.811	1.764	1.274	0.543	1.647	2.426	2.391	1.314
Yangtze-Kiang	2.680	1.265	1.583	1.566	1.897	2.153	1.136	0.962	0.820	1.824	1.503	1.107	1.125	2.147	2.524	1.509
Ord	5.895	2.786	3.114	3.533	3.206	3.570	2.726	2.146	2.602	2.503	2.205	1.317	2.866	3.696	3.761	2.284
Hwang Ho	2.605	2.671	2.695	3.302	2.902	2.547	3.334	3.393	3.542	1.949	1.672	1.080	2.611	3.319	3.773	1.701
Sagavanirktok	6.300	2.173	2.314	2.812	2.843	1.844	2.612	2.509	1.761	0.663	1.351	2.077	1.341	1.765	2.654	1.958
Irrawaddy	3.448	0.994	1.245	1.353	0.499	1.259	0.771	1.226	1.683	2.848	1.917	1.681	2.375	3.098	2.610	3.224
Magdalena	5.330	1.527	1.918	2.487	0.892	1.482	1.387	1.937	1.788	1.824	2.054	2.383	2.258	3.170	3.735	4.141
Red	6.048	1.839	2.318	2.896	1.878	1.877	1.588	1.780	1.740	1.686	1.865	1.890	2.425	3.424	3.846	3.413
Klang	7.995	5.152	5.148	5.236	3.937	4.639	5.363	5.469	6.055	6.191	4.834	4.654	6.322	6.459	5.733	5.053

Table 9 continued

River	Mekong	Mississippi	Nile	Parana	Lena	Niger	Ganges-Brahmaputra	Indus	Yangtze-Kiang	Ord	Hwang Ho	Sagavanirktok	Irrawaddy	Magdalena	Red	Klang
Amazon																
Burdekin																
Chao Phraya																
Orinoco																
Grijalva																
Tana																
Godavari																
Senegal																
Sao Francisco																
Colville																
Ebro																
Po																
Danube																
Pechora																
Shatt-al-Arab																
Mackenzie																
Mekong	0.0															
Mississippi	0.419	0.0														
Nile	0.352	0.085	0.0													
Parana	0.483	0.606	0.366	0.0												
Lena	1.137	0.848	1.288	2.325	0.0											
Niger	0.880	1.034	1.220	1.816	0.956	0.0										
Ganges-Brahm.	0.730	1.654	1.411	1.567	2.835	2.452	0.0									
Indus	1.006	1.816	1.701	1.382	2.701	3.537	0.958	0.0								
Yangtze-Kiang	0.603	1.100	1.247	1.357	1.588	2.016	0.775	0.525	0.0							
Ord	2.176	3.817	4.000	3.576	3.727	5.119	2.313	0.805	1.283	0.0						
Hwang Ho	2.585	2.336	2.173	1.546	4.105	5.469	2.571	2.497	1.778	2.145	0.0					
Sagavanirktok	2.716	2.493	3.084	2.683	2.409	3.216	5.132	3.130	2.320	3.254	3.399	0.0				
Irrawaddy	1.623	2.713	2.393	1.415	4.820	2.926	1.770	2.701	2.285	3.699	4.105	4.169	0.0			
Magdalena	2.701	3.184	3.197	1.904	5.104	3.663	3.980	3.278	2.524	4.568	3.667	2.128	1.746	0.0		
Red	2.786	3.476	3.742	2.630	4.654	4.112	3.633	2.587	1.967	2.481	3.324	1.475	1.727	0.821	0.0	
Klang	5.764	6.790	6.743	5.947	8.088	7.273	6.209	1.314	6.830	5.858	7.432	7.073	3.389	7.666	5.058	0.0

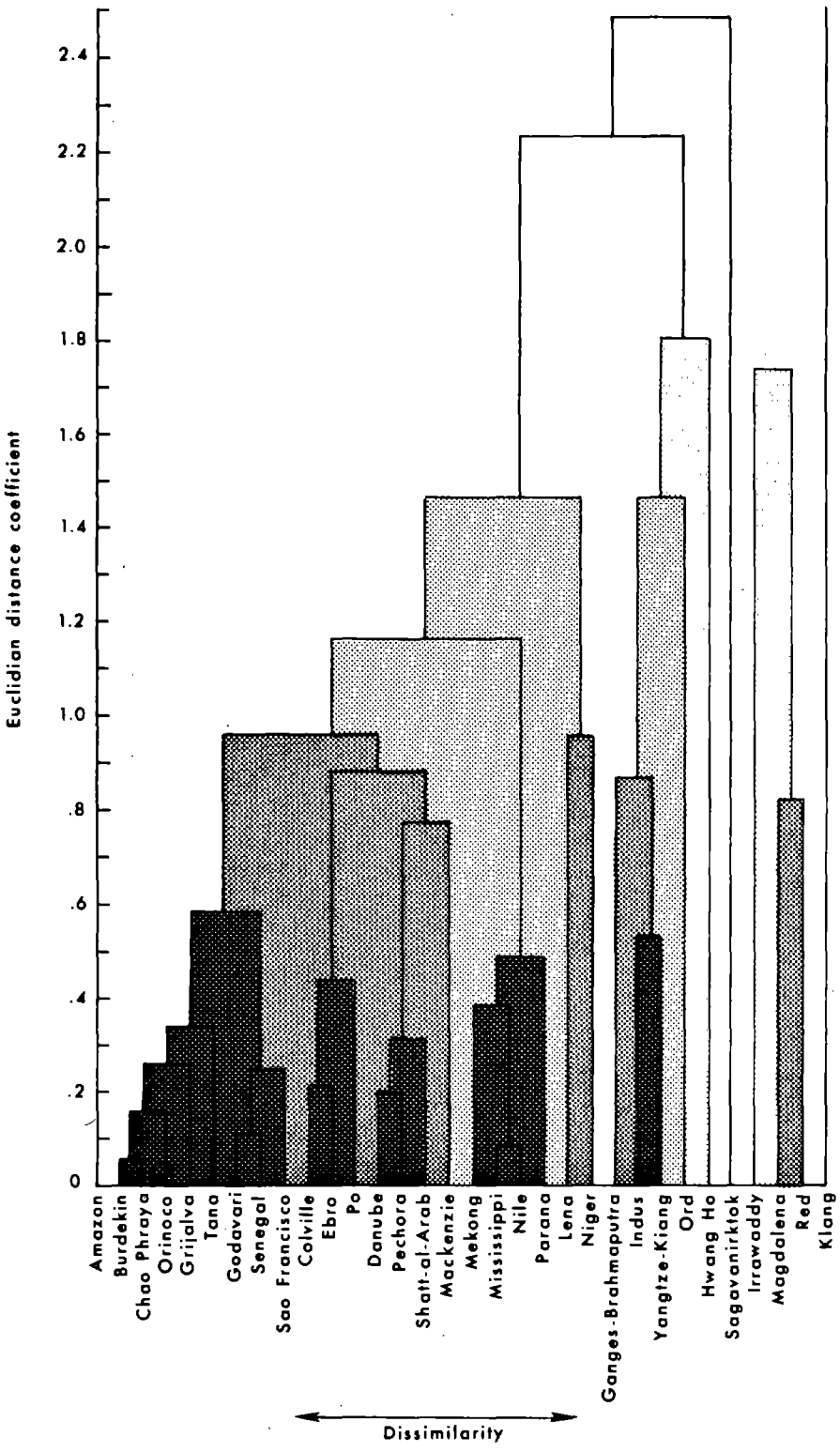

Figure 10. Cluster analysis dendrogram for drainage basins based on combined factor scores.

THE ALLUVIAL VALLEY

Unlike the drainage basin, which functions as a supplier of sediment and water and experiences net erosion, the alluvial valley is approximately a balanced system in which the river flows through its own deposits. Typically, there is neither net erosion nor deposition. It is through this conduit that riverine energy, fluid, and sediment mass, derived from the drainage basin, are transmitted to the delta. Sediment sorting and trading processes, which take place within the alluvial valley, affect the texture of delta sediments. In addition, the discharge regime, which ultimately affects deltaic processes, assumes its salient characteristics and, in a sense, matures within the alluvial valley. From a practical of view, more detailed discharge data are normally available for stations within the alluvial valley.

Separate cluster analyses were performed on two types of alluvial-valley data: (1) landform combinations and (2) discharge regime. Although comparisons on the basis of sediment discharge and texture would have been highly desirable, they were precluded by lack of sufficient data. However, sediment size and abundance are at least crudely implicit in the channel type and alluvial-valley landforms (Coleman and Wright, 1971).

Figure 11 is a dendrogram illustrating the similarities and dissimilarities of 31 alluvial-valley subsystems in terms of the relative abundance of several landforms, together with channel patterns. Five flood-plain features were considered in the landform analysis: river scars, swamps (densely vegetated), lakes, barren flats (including evaporite flats), and sand dunes. Each of these flood-plain features has been defined and illustrated by Coleman and Wright (1971). In addition, the prevalence of meandering or braided channel sections was included, to make a total of seven multistate variables. For purposes of cluster analysis, each of these landforms and channel patterns was treated as a separate variable. For each river system, each landform was assigned a score of 0, 0.33, 0.66, or 1.0, depending on whether the particular landform was absent, rare, common, or abundant, respectively. These scores are relative weightings indicating only the degree to which a landform is prevalent in the alluvial-valley landscape; they do not indicate areal percentages.

The dendrogram indicates that linkages occur over a broad range of distance (d_{jk}) values and, hence, that the variability spectrum of alluvial-valley landscapes is broad. Clusters, in this case, were accepted on the basis of linkages at or below the distance value of $d_{jk} = 0.85$. This criterion yielded seven clusters and three individuals which failed to link at the required level. The degree of segregation between clusters is indicated by the squared-distance coefficients from discriminant analyses, as presented in Table 10. (As was the case with the drainage-basin clusters, these coefficients are calculated directly from observed values rather than from standard scores.) The distance of each individual river valley from each cluster is indicated in Table 10. The distinguishing characteristics of each cluster are illustrated by the mean landform signatures presented in Figure 12. The histograms show the mean relative abundance of each landform type composing the alluvial-valley landscape.

Cluster I is characterized by the prevalence of swamps and braided channels, other features being absent or rare, and is exemplified by the alluvial-valley landscape of the Irrawaddy, as shown in Figure 13. Cluster II consists of only two members, the Magdalena and the Yangtze-Kiang, and is distinguished from cluster I by increases in the prevalence of meandering channel sections and in the abundance of lakes (Fig. 14). River scars, occasional barren flats, and braided channels characterize cluster III. The landscape of the Burdekin River valley of northeastern Australia (Fig. 15) is typical of this type. The alluvial-valley landscape of

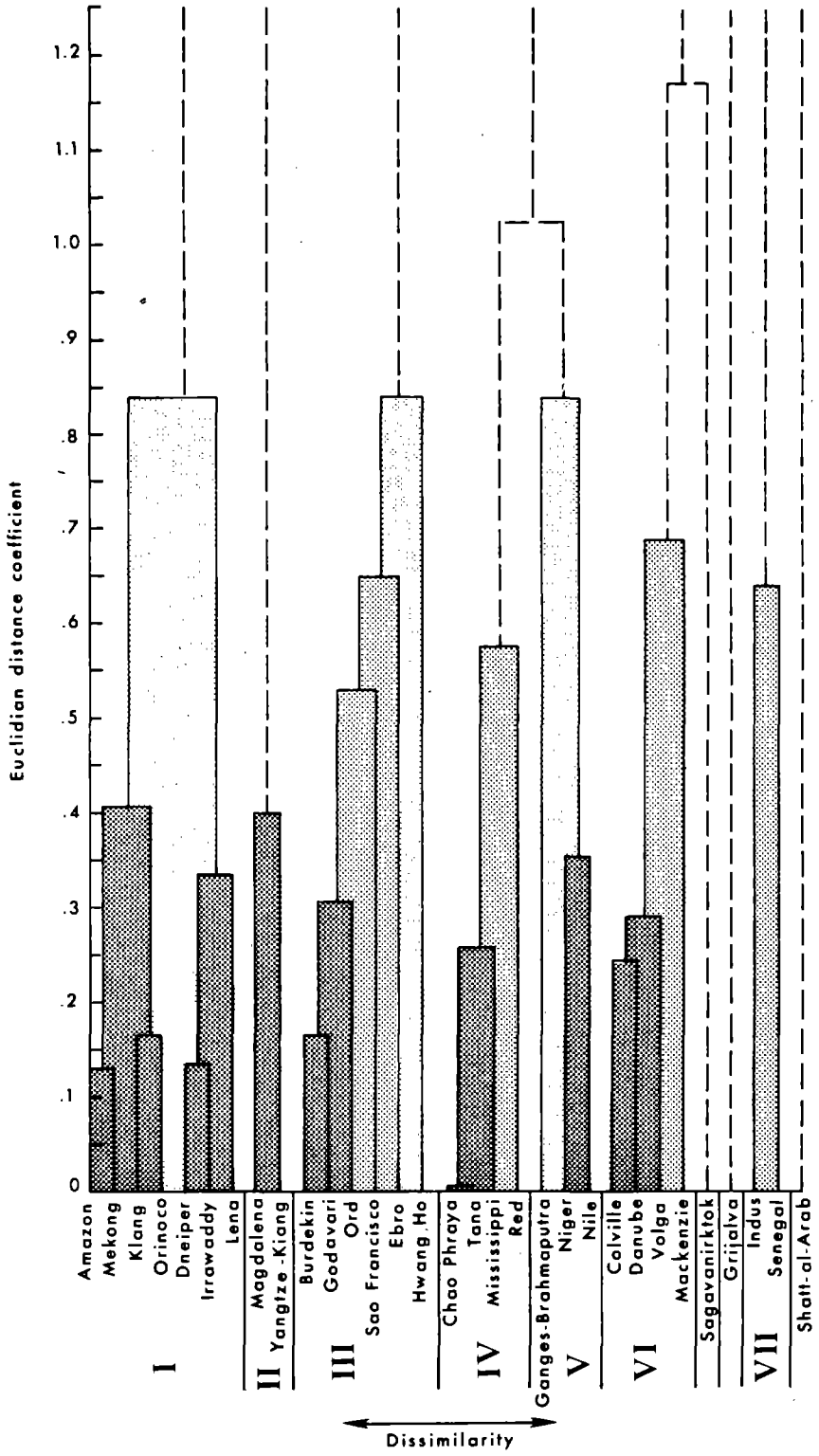

Figure 11. Cluster analysis dendrogram for alluvial-valley landform suites.

Table 10

Alluvial-Valley Landform Suite Discriminant Analysis--d^2 Values

Cluster	I	II	III	IV	V	VI	VII
I	0.00	39.57	80.01	55.50	30.83	101.82	100.41
II	39.57	0.00	131.04	67.32	46.16	59.47	69.18
III	80.01	131.04	0.00	54.31	74.17	179.95	144.60
IV	55.50	67.32	54.31	0.00	28.07	81.84	89.87
V	30.83	46.16	74.17	28.07	0.00	38.45	38.58
VI	101.82	59.47	179.95	81.84	38.45	0.00	25.78
VII	100.41	69.18	144.60	89.87	38.58	25.78	0.00

	Cluster						
Delta	I	II	III	IV	V	VI	VII
Amazon	1.94	51.91	78.81	59.44	31.38	111.81	103.09
Mekong	7.02	66.65	60.55	45.14	25.37	110.66	106.65
Klang	6.05	46.44	83.49	56.17	44.71	121.23	109.86
Orinoco	5.77	46.08	105.98	82.65	47.29	121.87	108.43
Dneiper	3.19	24.72	96.99	62.77	31.77	86.78	92.38
Irrawaddy	4.66	35.85	75.11	44.86	21.15	82.02	92.33
Lena	7.95	41.95	95.74	74.07	51.70	114.93	126.70
Magdalena	33.57	3.75	151.37	81.37	55.32	72.00	83.53
Yangtze-Kiang	53.08	3.75	118.21	60.76	44.49	54.43	62.32
Burdekin	114.40	178.56	5.46	75.98	114.24	237.88	198.48
Godavari	89.18	153.26	3.02	77.52	91.89	213.58	172.12
Ord	71.05	117.69	8.64	46.31	51.90	131.84	99.93
Sao Francisco	65.65	132.82	7.45	54.04	66.26	177.08	159.00
Ebro	94.57	123.56	9.18	56.04	87.06	181.57	152.58
Hwang Ho	89.26	124.41	10.27	59.97	77.69	181.77	129.52
Chao Phraya	73.68	88.45	66.11	2.05	38.48	93.22	102.60
Tana	73.68	88.45	66.11	2.05	38.48	93.22	102.60
Mississippi	49.13	49.61	72.12	4.51	16.28	56.42	70.96
Red	42.31	59.54	29.67	8.18	35.82	101.28	100.11
Ganges-Brahmaputra	34.03	48.54	93.41	41.09	7.24	56.26	59.56
Niger	39.27	48.85	71.21	24.82	4.11	30.03	39.19
Nile	34.23	56.13	72.93	33.34	3.70	44.09	32.03
Colville	122.06	70.76	180.96	102.03	46.29	5.94	21.66
Danube	125.96	75.94	205.96	94.62	52.52	1.95	29.00
Volga	89.19	67.02	176.11	89.46	34.61	4.12	27.92
Mackenzie	90.93	45.01	177.63	62.10	38.23	8.86	45.41
Sagavanirktok	66.05	69.73	117.82	83.88	27.82	25.83	37.03
Grijalva	184.01	152.08	71.19	71.10	141.12	184.93	187.76
Indus	110.05	82.21	139.29	102.49	44.43	39.15	3.10
Senegal	96.96	62.33	156.11	83.44	38.92	18.61	3.10
Shatt-al-Arab	101.04	69.24	124.72	108.22	80.50	110.73	45.14

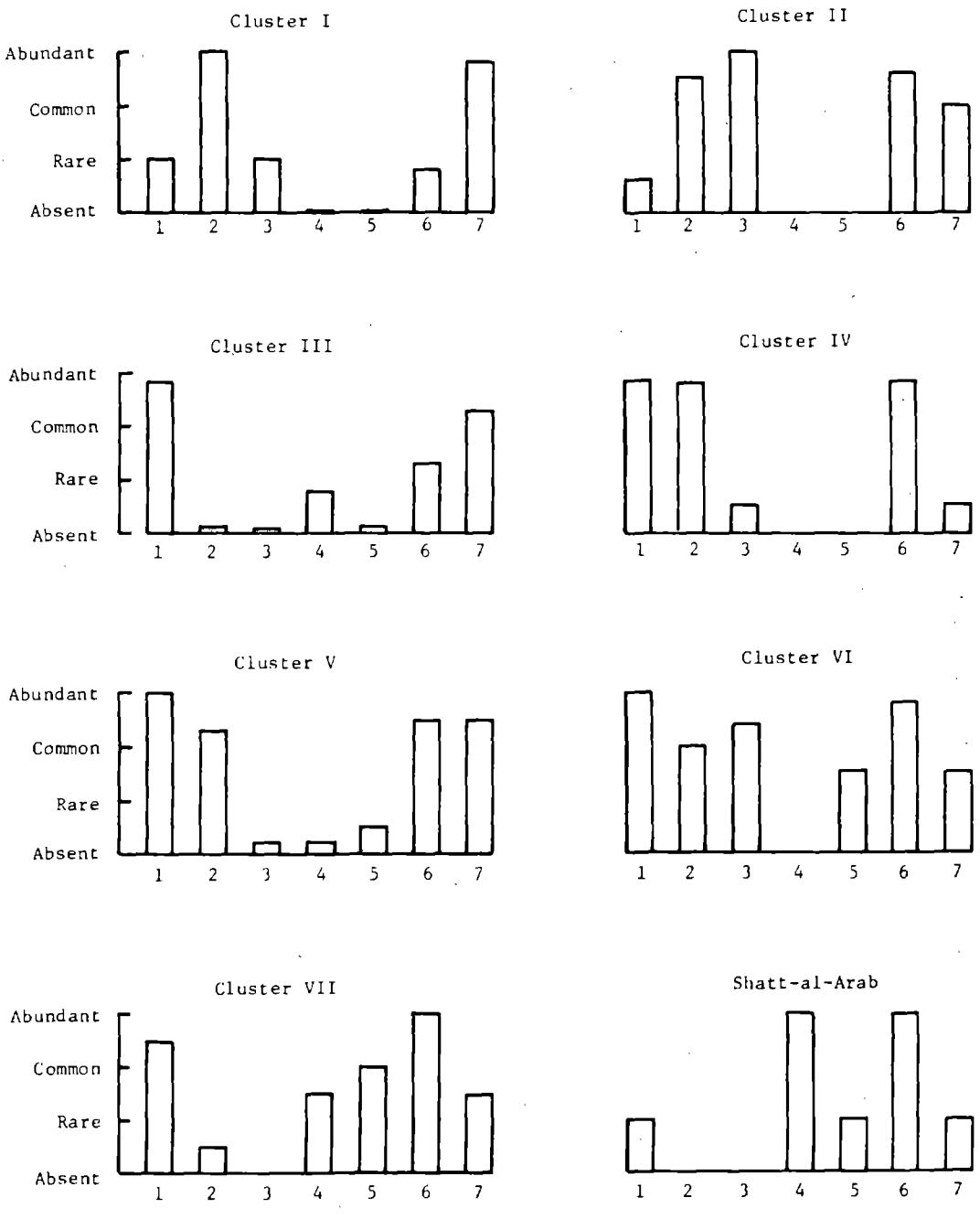

Figure 12. Mean relative abundance of alluvial-valley landforms in each cluster.

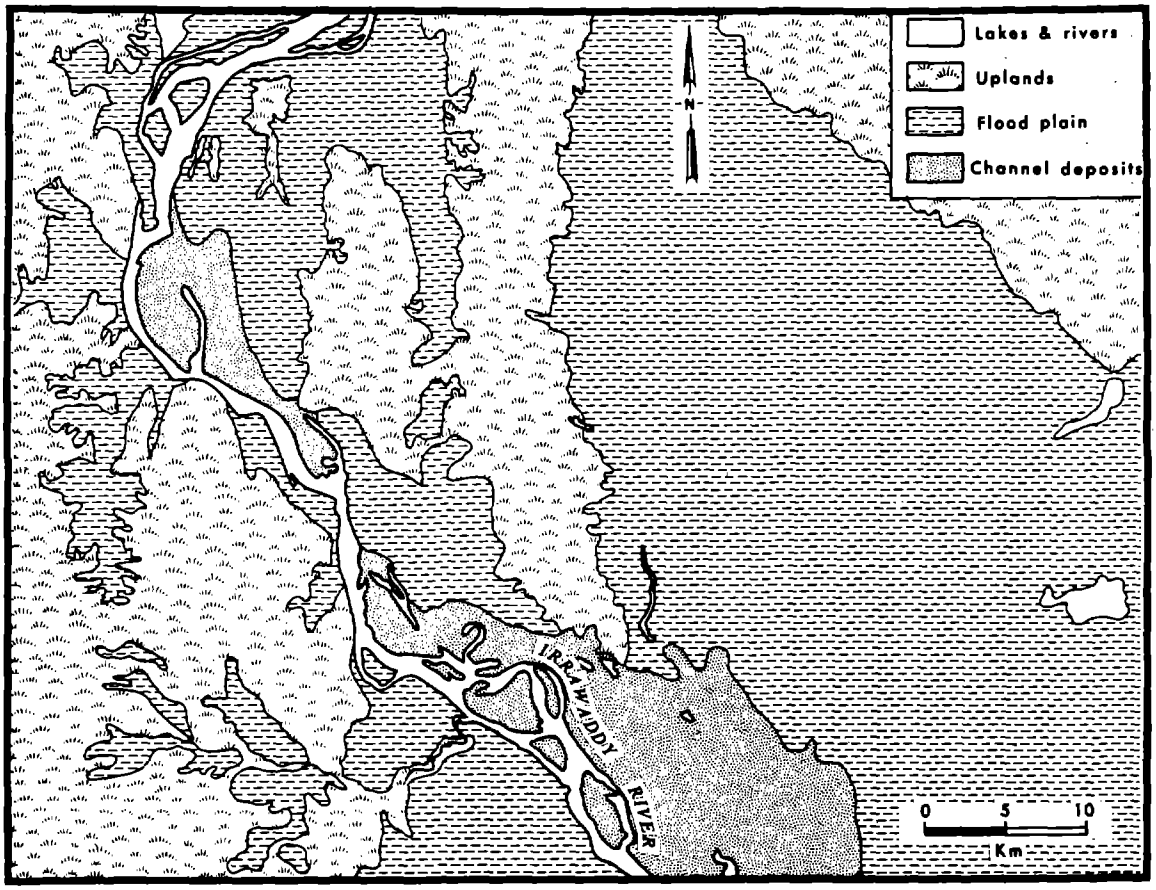

Figure 13. Map of a section of the alluvial valley of the Irrawaddy River.

of the Mississippi (Fig. 16) is representative of cluster IV, which is characterized by a predominantly meandering channel and abundant river scars and swamps. Cluster V consists of the Ganges-Brahmaputra, Niger, and Nile alluvial valleys. River scars, swamps, and marshes are the most abundant features; lakes, barren flats, and dunes are present but are relatively rare. Both meandering and braided channel segments are common. This valley type is illustrated in Figure 17 by the Ganges-Brahmaputra River. All features except barren flats are common in the alluvial valleys of cluster VI. Meandering dominates channel type. All the rivers in this cluster (Colville, Danube, Volga, and Mackenzie) are subject to freezing at least part of the year. Figure 18, showing the alluvial valley of the Mackenzie River, is representative of this type.

Cluster VII is separated from cluster VI by two unique rivers, the Sagavanirktok and the Grijalva. Like the Colville, the Sagavanirktok exhibits abundant river scars, lakes, and dunes but has a primarily braided channel. The Grijalva is distinguished by a completely meandering channel, together with abundant river scars and lakes and an almost total absence of other features. Cluster VII, consisting of the Indus and Senegal, contrasts with other clusters by virtue of an increase in the prevalence of barren flats and dunes and a sparsity of swamps and marshes. Figure 19 shows the alluvial valley of the Senegal.

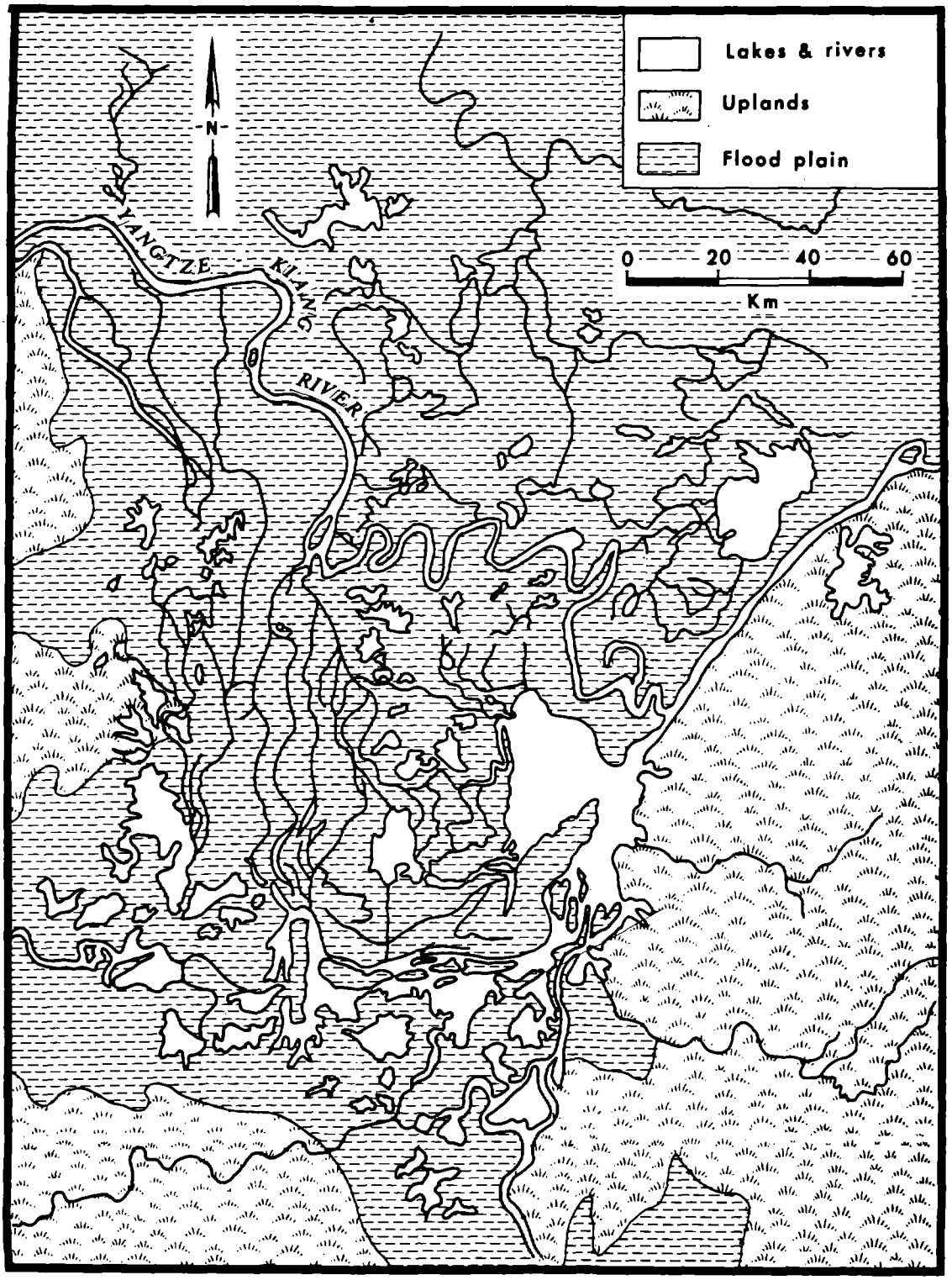

Figure 14. Map of a section of the alluvial valley of the Yangtze-Kiang River showing the meandering channel type and extensive lakes.

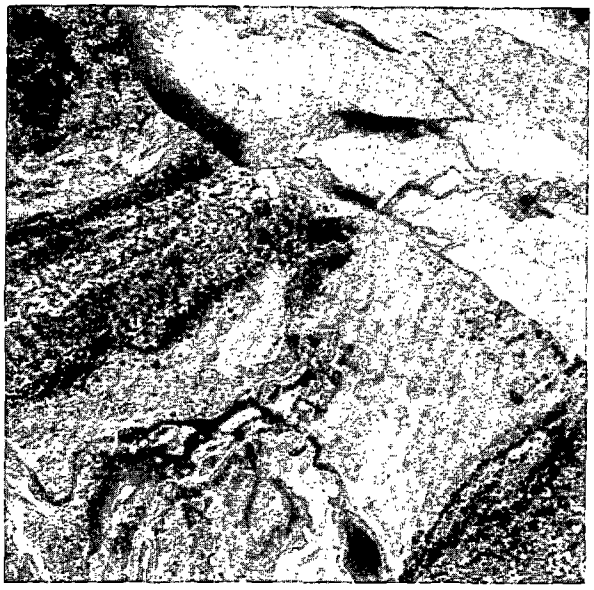

Figure 15. Oblique aerial photograph of a section of the alluvial valley of the Burdekin River showing the braided channel, barren flats, and channel scars typical of this type.

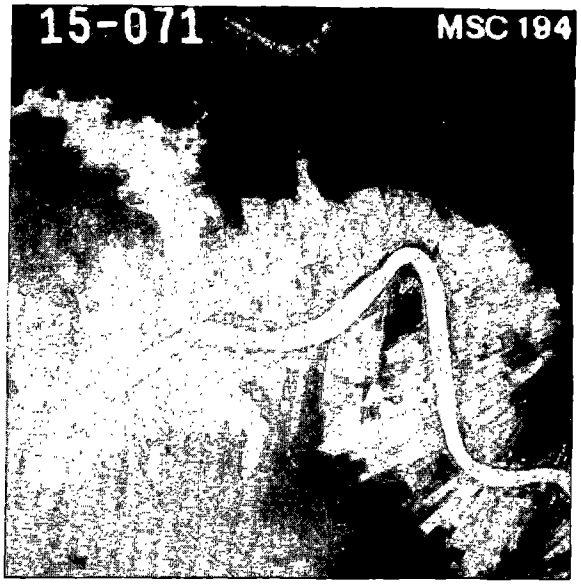

Figure 16. Vertical aerial photograph of the alluvial valley of the lower Mississippi River showing river meanders, natural levees, crevasse splays, and heavily vegetated backswamp.

Figure 17. Oblique aerial photograph of a section of the alluvial valley of the Ganges-Brahmaputra River showing braided channel surrounded by river-scarred flood plain.

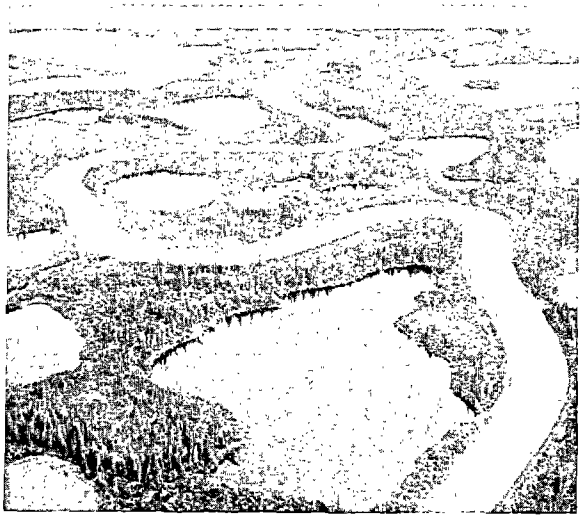

Figure 18. Oblique aerial photograph of a section of the alluvial valley of the Mackenzie River showing a meandering channel flanked by extensive lakes.

Figure 19. Oblique aerial photograph of a section of the alluvial valley of the Senegal River showing barren sand plains and dunes flanking a meandering channel.

The Shatt-al-Arab possesses the most unique alluvial valley; it is characterized by a meandering channel (especially in its lower reaches) and abundant evaporite flats.

Four salient features of the discharge regime were combined in the second set of alluvial valley clusters: mean annual discharge, the annual coefficient of variability for mean monthly discharge (defined as $\sigma_d/\bar{Q}$, where σ_d is the standard deviation of discharge for an average year and $\bar{Q}$ is the mean), total discharge range (the different between maximum and minimum), and the discharge flood peakedness index K_f ($K_f = T_l/T_g$, where T_l is the number of days per average year that discharge is less than the mean and T_g is the number of days that discharge exceeds the mean). The significances of these parameters were discussed previously by Coleman and Wright (1971).

Variations in discharge similarities, based on the values presented in Table 11, are illustrated by the linkage dendrogram shown in Figure 20. The diagram suggests numerous close similarities between discharge regimes; ten linkages occur below the 0.10 distance coefficient. For comparative purposes, clusters were accepted on the basis of linkages occurring below a d_{jk} cutoff value of 0.50. Five relatively discrete clusters and four unique individuals (Amazon, Parana, Ganges-Brahmaputra, and Lena) resulted. The degrees of segregation between the clusters are indicated by Table 12 from the results of discriminant analysis. Clusters I and III are the most similar, whereas clusters II and IV are the most mutually dissimilar. The four unique rivers are separated from all clusters by extremely large distances (Table 12).

The mean discharge characteristics of each cluster are indicated in Table 11. A comparison of the dendrograms for alluvial-valley morphology and discharge regime (Figs. 11 and 20) suggests that, even though there are a few pairs of river systems which are similar to one another in both respects, the two sets of clusters generally

Table 11

Alluvial-Valley Discharge Regime Data

	River	Annual Mean Discharge (m^3/sec)	CV Annual Discharge	Discharge Range (m^3/sec)	Flood Peakedness
	Amazon	149,739.94	0.29	118,469.88	1.06
Cluster I	Burdekin	7,751.60	1.34	24,359.00	2.43
	Godavari	8,159.42	1.40	11,170.00	2.04
	Hwang Ho	2,571.21	1.40	12,753.00	2.04
	Senegal	773.91	1.46	3,450.00	2.30
	Ord	166.31	1.70	7,300.00	2.43
	Mean	2,844.50	1.46	11,806.41	2.25
	CV	0.914	0.863	0.598	0.078
Cluster II	Dneiper	1,370.81	0.61	2,646.00	2.32
	Niger	384.81	0.78	737.21	2.38
	Nile	2,611.71	0.98	7,482.00	2.65
	Shatt-al-Arab	1,965.71	0.79	4,503.00	2.66
	Volga	8,378.33	0.97	23,010.00	3.10
	Mean	2,942.28	0.83	7,675.66	2.62
	CV	0.957	0.166	0.389	0.105
	Parana	11,756.70	0.24	8,260.00	2.17
Cluster III	Chao Phraya	883.00	1.07	2,838.00	1.92
	Red	3,912.80	0.87	2,300.00	1.70
	Irrawaddy	12,564.00	0.92	30,252.00	1.61
	Mekong	10,314.20	0.95	26,380.00	1.55
	Colville	491.01	1.10	1,075.00	1.00
	Mean	5,633.01	0.98	12,569.00	1.56
	CV	0.876	0.090	1.03	0.196
Cluster IV	Danube	5,427.00	0.25	3,788.00	1.52
	Sao Francisco	120.71	0.41	167.21	1.48
	Po	1,481.41	0.22	77.00	1.18
	Ebro	240.51	0.66	416.00	1.05
	Grijalva	1,011.41	0.70	2,175.00	1.40
	Indus	2,070.00	0.83	4,456.00	1.25
	Mackenzie	8,582.50	0.67	17,300.00	1.35
	Tana	171.59	0.57	302.80	1.67
	Mean	2,388.14	0.54	3,585.26	1.36
	CV	1.194	0.386	1.514	0.137
Cluster V	Mississippi	15,814.20	0.46	20,810.00	0.75
	Orinoco	25,067.00	0.57	38,680.00	1.12
	Mean	20,440.59	0.52	29,745.00	0.94
	CV	0.226	0.107	0.300	0.198
	Ganges-Brahmaputra	30,531.99	0.90	76,381.94	1.66
	Lena	11,402.00	1.65	64,319.98	3.56
	Overall Mean	11,052.25	0.85	17,788.24	1.84
	Overall CV	2.47	0.48	1.49	0.36

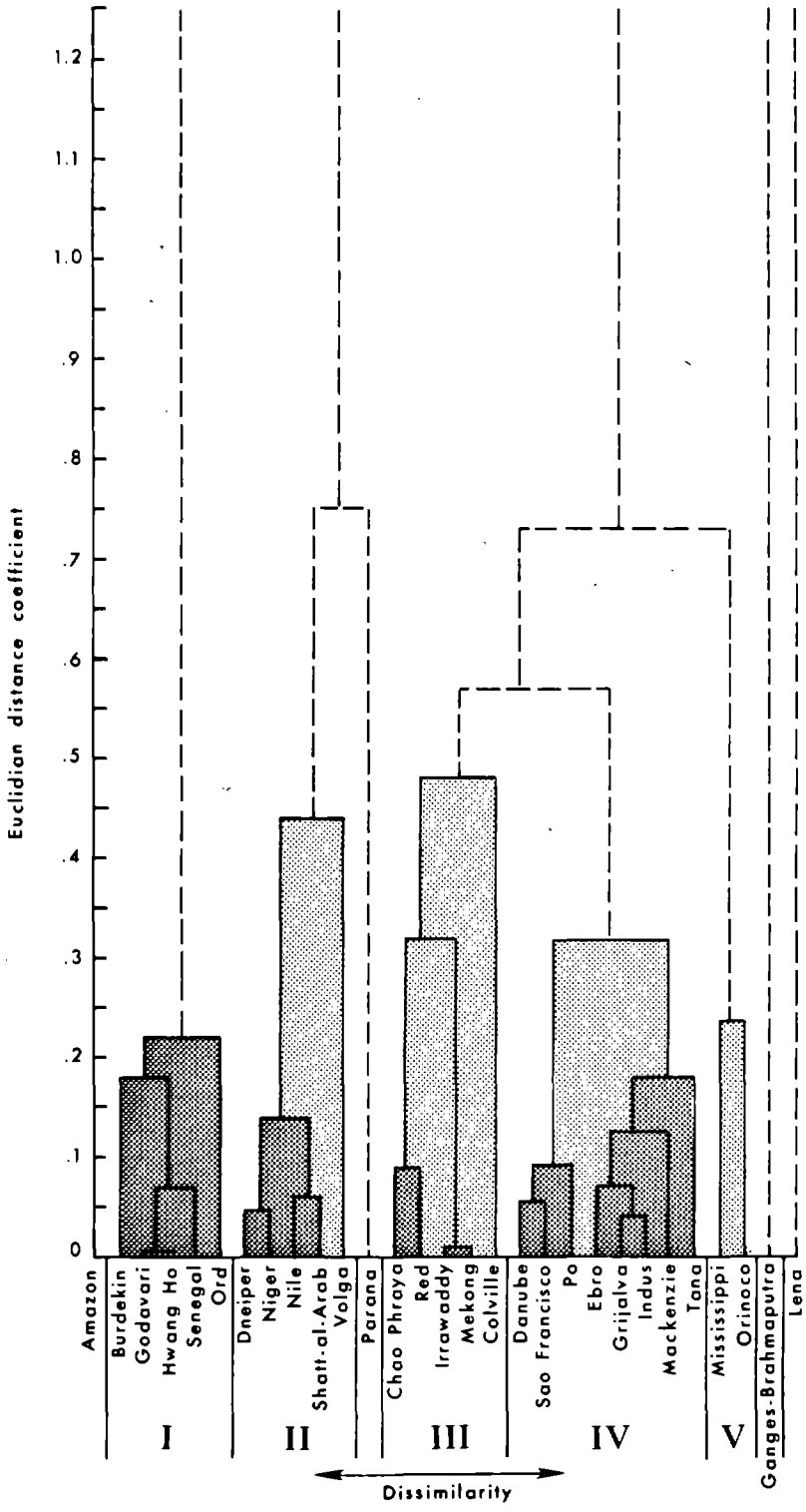

Figure 20. Cluster analysis dendrogram for alluvial valley discharge regimes.

Table 12

Alluvial-Valley Discharge Regime Discriminant Analysis--d^2 Values

Cluster	I	II	III	IV	V
I	0.00	68.66	8.98	27.14	16.55
II	68.66	0.00	81.35	148.51	135.21
III	8.98	81.35	0.00	27.43	38.07
IV	27.14	148.51	27.43	0.00	19.20
V	16.55	135.21	38.07	19.20	0.00

River	Cluster I	II	III	IV	V
Amazon	10,878.48	11,044.53	10,541.50	10,785.03	9,093.30
Burdekin	3.90	14.74	18.50	36.70	140.01
Godavari	1.01	21.59	10.15	30.59	115.42
Hwang Ho	1.40	20.37	13.26	31.04	134.46
Senegal	2.43	20.98	19.24	42.39	128.31
Ord	3.02	29.29	32.57	60.59	168.80
Dneiper	28.21	2.73	24.72	16.80	137.64
Niger	19.43	1.11	22.17	20.02	138.63
Nile	12.93	0.92	25.60	31.26	148.81
Shatt-al-Arab	22.24	0.25	30.40	29.46	152.07
Volga	23.21	5.00	42.83	46.64	175.39
Parana	90.50	62.22	52.74	50.84	48.57
Chao Phraya	6.76	12.02	5.51	14.21	104.44
Red	24.90	28.61	5.92	14.52	55.94
Irrawaddy	25.23	34.99	3.95	13.16	63.69
Mekong	22.27	32.80	3.17	11.22	73.24
Colville	27.99	51.69	5.83	16.17	70.36
Danube	59.72	35.67	20.21	7.08	61.39
Sao Francisco	45.98	24.27	20.09	3.35	114.09
Po	65.52	41.41	24.94	4.14	92.76
Ebro	39.66	39.06	9.17	2.29	83.72
Grijalva	28.13	23.76	5.94	1.06	89.16
Indus	26.57	32.50	2.73	3.66	24.72
Mackenzie	36.80	37.28	4.58	4.73	53.45
Tana	31.66	14.97	13.62	3.13	111.00
Mississippi	121.45	131.69	54.67	61.20	2.60
Orinoco	154.17	170.53	87.85	106.71	2.60
Ganges-Brahmaputra	82.43	98.98	50.12	67.17	82.56
Lena	193.07	189.61	261.58	269.54	554.55

exhibit minimal coincidence. The implication is simply that the composite alluvial-valley landscape is not dependent solely on discharge regime.

The discharge regimes of the Amazon, Ganges-Brahmaputra, and Lena are anomalous in the sense that they are highly dissimilar to each other and to the five types just described. The Amazon and Lena are at opposite ends of the spectrum of discharge regimes. The former is distinguished by its extreme mean annual discharge (world's largest) and low variability and flood peakedness, whereas the latter exhibits extreme variability and flood peakedness. Although the Ganges-Brahmaputra

does not display any extremes, mean annual discharge, discharge coefficient of variability, discharge range, and flood peakedness values are all high.

Relatively short but intense wet seasons cause the rivers of cluster I to be characterized by low mean annual discharge values combined with a high temporal variability (CV) and flood peakedness. This type of discharge regime is represented by the discharge curve of the Burdekin (Fig. 21A). The signature of cluster II is similar in many respects to that of cluster I but exhibits a significant decrease in the discharge variability and a significant increase in flood peakedness. The five rivers in this cluster experience highly seasonal discharge regimes, as in the case of cluster I. The discharge curve of the Niger (Fig. 21B) offers an example of this type of regime. Although the Parana remains isolated at the selected cutoff distance, it is most similar to this cluster, but it has an abnormally low coefficient of variability.

Cluster III is characterized by more moderate discharge variability and flood peakedness and slightly higher mean annual discharge and discharge range. The discharge regime of the Mekong River (Fig. 21C) is the model for this type.

Still further decreases in discharge variability and flood peakedness characterize cluster IV, which is the largest, encompassing eight river systems. The discharge curve of the Indus River (Fig. 21D) best illustrates this type of regime.

The Mississippi and Orinoco compose cluster V. In this case, absolute discharge and discharge range are high, but the coefficient of the variability is low and the flood peakedness index has a value near 1.0, indicating normal flood intensity. The Mississippi is representative (Fig. 21E).

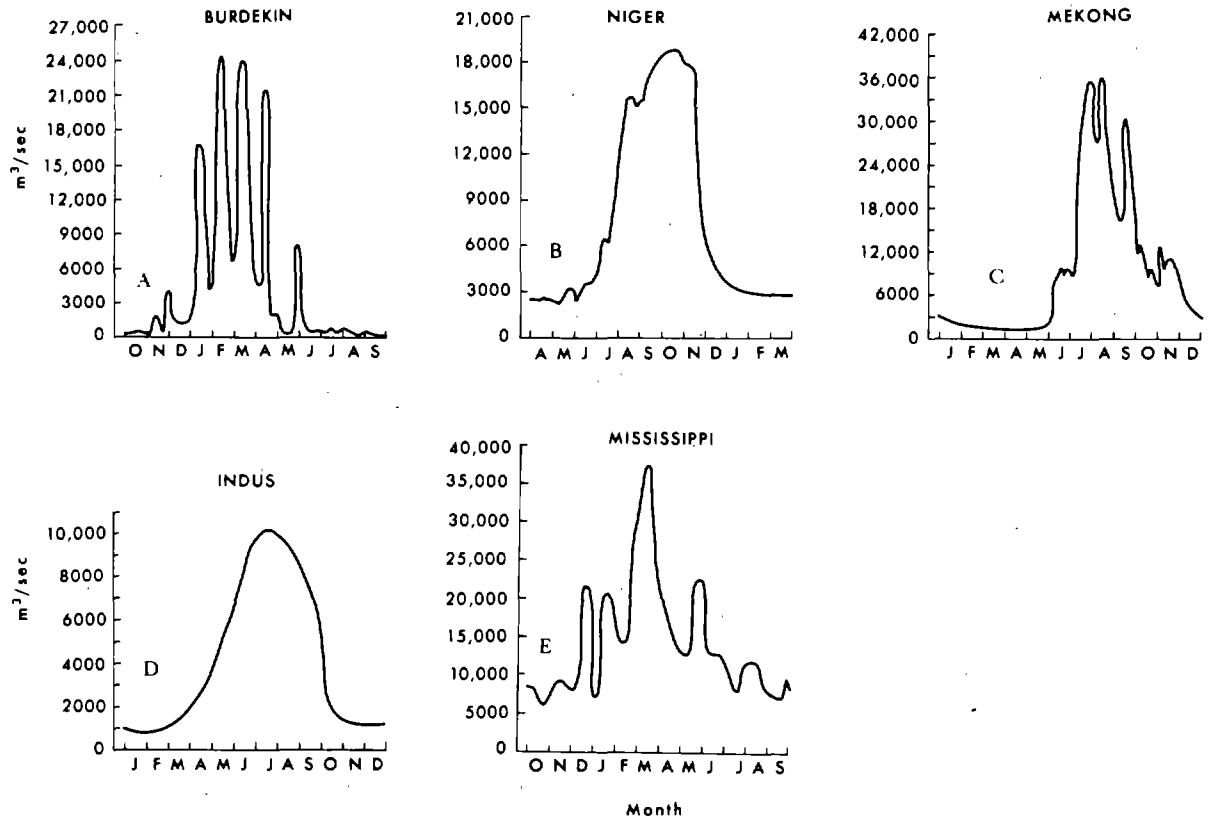

Figure 21. Examples of typical alluvial valley annual discharge curves (based on data for individual years).

THE RECEIVING BASIN

The receiving basin serves as a sink for sediments and energy discharged by the river; however, it is far from passive. In a large number of cases, marine forces play the major roles in molding the delta and determining its landscape and geometry. Of fundamental importance are the wind, wave, and tide regimes of the seas and the subaqueous morphology of the continental shelves fronting the deltas. Hence, receiving basins were compared by means of two cluster sets: one based on subaqueous configurations and the other on deepwater energy regimes.

The slope and shape of the subaqueous profile fronting a delta naturally affect the rate of horizontal sediment accumulation: deltas can prograde faster over flat, shallow shelves than over steep ones. In addition, previously compiled comparisons of deltas and their associated wave-power climates (Wright and Coleman, 1971b, 1972, 1973) have demonstrated that, owing to the effects of refraction and frictional attenuation, wave power which reaches the delta shoreline is as much or more a function of offshore slope as of deepwater wave characteristics. Consequently, one of the receiving-basin cluster sets has been based on the following morphometric parameters: (1) offshore slope between the shoreline and the 20-meter depth contour; (2) offshore slope between the shoreline and the 10-meter contour; and (3) the subaqueous hypsometric integral. The subaqueous hypsometric integral is defined by the relationship

$$H_s = \int_0^{Z_{max}} (A/A_{max})\, d(Z/Z_{max})$$

where A is the area of a contour, A_{max} is the area of the basal contour, Z is the vertical distance of the contour above the basal contour, and Z_{max} is the total vertical distance separating the shoreline from the basal depth, which for this study was taken as 12 meters. As in the case of the basin, hypsometric integral values greater than 0.5 indicate convexity, values less than 0.5 indicate concavity, and 0.5 indicates a linear slope.

The results of cluster analysis based on these three offshore profile descriptors are illustrated by the dendrogram shown in Figure 22, and cluster central tendencies and overall means for all deltas are indicated in Table 13. Corresponding d^2 values from discriminant analysis are presented in Table 14. Linkages at distance coefficients less than 0.4 yield four clusters and five unique individual deltas.

The eight deltas of cluster I are fronted by very gentle but moderately concave-upward offshore slopes. The bathymetry of the nearshore zone of the Amazon Delta (Fig. 23) illustrates this type.

Cluster II is characterized by extremely low-gradient, linear to slightly convex offshore slopes such as those of the Mississippi (Fig. 24) or Ganges-Brahmaputra (Fig. 25). This group includes 33 percent of the deltas examined. The writers have shown previously that this type of bathymetry is most effective in attenuating incident wave energy (Wright and Coleman, 1972, 1973). Nearly linear offshore slopes and above-average steepnesses front the three deltas of cluster III, of which the Danube (Fig. 26) is an example.

The four members of cluster IV are mutually very similar, linking at distances less than 0.025. Extremely gentle and convex profiles are the distinguishing characteristics. The broad, shallow subaqueous zone of the Klang (Fig. 27) is typical.

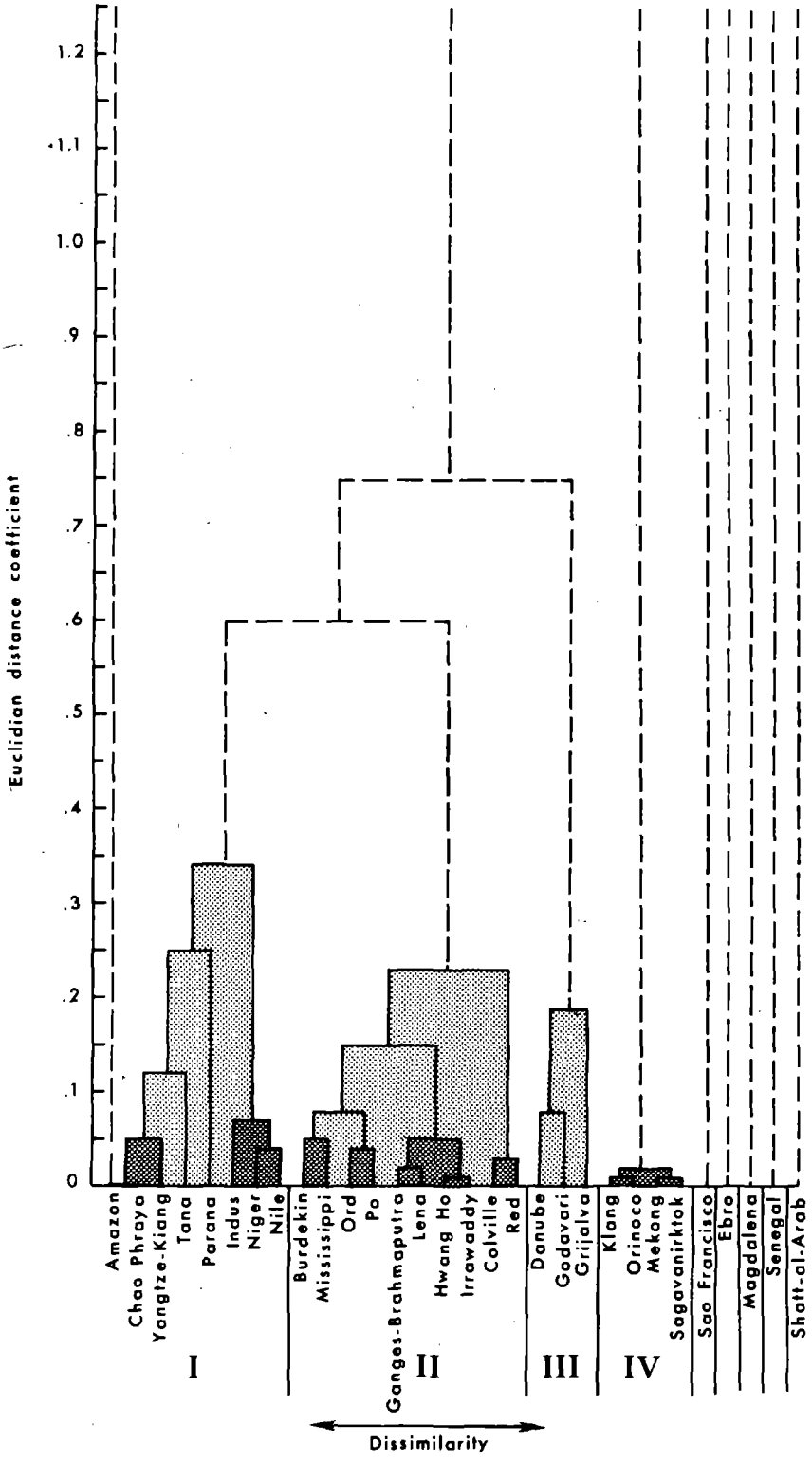

Figure 22. Cluster analysis dendrogram for receiving-basin morphology.

Table 13

Receiving-Basin Morphology Data

	River	Slope, 10 m (degrees)	Slope, 20 m (degrees)	Hypsometric Integral
Cluster I	Amazon	0.0041	0.0051	0.4100
	Chao Phraya	0.0041	0.0061	0.4170
	Yangtze-Kiang	0.0111	0.0131	0.4480
	Tana	0.0710	0.0321	0.4250
	Parana	0.0031	0.0031	0.3501
	Indus	0.0960	0.0960	0.3961
	Niger	0.0660	0.0620	0.3601
	Nile	0.1030	0.0730	0.3701
	Mean	0.0448	0.0338	0.3970
	CV	0.9129	0.9311	0.0864
Cluster II	Burdekin	0.0451	0.0920	0.5040
	Mississippi	0.0740	0.0700	0.4840
	Ord	0.0451	0.0391	0.4840
	Po	0.0331	0.0561	0.4540
	Ganges-Brahmaputra	0.0111	0.0151	0.4950
	Lena	0.0151	0.0081	0.4720
	Hwang Ho	0.0261	0.0151	0.5090
	Irrawaddy	0.0211	0.0411	0.6290
	Colville	0.0380	0.0211	0.5470
	Red	0.0481	0.0371	0.5690
	Mean	0.0357	0.0368	0.5147
	CV	0.4986	0.7228	0.1023
Cluster III	Danube	0.1520	0.1410	0.5050
	Godavari	0.1270	0.1280	0.4630
	Grijalva	0.1940	0.0740	0.5000
	Mean	0.1577	0.1144	0.4894
	CV	0.7759	0.2544	0.0384
Cluster IV	Klang	0.0301	0.0411	0.6290
	Orinoco	0.0231	0.0281	0.6270
	Mekong	0.0351	0.0431	0.6410
	Sagavanirktok	0.0331	0.0351	0.6530
	Mean	0.0303	0.0368	0.6375
	CV	0.1518	0.1603	0.0165
	Sao Francisco	0.1870	0.1120	0.3101
	Ebro	0.3050	0.3600	0.4990
	Magdalena	0.4690	0.3690	0.3671
	Senegal	0.4790	0.1700	0.2601
	Shatt-al-Arab	0.1000	0.4700	0.4980
	Overall Mean	0.0949	0.0876	0.4722
	Overall CV	1.2803	1.2934	0.2210

Table 14

Receiving-Basin Morphology Discriminant Analysis--d^2 Values

Cluster	I	II	III	IV
I	0.00	13.10	25.61	65.31
II	13.10	0.00	16.62	19.95
III	25.61	16.62	0.00	40.07
IV	65.31	19.95	40.07	0.00

River	I	II	III	IV
Amazon	1.99	12.36	36.09	61.65
Chao Phraya	2.16	10.76	34.60	57.86
Yangtze-Kiang	3.83	4.79	27.21	42.37
Tana	2.06	10.97	16.81	57.32
Po	5.01	29.82	52.90	97.01
Indus	4.49	15.01	13.70	63.91
Niger	1.85	22.51	28.70	84.01
Nile	4.38	24.26	20.60	84.12
Burdekin	23.56	4.95	19.04	18.71
Mississippi	10.37	2.16	8.03	27.80
Ord	8.50	0.59	14.32	26.78
Parana	6.34	2.75	19.31	34.84
Ganges-Brahmaputra	11.38	0.92	24.06	24.37
Lena	6.48	2.59	24.30	33.99
Hwang-Ho	13.20	0.55	19.85	20.95
Irrawaddy	17.29	0.80	21.68	16.52
Colville	23.49	2.04	18.67	11.33
Red	32.36	4.64	18.91	6.18
Danube	33.46	17.32	2.48	32.45
Godavari	18.59	12.00	3.27	39.34
Grijalva	39.34	35.10	8.81	62.98
Klang	61.90	18.06	38.12	0.09
Orinoco	58.99	16.55	38.47	0.26
Mekong	68.02	21.48	40.37	0.07
Sagavanirktok	73.02	24.37	43.98	0.26
Sao Francisco	30.50	66.75	39.44	145.58
Ebro	151.31	129.84	73.51	130.77
Magdalena	209.02	224.55	121.83	275.18
Senegal	273.13	337.16	230.10	444.64
Shatt-al-Arab	364.34	309.11	308.22	282.03

The offshore slopes of the remaining five deltas exhibit gradients which exceed the average by varying degrees and hypsometric integrals which range from linear to strongly concave. Of these five deltas, the offshore zone of the Senegal Delta deserves special mention because it represents the extreme in terms of its steep nearshore (0-10 meter) gradient and pronounced profile concavity. The bathymetry and average subaqueous profile of the Senegal are shown in Figure 28. This type of profile is more typical of barrier coasts than of deltas. Because this profile is very ineffective in attenuating wave energy, the waves which operate on the Senegal Delta shoreline are exceptionally powerful (Wright and Coleman, 1972, 1973).

The subaqueous configurations just described are important to deltaic process

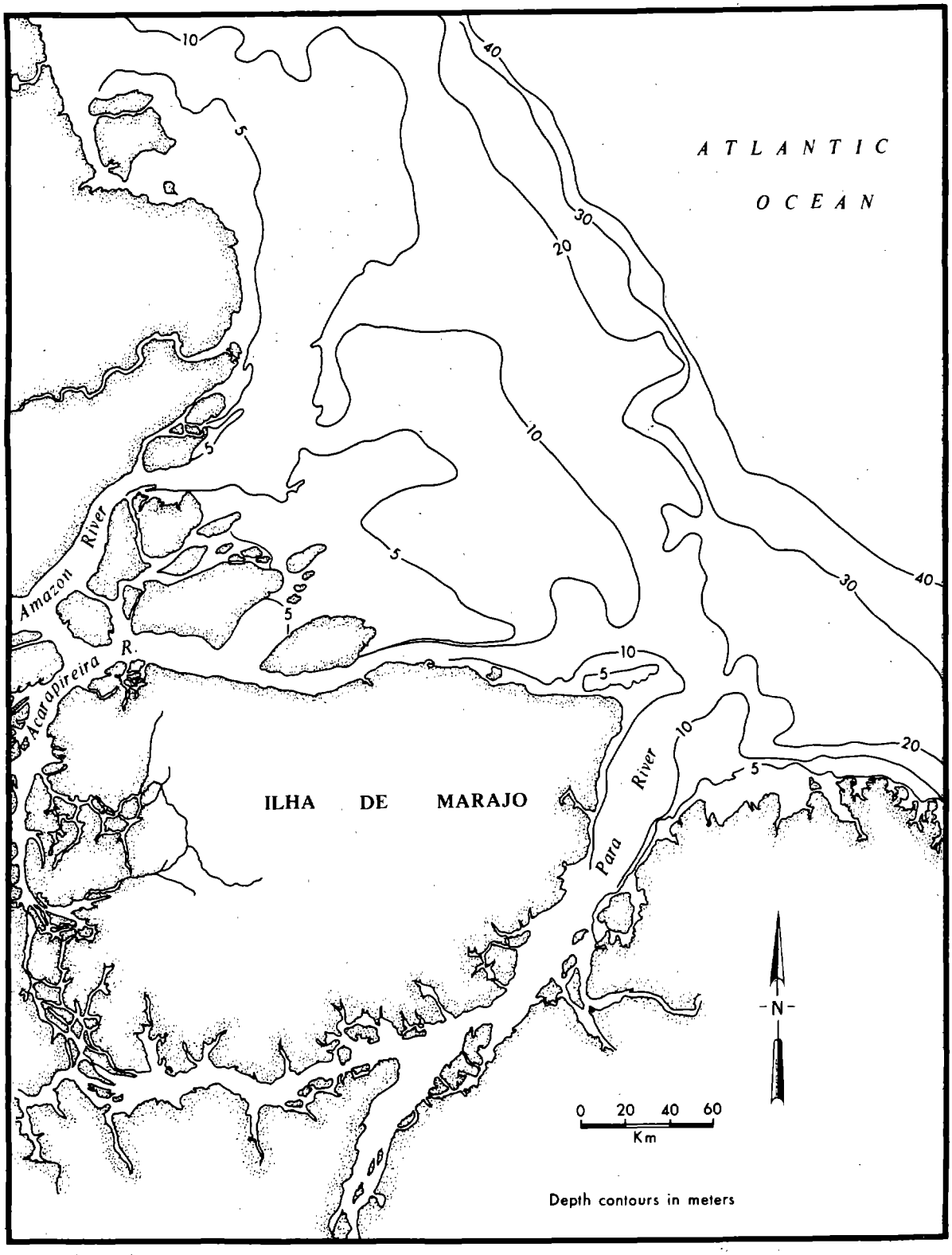

Figure 23. Bathymetric chart of the Amazon Delta.

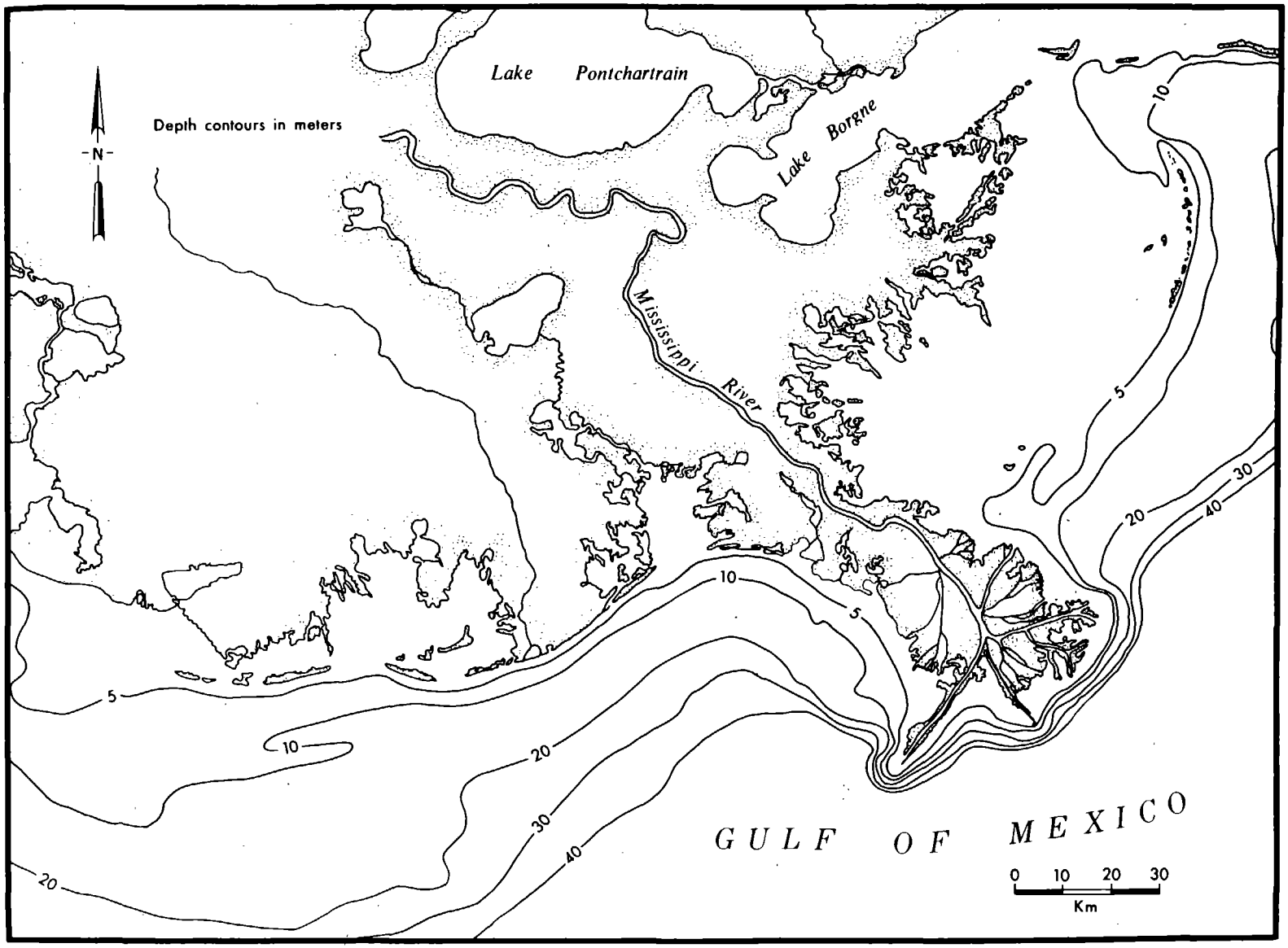

Figure 24. Bathymetric chart of the Mississippi Delta.

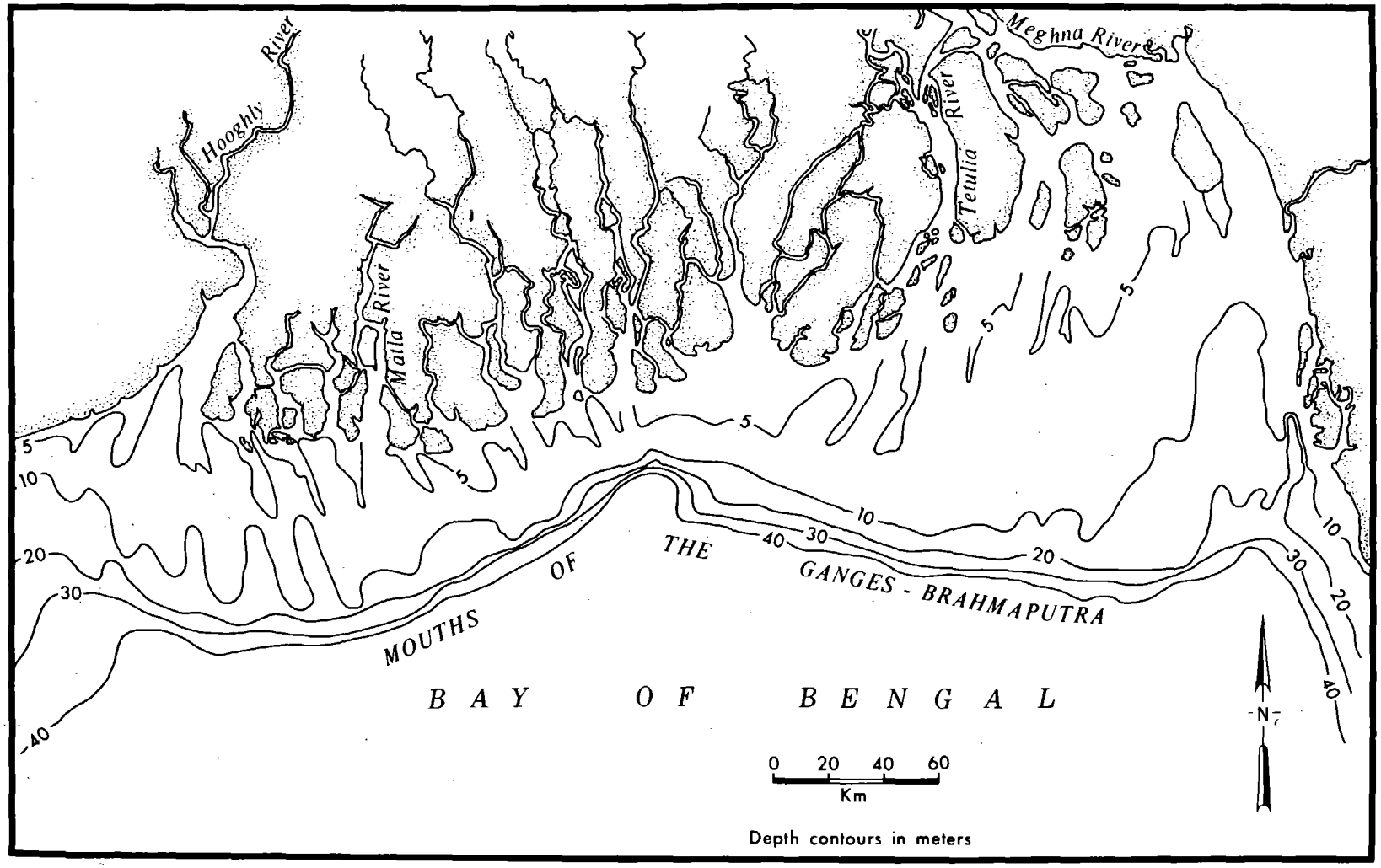

Figure 25. Bathymetric chart of the Ganges-Brahmaputra Delta.

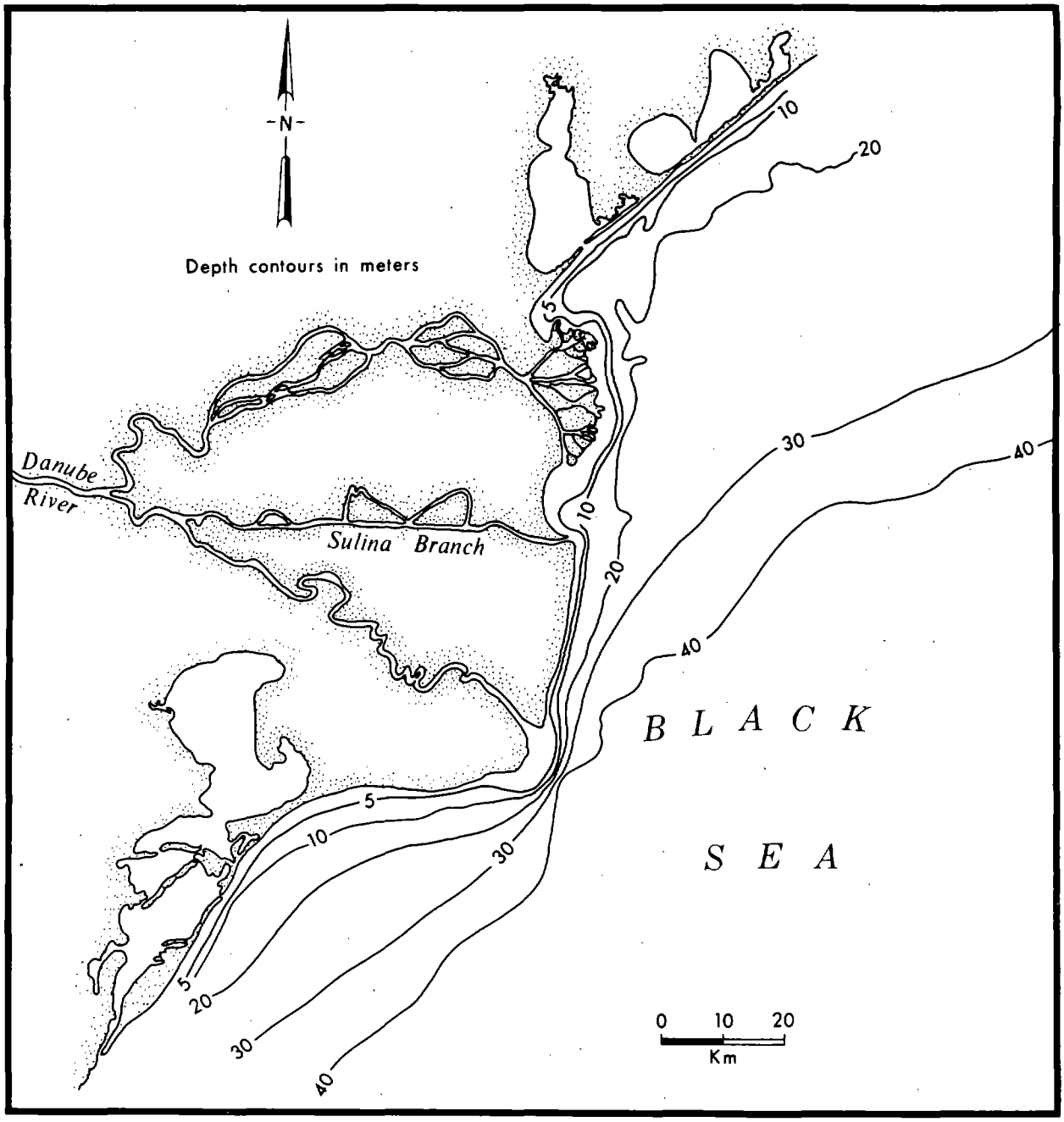

Figure 26. Bathymetric chart of the Danube Delta.

regimes because of their roles in modifying the forces which remold riverborne sediments. The magnitudes of the marine forces prior to their modification are also fundamental, even though it has been demonstrated that it is the nearshore wave climate, after modification, which controls the delta form (Wright and Coleman, 1972, 1973). The wave, tide, and wind regimes of the receiving basin are primary agents which oppose riverine forces and contribute to the morphologic development of the delta. Comparisons of the similarities between receiving-basin deepwater energy

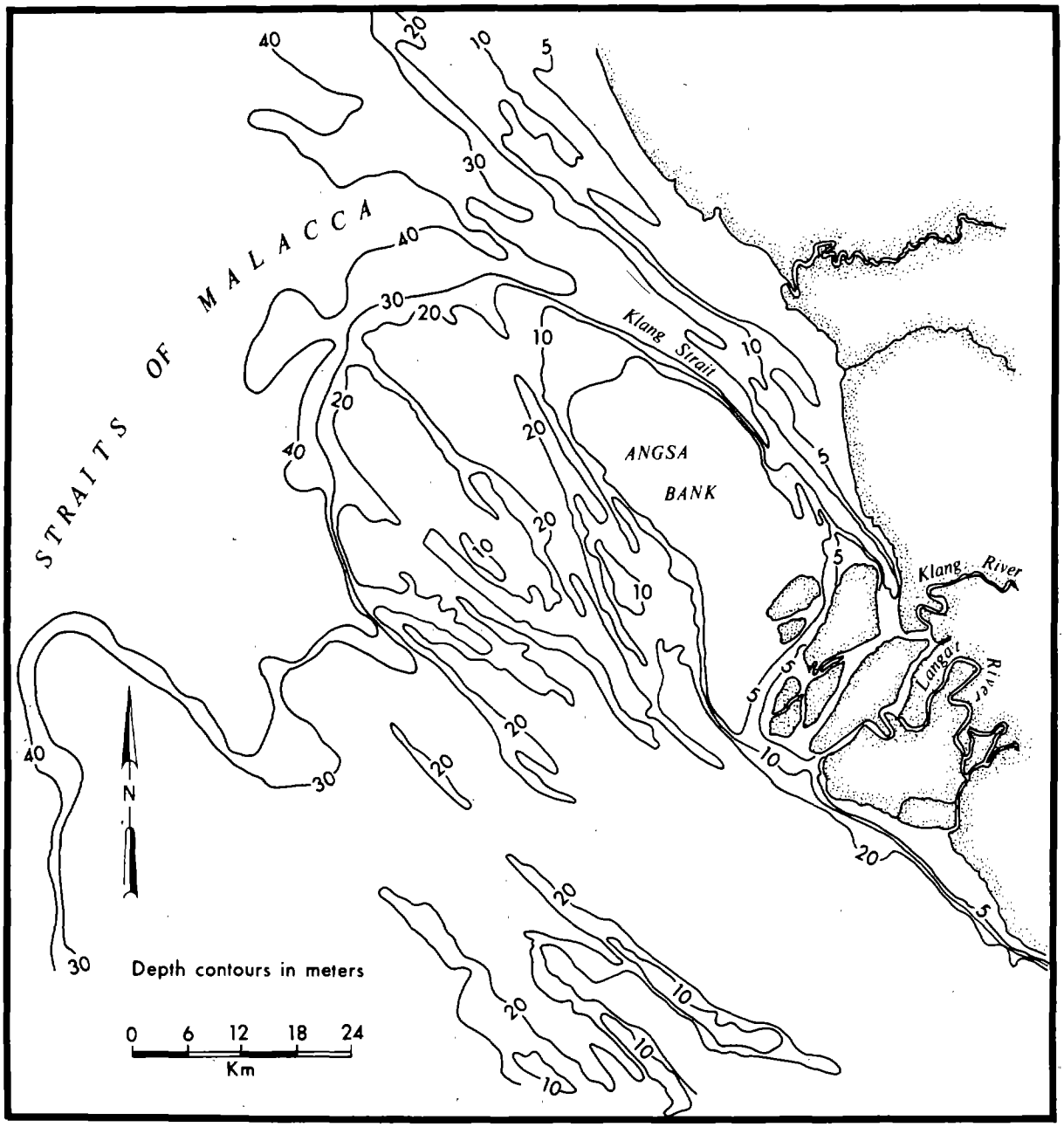

Figure 27. Bathymetric chart of the Klang Delta.

regimes were based on the following parameters: (1) annual root-mean-square significant wave height $\left(\sqrt{\bar{H}_{sig}^{2}}\right)$; (2) mean annual significant wave period ($\bar{T}_{sig}$); (3) mean annual spring tide range; (4) the ratio F_{al}/F_{on} of the mean annual frequency of alongshore winds to onshore winds; and (5) the ratio F_{off}/F_{on} of the mean annual frequency (F_{off}) of offshore winds to onshore winds.

Cluster analysis results for receiving-basin energy regime (Fig. 29) reveal

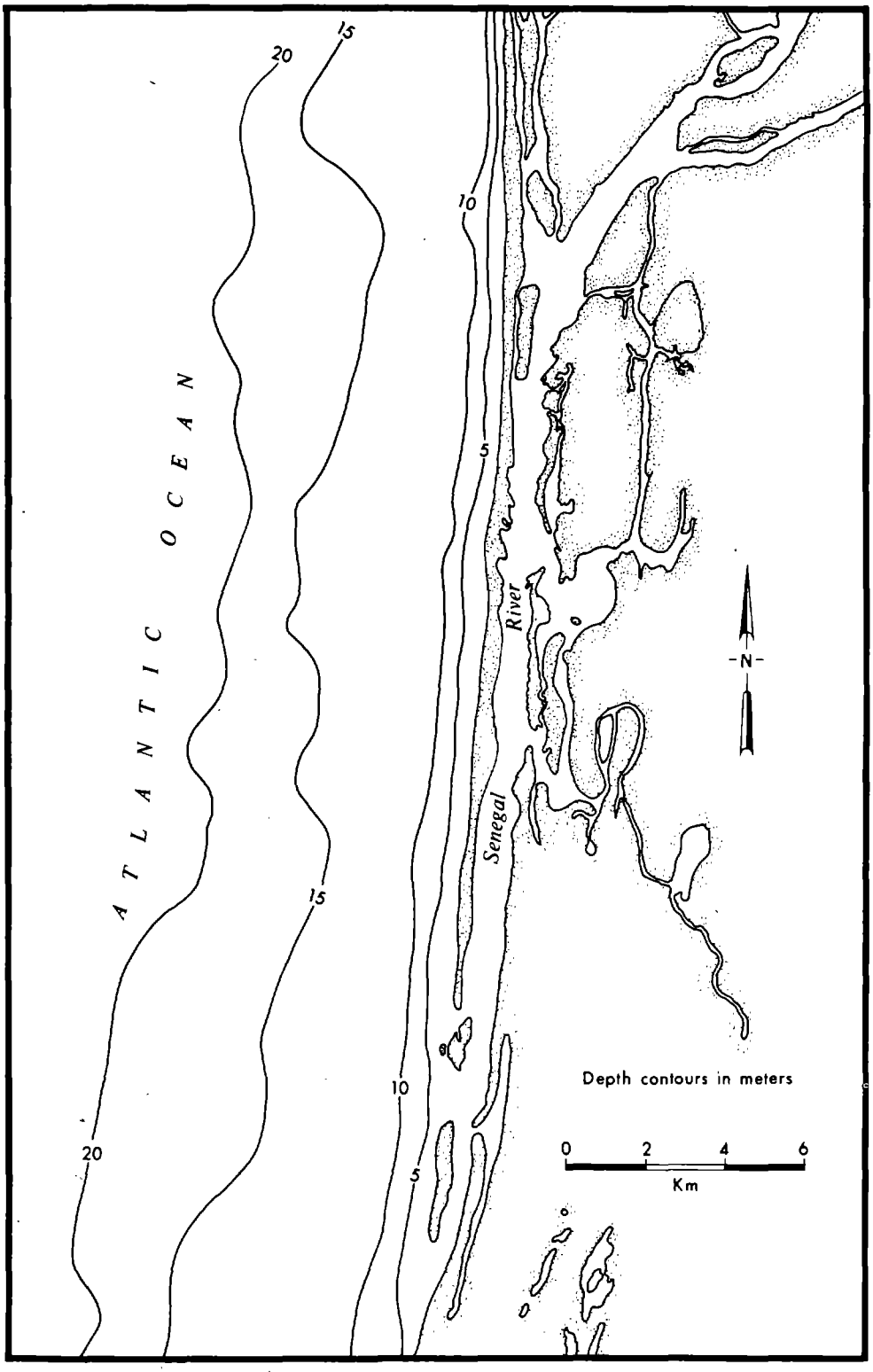

Figure 28. Bathymetric chart of the Senegal Delta.

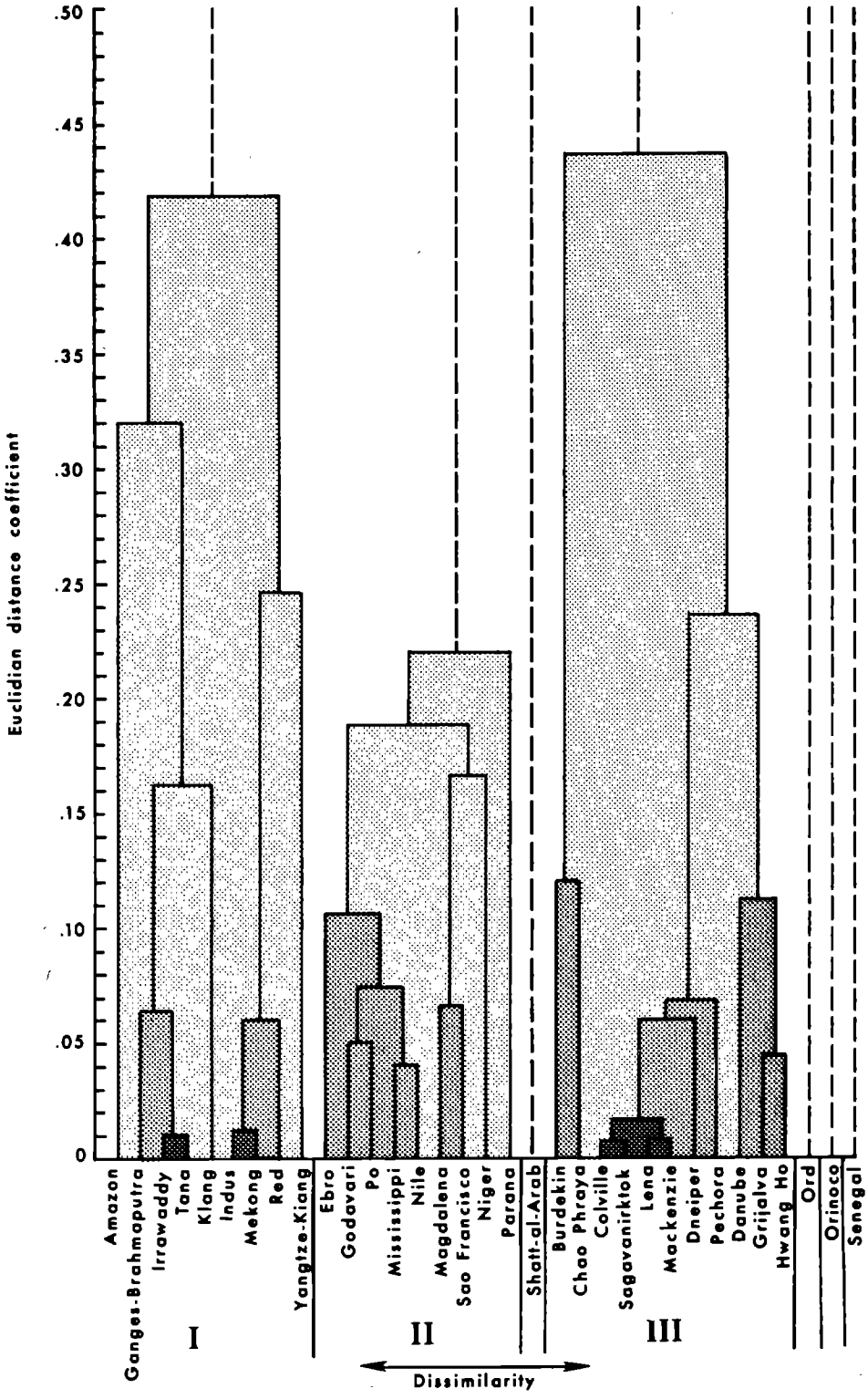

Figure 29. Cluster analysis dendrogram for receiving basins based on deepwater energy parameters.

three large and internally variable clusters and four individuals occurring below the 0.45 similarity level. Table 15 indicates the characteristics of each delta and cluster. Discriminant analysis results for these clusters are presented in Table 16.

The receiving basins into which the nine deltas of cluster I debouch are characterized by mesotidal ranges (mean tide range for this group is 3.23 meters), predominantly onshore winds, and moderate wave energy. The receiving basins fronting the Indus and Mekong have energy regimes of this type. Cluster II is distinguished from cluster I by a microtidal environment; tidal ranges average less than 1 meter for the cluster. The energy regime which affects the Mississippi Delta is typical of this type. The third cluster exhibits both low tide range and low wave energy. Most of the deltas experiencing this regime are situated in enclosed or semienclosed seas (such as the Danube in the Black Sea) or in arctic environments, where there is no wave activity for a large part of the year.

Various extreme receiving-basin energy regimes, as indicated by Table 15, are responsible for the isolation of the four remaining deltas. Two of these, the Ord and the Senegal, deserve special mention. The Ord Delta of western Australia experiences a macrotidal environment and a tropical monsoon climate, with associated seasonal reversals of wind direction, and is fronted by the shallow, partially protected Timor Sea. Consequently, spring tide range is near 6 meters, offshore and alongshore winds are more common than onshore winds, and waves normally tend to be low and short. In contrast to the Ord, the Senegal River debouches into the Atlantic Ocean in an area where tide range is only slightly greater than 1 meter, wave energy is high, and prevailing winds are directed alongshore from the north.

Because of the close coupling between the receiving-basin energy regime and the morphology of the nearshore bottom, an attempt was made to compare receiving basins in terms of the combination of morphology and energy. As in the case of the drainage basins, this was done by first performing factor analyses on original data and clustering on the resultant factor scores. Factor analyses were performed on each of the two data sets (morphology and energy regime); the results are presented in Table 17. The three morphologic variables reduce to one factor (Table 17), whereas two factors are required to explain a sufficient fraction of the variance in energy parameters. Appreciable percentages of the variance of all five parameters are contained in both factors; however, factor 1 receives the heaviest loadings from tide range and wave dimensions, but the two wind parameters make the greatest contribution to factor 2. Tide range contributes the least to both factors.

Cluster analysis on the scores of the three factors indicated six clusters and three individuals resulting from linkages at d_{jk} values of 0.25 or less (Fig. 30). The central tendencies of each cluster are presented in Table 18.

THE DELTA PLAIN

The three subsystems just described all contribute to the production of the delta plain. The geometry, landforms, and environments of the delta plain and delta shoreline result from accumulation of sediments dispersed by the river and the reworking of these sediments by marine forces. Delta morphology reflects the totality of hydrologic regime, sediment load, geologic structure and tectonic stability, climate and vegetation, tides, winds, waves, density contrasts, coastal currents, and numerous spatiotemporal interactions of all these factors. As a consequence of spatial variations in magnitudes and intensities of these factors, deltaic responses vary in terms of absolute dimensions, relative proportions of various delta components (see Coleman and Wright, 1971), distributary patterns and forms of river mouths,

Table 15

Marine Energy Regime Data

	River	Spring Tide Range (m)	Winds Longshore Onshore	Winds Offshore Onshore	RMS Wave Height (m)	$\bar{T}$ (sec^{-1})
	Amazon	4.93	0.81	0.08	1.62	4.93
	Ganges-Brahmaputra	3.63	0.56	0.76	1.42	4.60
	Irrawaddy	2.71	0.55	0.79	1.42	4.60
	Tana	2.93	0.02	0.42	1.38	4.57
Cluster	Klang	4.15	0.38	0.52	1.24	3.85
I	Indus	2.62	0.88	1.15	1.84	5.16
	Mekong	2.59	0.22	0.87	1.92	5.34
	Red	1.86	0.10	0.49	1.92	5.34
	Yangtze-Kiang	3.66	0.85	2.39	2.14	5.64
	Mean	3.23	0.48	0.83	1.65	4.89
	CV	0.28	0.63	0.75	0.18	0.11
	Ebro	0.00	0.25	2.50	1.53	4.52
	Godavari	1.19	0.90	1.04	1.42	4.60
	Po	0.73	0.70	2.30	1.53	4.52
	Mississippi	0.43	0.60	0.58	1.27	4.12
Cluster	Nile	0.43	0.70	0.30	1.53	4.52
II	Magdalena	1.10	1.60	0.13	1.62	5.18
	Sao Francisco	1.86	1.06	0.07	1.49	5.18
	Niger	1.43	0.20	0.03	1.11	4.44
	Parana	0.64	0.00	0.92	1.89	5.48
	Mean	0.87	0.67	0.87	1.49	4.74
	CV	0.63	0.69	1.01	1.14	0.08
	Shatt-al-Arab	2.53	1.25	4.50	0.99	3.15
	Burdekin	2.23	1.00	0.58	0.59	1.50
	Chao Phraya	2.38	0.32	0.68	0.23	0.57
	Colville	0.21	0.92	0.71	0.07	0.07
	Sagavanirktok	0.21	0.49	0.07	0.07	0.07
	Lena	0.21	0.13	0.95	0.24	0.42
Cluster	Mackenzie	0.34	0.40	1.20	0.15	0.28
III	Dneiper	0.00	2.10	1.62	0.23	0.33
	Pechora	0.73	1.25	0.36	0.30	0.63
	Danube	0.00	0.35	1.18	0.51	1.63
	Grijalva	0.79	1.82	1.73	0.64	1.64
	Hwang Ho	1.13	0.38	0.38	0.58	1.52
	Mean	0.75	0.83	0.86	0.33	0.79
	CV	1.08	0.75	0.59	0.62	0.78
	Ord	5.85	2.54	2.00	0.78	2.47
	Orinoco	1.77	14.00	20.00	1.19	4.56
	Senegal	1.22	21.70	10.70	1.61	5.54
	Overall Mean	1.71	1.78	1.87	1.10	3.36
	Overall CV	0.86	2.36	1.98	0.58	0.58

Table 16

Marine Energy Regime Discriminant Analysis--d^2 Values

Cluster	I	II	III
I	0.00	14.35	69.54
II	14.35	0.00	72.61
III	69.54	72.61	0.00

River	I	II	III
Amazon	5.08	32.37	81.92
Ganges-Brahmaputra	1.97	14.53	71.31
Irrawaddy	2.97	6.60	67.85
Tana	3.31	9.92	72.55
Klang	5.63	29.51	51.89
Indus	1.67	11.75	69.73
Mekong	2.41	15.68	77.74
Red	6.31	13.06	77.40
Yangtze-Kiang	8.02	33.17	92.85
Ebro	22.55	6.81	73.09
Godavari	13.24	0.58	68.88
Po	15.23	4.83	65.48
Mississippi	19.73	1.32	61.44
Nile	17.27	4.45	58.54
Magdalena	23.11	5.69	86.46
Sao Francisco	18.37	4.28	96.68
Niger	25.45	6.61	92.85
Parana	14.37	5.50	90.16
Shatt-al-Arab	53.84	58.58	80.93
Burdekin	49.10	64.81	4.81
Chao Phraya	70.14	90.68	6.73
Colville	95.70	94.40	2.22
Sagavanirktok	96.68	97.29	3.89
Lena	82.02	85.23	2.49
Mackenzie	83.62	85.50	1.86
Dneiper	105.00	99.25	8.93
Pechora	82.80	85.86	2.14
Danube	47.39	38.10	8.87
Grijalva	56.37	54.34	6.99
Hwang Ho	48.57	55.67	3.48
Ord	58.47	94.04	62.29
Orinoco	1,728.10	1,653.09	1,774.14
Senegal	1,977.40	1,869.39	1,954.81

Table 17

Factor Analysis of Receiving Basins

Variable	Morphology: Mean	Morphology: Standard Deviation	Correlation Matrix: Slope, 10 m	Correlation Matrix: Slope, 20 m	Correlation Matrix: Hypsometric Integral	Factor Matrix: Unrotated
Slope, 10 m (degrees)	0.0949	0.12	1.00	0.68	-0.46	0.67
Slope, 20 m (degrees)	0.0876	0.12	0.68	1.00	-0.17	0.59
Hypsometric Integral	0.47	0.10	-0.46	-0.17	1.00	-0.45

Factor	1	2	3
Eigenvalue	1.90	0.84	0.26

Variable No.	Variable	Marine Energy Regime: Mean	Marine Energy Regime: Std. Deviation	Correlation Matrix: 1	2	3	4	5	Factor Matrices: Unrotated Factor 1	Factor 2
1.	Tide (m)	1.71	1.50	1.00	-0.02	-0.01	0.36	0.36	0.31	-0.30
2.	Winds, Longshore/Onshore	1.78	4.29	-0.02	1.00	0.83	0.11	0.20	0.34	0.62
3.	Winds, Offshore/Onshore	1.87	3.78	-0.01	0.83	1.00	0.10	0.18	0.33	0.62
4.	Root-Mean-Square Wave Height (m)	1.10	0.63	0.36	0.11	0.10	1.00	0.98	0.57	-0.31
5.	Wave Period (sec^{-1})	3.36	1.98	0.36	0.20	0.18	0.98	1.00	0.60	-0.24

Factor	1	2	3	4	5
Eigenvalue	2.33	1.71	0.77	0.17	0.02

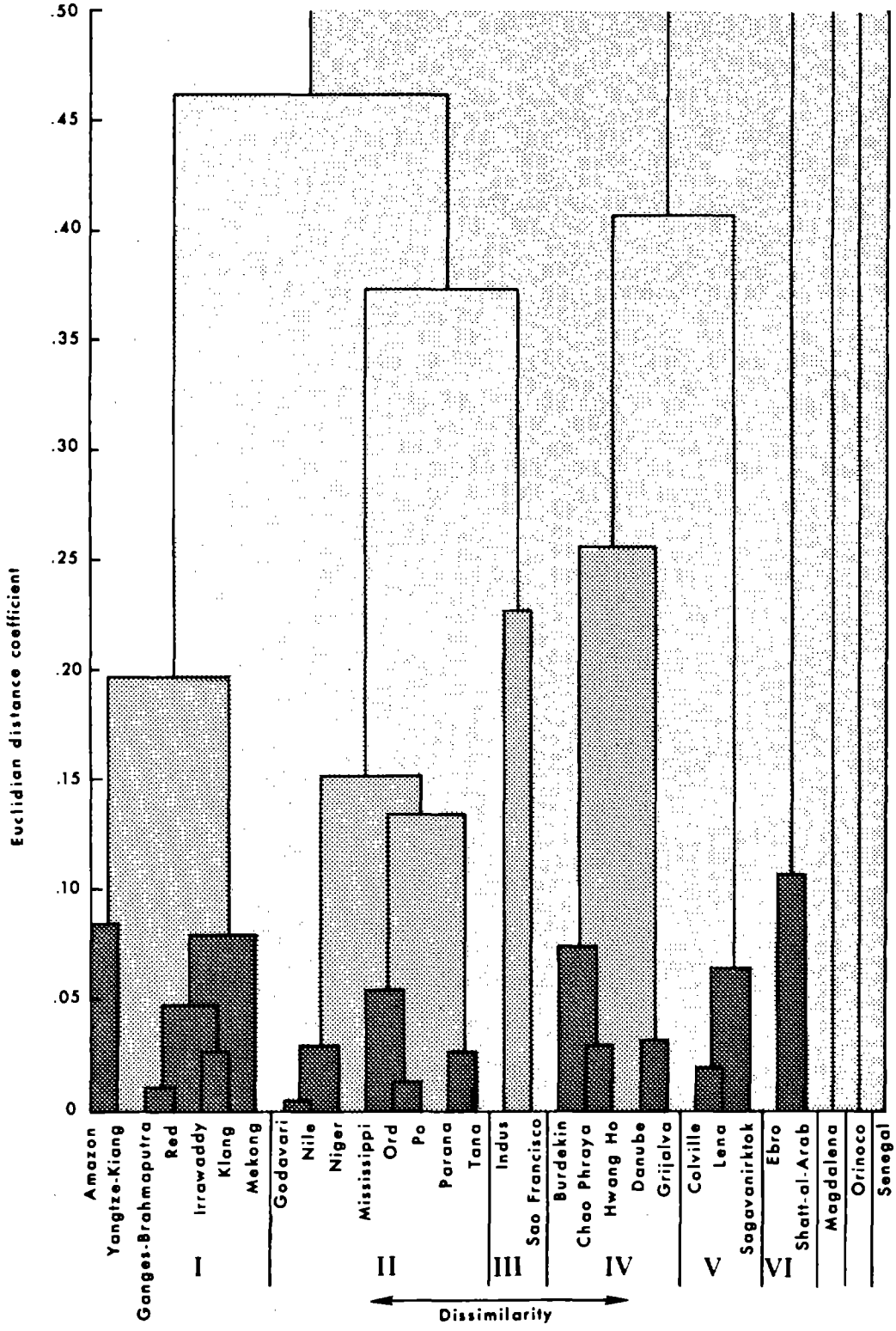

Figure 30. Cluster analysis dendrogram for receiving basins based on combined factor scores.

Table 18

Central Tendencies of Receiving Basin Composite Clusters

	Slope, 10 m		Slope, 20 m		Hypsometric Integral		Spring Tide Range	
Cluster	Mean	CV	Mean	CV	Mean	CV	Mean	CV
I	0.023	0.681	0.028	0.577	0.546	0.174	3.37	0.31
II	0.051	0.664	0.058	0.631	0.424	0.133	1.70	1.09
III	0.142	0.455	0.104	0.109	0.353	0.172	2.24	0.24
IV	0.049	1.202	0.066	0.854	0.487	0.081	1.31	0.77
V	0.029	0.420	0.024	0.556	0.557	0.163	0.21	0.00
VI	0.203	0.716	0.415	0.187	0.499	0.001	1.27	1.41

	Winds Longshore/Onshore		Winds Offshore/Onshore		Root-Mean-Square Wave Height		Period	
Cluster	Mean	CV	Mean	CV	Mean	CV	Mean	CV
I	0.50	0.57	0.84	0.87	1.67	1.99	4.90	0.12
II	0.71	1.15	0.95	0.86	1.36	0.24	4.35	0.19
III	0.97	0.13	0.61	1.25	1.67	1.49	5.17	0.00
IV	0.77	0.84	0.91	0.60	0.51	0.31	1.37	0.33
V	0.51	0.77	0.58	0.79	0.13	0.77	0.19	1.08
VI	0.75	0.94	3.50	0.40	1.26	0.30	3.84	0.25

landform suites of interdistributary areas, and dimensionless geometry of the delta. Morphology similarities and dissimilarities between deltas are subjects of this section. The following section will deal with some of the more salient process-form interactions responsible for these likenesses and contrasts. Differences in total area of the delta plain are among the more obvious delta variations. In Table 19 each delta is listed in order of size from largest to smallest, together with its total area in square kilometers. The Amazon Delta is the largest, with a total area of 467,078 km^2, and the Ebro is the smallest, with an area of 624 km^2. Among the deltas listed, the Mississippi ranks eighth in size. The area mean and standard deviation for the deltas considered are 34,000 km^2 and 8,306 km^2, respectively.

Although total area is an important aspect of absolute delta variability, it conveys minimal information relevant to delta environments or the processes of delta development. The dimensionless ratios between the various components of the delta are probably somewhat more meaningful because they are, at least indirectly, functions of the relative magnitudes of several processes, as discussed by Coleman and Wright (1971). Cluster analyses were performed for the three ratios A_u/A_l, $A_{subaerial}/A_{subaqueous}$, and $A_{abandoned}/A_{active}$, indexing respectively the ratios of the area of the upper delta plain (above the position of tidal inundation) to that of the lower delta plain (the subaerial delta below the position of tidal inundation), the area of the subaerial portion of the delta relative to that of the subaqueous delta, and the area of the abandoned portion of the subaerial delta relative to the area of the active subaerial delta.

Table 19

Total Area (km^2) of Delta Plain

Amazon	467,078	Niger	19,135	Ord	3,896
Ganges-Brahmaputra	105,641	Shatt-al-Arab	18,497	Tana	3,659
Mekong	93,781	Grijalva	17,028	Danube	2,740
Yangtze-Kiang	66,669	Po	13,398	Burdekin	2,112
Lena	43,563	Nile	12,512	Klang	1,817
Hwang Ho	36,272	Red	11,903	Magdalena	1,689
Indus	29,524	Chao Phraya	11,329	Colville	1,687
Mississippi	28,568	Mackenzie	8,506	Sagavanirktok	1,178
Volga	27,224	Godavari	6,322	Sao Francisco	734
Orinoco	20,642	Parana	5,440	Ebro	624
Irrawaddy	20,571	Senegal	4,254		

The dendrogram (Fig. 31) shows numerous linkages at very low distance levels, indicating the existence of close similarities. Acceptance of clusters on the basis of linkages at or below distance coefficients of 0.10 results in only four clusters and four individual deltas. The values of the three ratios for each delta and the means and coefficients of variability for clusters are presented in Table 20. The between-cluster distance-squared coefficients and the distance-squared values for each delta from the discriminant analyses are given in Table 21.

Cluster I is distinguished by high values for the ratios $A_{subaerial}/A_{subaqueous}$ and $A_{abandoned}/A_{active}$, combined with a normal value for the ratio A_u/A_l. The delta component pattern of the Indus Delta (Fig. 32) is typical of this type.

Moderate values for all three ratios characterize cluster II. This cluster contains fifteen (47 percent) of the deltas included in the cluster analysis, suggesting that this pattern is the most common. The delta component patterns of the Irrawaddy (Fig. 33) exemplify this type.

The Mississippi Delta (Fig. 34) illustrates the delta component relationships of cluster III, which is characterized by relatively greater predominance of subaerial and abandoned delta portions. The discriminant analysis results (Table 21) suggest that this type is transitional between types I and II.

Cluster IV contains only two deltas, the Danube (Fig. 35) and the Po, both of which are situated in tideless seas. This type is highly distinct from the other three clusters owing to very high values for the ratios A_u/A_l and $A_{subaerial}/A_{subaqueous}$ Extreme values for one or more of the three ratios (Table 20) are responsible for the isolation of the remaining deltas.

Many of the differences in delta shape are describable in terms of several macroscale morphometric parameters.

Delta Morphometry

Overall delta shape is a major distinguishing characteristic between individual

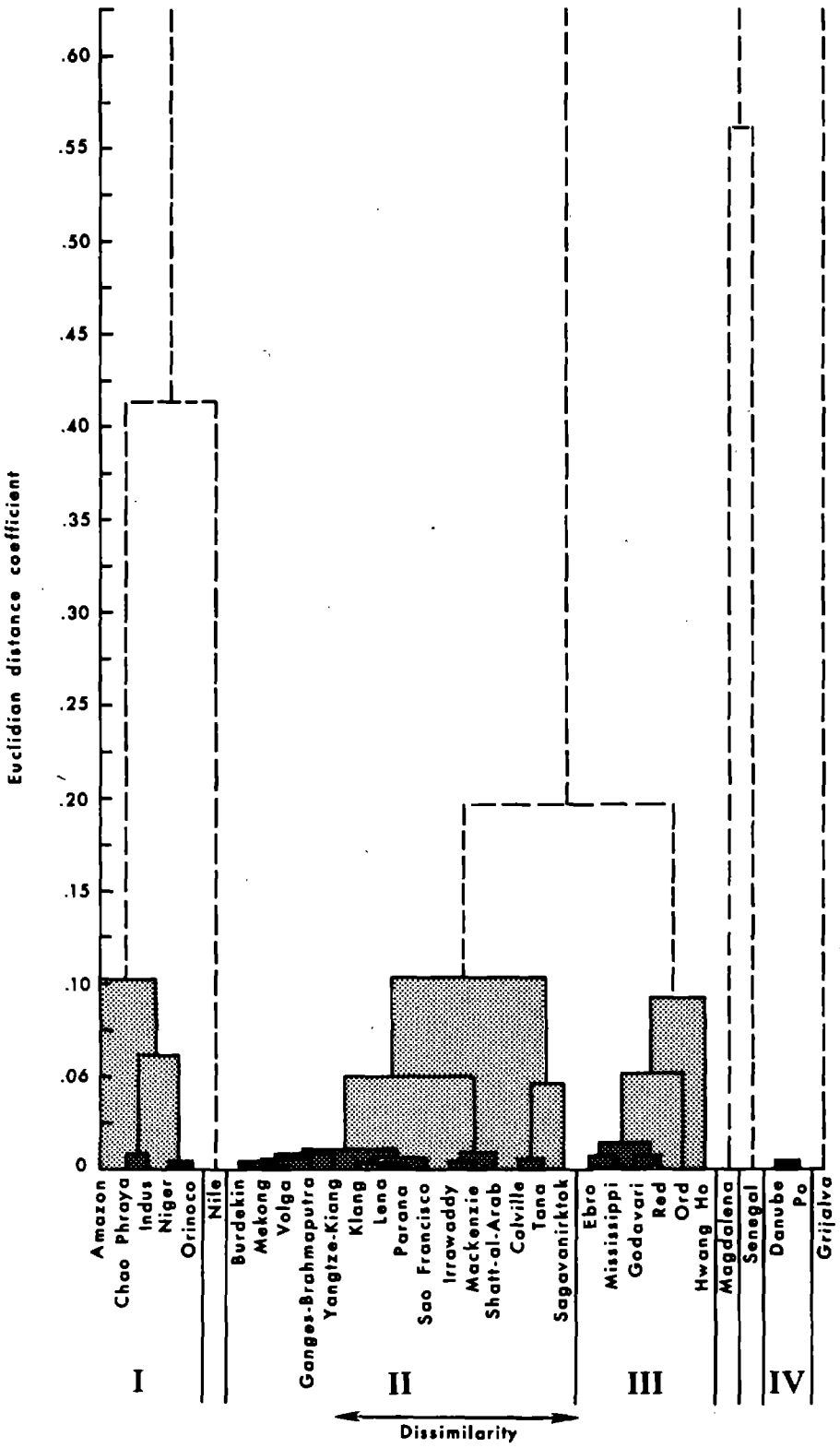

Figure 31. Cluster analysis dendrogram for deltas based on delta component ratios.

Table 20

Delta Components Data

	Delta	A_u/A_l	$\frac{A_{subaerial}}{A_{subaqueous}}$	$\frac{A_{abandoned}}{A_{active}}$
Cluster I	Amazon	2.69	6.35	0.00
	Chao Phraya	2.45	7.38	8.95
	Indus	2.02	8.15	6.41
	Niger	1.05	8.53	1.60
	Orinoco	0.24	8.61	0.19
	Mean	1.69	7.80	3.43
	CV	0.54	0.11	1.05
	Nile	7.46	9.04	8.68
Cluster II	Burdekin	1.51	2.12	3.96
	Mekong	1.11	1.98	1.85
	Volga	1.13	1.97	0.73
	Ganges-Brahmaputra	0.58	2.42	1.62
	Yangzte-Kiang	0.00	1.70	1.66
	Klang	0.94	1.00	0.00
	Lena	1.48	1.21	0.26
	Parana	1.17	1.51	0.00
	Sao Francisco	0.78	1.36	2.30
	Irrawaddy	0.70	0.09	2.94
	Mackenzie	1.17	0.00	0.00
	Shatt-al-Arab	0.40	0.62	5.66
	Colville	2.69	0.51	0.00
	Tana	3.33	0.97	1.52
	Sagavanirktok	4.96	0.93	0.00
	Mean	1.46	1.23	1.50
	CV	0.85	0.58	1.08
Cluster III	Ebro	1.74	4.60	5.33
	Mississippi	0.68	5.23	5.33
	Godavari	1.27	4.55	1.17
	Red	0.53	3.94	0.49
	Ord	0.00	3.20	1.39
	Hwang Ho	3.12	3.30	3.41
	Mean	1.22	4.14	2.85
	CV	0.83	0.18	0.69
	Magdalena	1.15	14.81	5.32
	Senegal	3.88	20.10	1.22
Cluster IV	Danube	19.80	8.60	3.10
	Po	19.50	7.96	3.98
	Mean	19.65	8.28	3.54
	CV	0.01	0.04	0.12
	Grijalva	22.10	6.70	137.00
	Overall Mean	3.49	4.67	6.75
	Overall CV	1.65	0.95	3.48

Table 21

Delta Component Discriminant Analysis--d^2 Values

Cluster	I	II	III	IV
I	0.00	79.88	26.03	262.43
II	79.88	0.00	14.94	446.50
III	26.03	14.94	0.00	356.68
IV	262.43	446.50	356.68	0.00

	Cluster			
Delta	I	II	III	IV
Amazon	5.21	56.10	15.85	258.44
Chao Phraya	6.58	78.47	27.33	257.07
Indus	1.89	90.95	32.74	251.54
Niger	1.76	96.46	36.31	270.54
Orinoco	4.25	97.13	37.64	294.26
Nile	37.70	175.69	98.69	118.62
Burdekin	61.06	2.32	7.73	414.48
Mekong	64.50	0.94	8.64	430.18
Volga	64.48	1.12	8.97	429.02
Ganges-Brahmaputra	58.06	2.46	6.54	432.41
Yangzte-Kiang	77.61	1.60	14.14	479.38
Klang	88.44	0.75	19.09	472.65
Lena	80.09	0.29	15.46	445.65
Parana	74.70	0.64	13.24	444.52
Sao Francisco	80.86	0.46	15.13	465.67
Irrawaddy	115.91	4.18	32.12	522.54
Mackenzie	113.84	3.24	31.51	506.36
Shatt-al-Arab	107.03	5.87	28.60	515.93
Colville	92.18	1.81	22.15	433.18
Tana	79.04	2.53	16.93	395.74
Sagavanirktok	78.28	9.62	21.75	347.63
Ebro	20.50	22.55	1.73	330.90
Mississippi	16.50	28.32	2.80	347.99
Godavari	20.52	20.18	0.98	342.52
Red	31.75	13.03	1.49	383.80
Ord	46.43	6.80	3.79	425.47
Hwang Ho	34.36	12.64	3.07	323.26
Magdalena	86.85	332.90	207.14	260.75
Senegal	308.67	698.04	512.96	321.67
Danube	272.16	464.87	371.51	0.30
Po	253.32	428.73	342.46	0.30
Grijalva	3,646.56	3,764.95	3,678.07	3,424.01

deltas and is of fundamental importance from a geologic point of view. For purposes of cluster comparisons, five morphometric variables, as defined by Coleman and Wright (1971), were selected: (1) the ratio of delta shoreline length to chord width (LS/W), an index of shoreline irregularity, (2) the ratio of the delta longitudinal axis to delta width (L/W), (3) the ratio of the longitudinal axis of the deltaic bulge to bulge width (L_b/W_b; the protrusion index), (4) delta bulge asymmetry as indexed by the ratio of the bulge volume on one side of the bulge bisector to the volume on the opposite side (in order to obtain values between 0 and 1 the

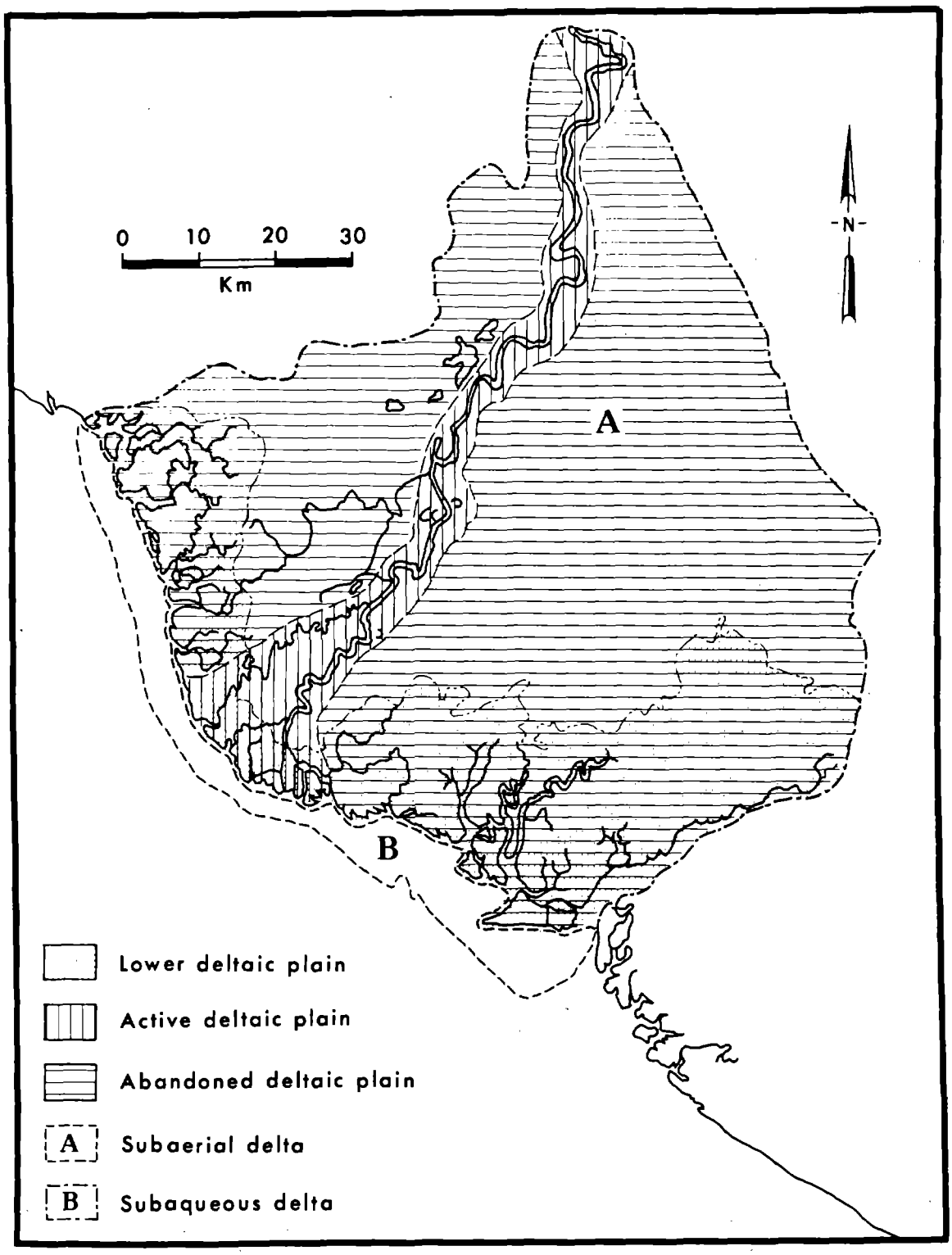

Figure 32. Map of the components of the Indus Delta.

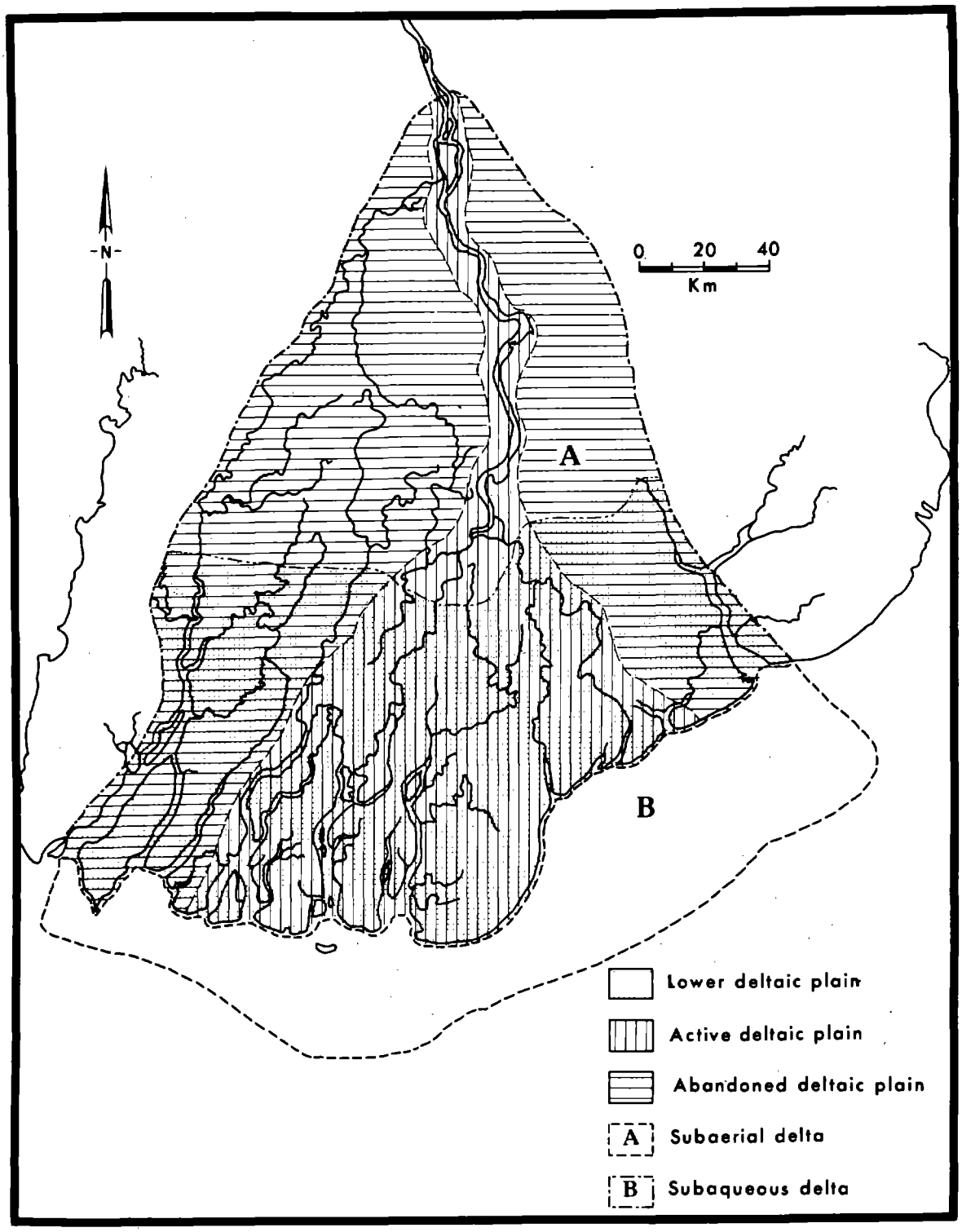

Figure 33. Map of the components of the Irrawaddy Delta.

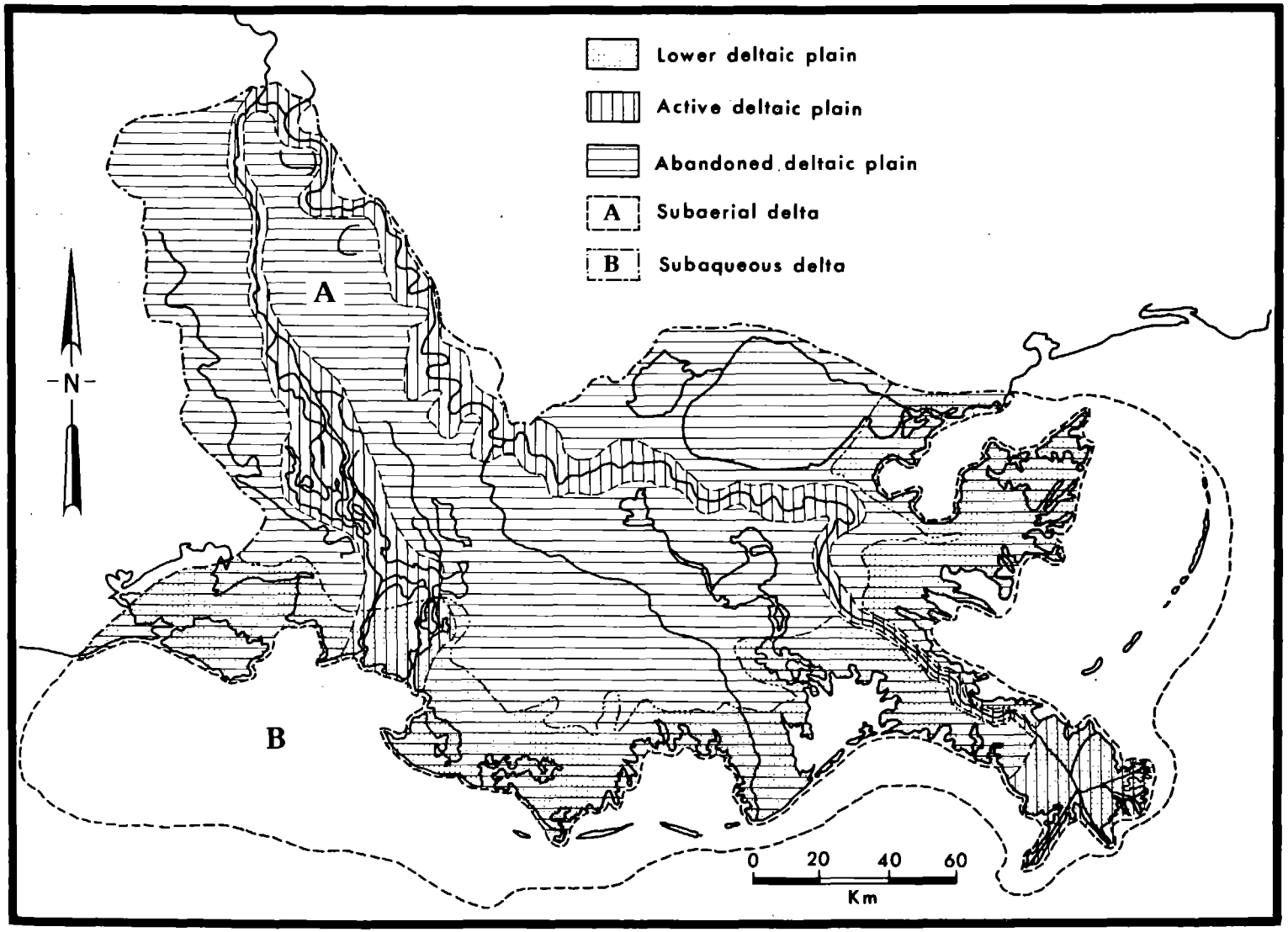

Figure 34. Map of the components of the Mississippi Delta.

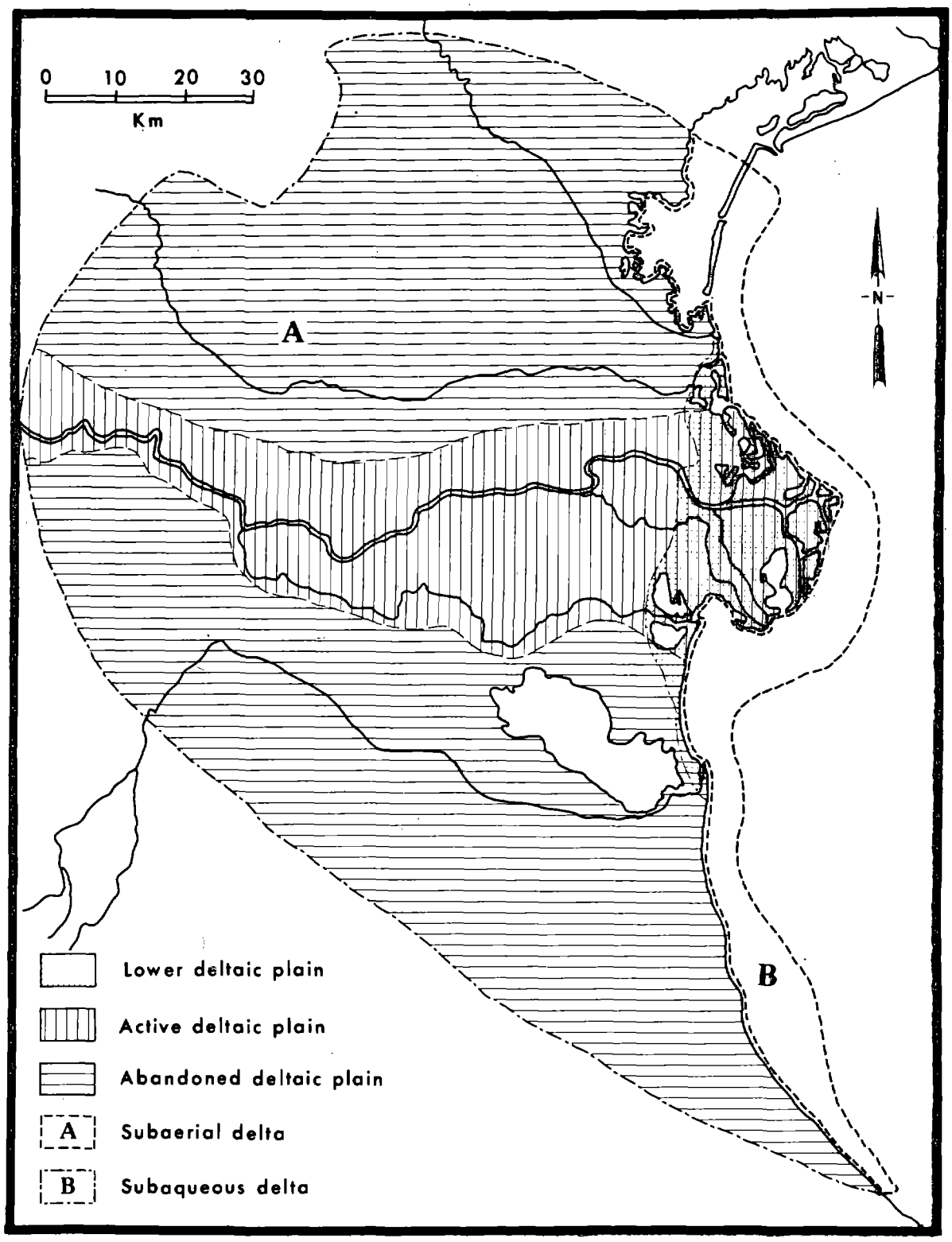

Figure 35. Map of the components of the Danube Delta.

smaller value was always divided by the larger value), and (5) the delta bulge volume distribution parameter β (defined by Coleman and Wright, 1971, and Wright and Coleman, 1973).

Because clustering on actual input values produced only marginally satisfactory results, clusters were based on factor scores obtained by subjecting the morphometric variables to a factor analysis. This procedure yielded tighter and more discrete clusters, as revealed by a comparison of discriminant analyses performed by cluster results from factor scores and raw data.

Factor analysis reduced the original five variables to two factors, as indicated by Table 22. The factor matrices (Table 22) indicate the fraction of the variance of each variable accounted for by each factor. Cluster analysis on the resulting factor scores produced the dendrogram shown in Figure 36. Acceptance of clusters at distance coefficients less than 0.5 yields six clusters and two individuals. The central tendencies of each cluster are indicated by Table 23. Associated discriminant analysis results are presented in Table 24.

The three deltas of cluster I are distinguished by relatively straight shorelines, moderately high long-axis-to-width ratios but very low protrusion index values, and moderately skewed deltaic bulges. This type of configuration is represented by the Amazon and Senegal (Figs. 19 and 23). The characteristics of cluster II appear to be the most common inasmuch as they are exhibited by ten of the deltas examined. Crenulate shorelines, as indicated by high values for the ratio S/W, less elongate deltaic plains, and more pronounced but relatively symmetrical bulges are typical of this type. The planar configurations of the Mississippi (Figs. 24 and 37) and Danube (Figs. 26 and 38) are representative.

Cluster III is somewhat similar to cluster II except that the seven deltas of this group exhibit generally straighter shorelines and less pronounced bulges. The Nile (Fig. 39) is an example.

Highly crenulate shorelines, together with linear delta volume distribution patterns (β near 0.5) characterize the four deltas of cluster IV. The Ganges-Brahmaputra (Fig. 40) is an example of this type.

The two deltas of cluster V have highly irregular shorelines and elongate delta plains and exhibit significant protrusions. In cluster VI, the Chao Phraya (Fig. 41) and Tana also exhibit elongate delta plains but have weak and highly asymmetric bulges.

Delta Landform Suites

Variations in the relative dominance of different landforms or suites of landforms in the interdistributary regions of the delta plain account for some of the most readily conspicuous contrasts between deltas. As in the case of alluvial-valley landscapes, clustering was based on multistate data obtained by treating each of several features as a separate variable and assigning each a score of 0, 0.33, 0.66, or 1.0, indicating respectively absent, rare, common, or abundant. The relative abundances of five interdistributary features were considered: (1) active coastline barriers, (2) stranded interdistributary beach ridges, (3) bays and lakes, (4) marshes and swamps, and (5) tidal flats and tidal creeks. In combination, these five characteristics provide a rough index of the overall interdistributary landscape.

The dendrogram for interdistributary landscape type (Fig. 42) suggests

Table 22

Factor Analysis of Delta Morphometry

Variable No.	Variable	Mean	Std. Deviation	Correlation Matrix: Variable Number 1	2	3	4	5	Factor Matrices: Unrotated Factor 1	Unrotated Factor 2	Rotated Factor 1	Rotated Factor 2
1.	Shoreline Length/Width	1.55	0.41	1.00	-0.24	0.36	0.32	-0.12	0.70	0.30	0.32	0.69
2.	Delta Length/Delta Width	1.04	0.57	-0.24	1.00	0.15	-0.22	0.24	-0.48	0.65	-0.79	0.17
3.	Protrusion Index	0.42	0.27	0.36	0.15	1.00	0.19	-0.10	0.46	0.76	-0.16	0.88
4.	Right Volume/Left Volume	0.70	0.20	0.32	-0.22	0.19	1.00	-0.36	0.75	-0.07	0.61	0.45
5.	Mean Vol. Distribution Parameter	0.44	0.10	-0.12	0.24	-0.10	-0.36	1.00	-0.60	0.33	0.67	-0.15
			Factor	1	2	3	4	5				
	Eigenvalue			1.85	1.21	0.87	0.67	0.46				

appreciable dissimilarities between deltas in terms of the properties considered. Deltas were grouped, on the basis of linkages occurring at distance coefficients less than 0.6, into seven clusters, and six deltas remained unique at the given level of cluster acceptance (however, all but one of the deltas fuse below $I_{in} = 1.0$). Distance-squared values from discriminant analysis, indicating the relative degree of dissimilarity between clusters and between deltas and clusters, are presented in Table 25. The characteristic landscape signatures of each cluster are illustrated diagrammatically by the histograms shown in Figure 43.

Cluster I is the largest, containing eight (24 percent) of the deltas examined. Marshes and swamps, together with tidal creeks and flats, are the abundant features; active barriers, beach ridges, and bays and lakes are present but relatively sparse. Figure 44, showing the dense vegetation in the delta of the Amazon, illustrates the importance of vegetation in this type. Equally representative of this landscape type is the delta plain of the Ganges-Brahmaputra, with its intricate network of tidal creeks, as seen from the high-altitude ERTS infra-red image in Figure 40.

Widely spaced beach ridges, separated by broad expanses of tidal flats and mangrove-swamp-fringed tidal creeks, are common features among the five deltas of cluster II. An example of this type of landscape from an arid region where barren flats are the prevailing feature is offered by the Ord Delta (Fig. 45). Analogous patterns from a moister environment are represented by the landscape of the Mekong Delta, as seen in the form of an ERTS satellite image in Figure 46. Widely spaced interdistributary beach ridges, separated by swamp, are typical of this type.

The Burdekin, Niger, and Tana, the three deltas comprising cluster III, are characterized by a greater abundance of coastline barriers and beach ridges than cluster I or II and a total absence of interdistributary lakes and bays; however, as in the case of clusters I and II, marshes and swamps and tidal features are common to abundant. Beach-ridge plains and swales filled with marsh, swamp, or barren tidal flats are prominent. The Burdekin Delta (Fig. 47) illustrates this type.

Two arctic rivers, the Colville and Sagavanirktok, make up cluster IV. An abundance of thaw lakes, as exhibited by the delta plain of the Colville (Fig. 48), and a comparative sparsity of active coastline barriers typify this type.

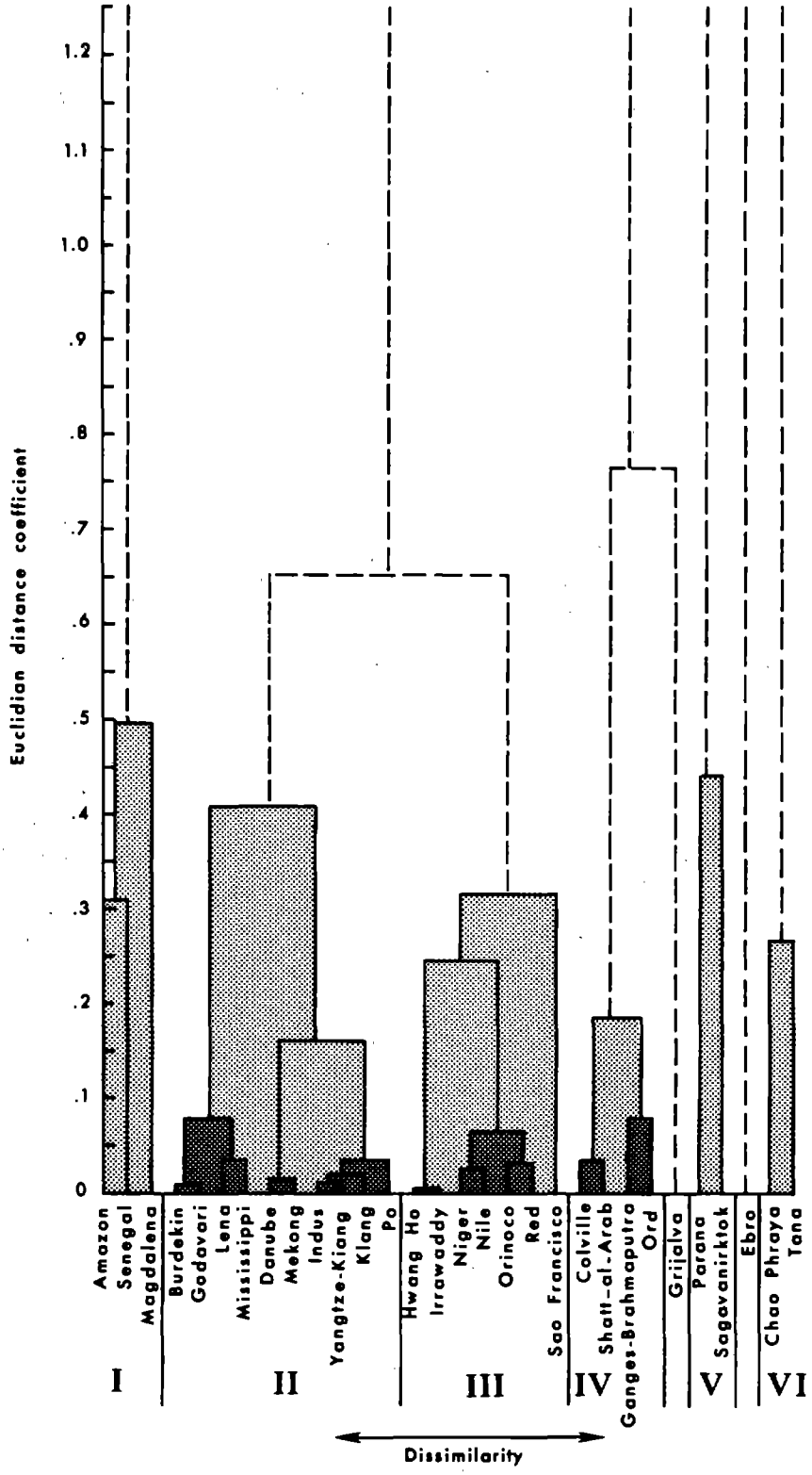

Figure 36. Cluster analysis dendrogram for deltas based on factor scores for dimensionless morphometry.

Table 23

Delta Morphometry Data

	River	L_s/W	L/W	L_b/W_b	Bulge Asymmetry (V_{min}/V_{max})	$\bar{\beta}$
Cluster I	Amazon	1.20	1.40	0.046	0.472	0.521
	Senegal	1.02	2.74	0.117	0.631	0.336
	Magdalena	1.02	1.03	0.325	0.613	0.418
	Mean	1.08	1.72	0.163	0.572	0.425
	CV	0.096	0.52	0.890	0.152	0.218
Cluster II	Burdekin	1.66	0.55	0.419	0.776	0.331
	Godavari	1.76	0.63	0.351	0.903	0.395
	Lena	1.85	0.58	0.487	0.694	0.395
	Mississippi	2.03	0.37	0.381	0.849	0.478
	Danube	1.65	0.90	0.432	0.884	0.485
	Mekong	2.2	1.18	0.194	0.819	0.52
	Indus	1.42	0.26	0.224	0.833	0.360
	Yangtze-Kiang	1.55	1.23	0.321	0.730	0.428
	Klang	1.35	0.68	0.553	0.392	0.353
	Po	1.39	0.80	0.529	0.558	0.344
	Mean	1.68	0.768	0.389	0.744	0.409
	CV	0.164	0.355	0.309	0.207	0.162
Cluster III	Hwang Ho	1.36	0.32	0.241	0.826	0.355
	Irrawaddy	1.65	1.12	0.241	0.75	0.470
	Niger	1.24	0.62	0.336	0.719	0.325
	Nile	1.20	0.82	0.209	0.826	0.384
	Orinoco	1.81	0.76	0.221	0.680	0.385
	Red	1.33	1.06	0.170	0.921	0.405
	Sao Francisco	1.08	0.52	0.124	0.740	0.385
	Mean	1.38	0.746	0.220	0.780	0.387
	CV	0.187	0.384	0.300	0.105	0.116
Cluster IV	Colville	1.73	1.16	0.693	0.834	0.485
	Shatt-al-Arab	1.30	1.01	0.893	1.000	0.578
	Ganges-Brahmaputra	1.51	0.75	0.755	0.460	0.447
	Ord	2.28	0.76	0.575	0.400	0.458
	Mean	1.71	0.92	0.729	0.674	0.492
	CV	0.25	0.22	0.182	0.431	0.121
Cluster V	Parana	1.81	1.53	1.06	0.625	0.340
	Sagavanirktok	1.64	2.30	1.10	0.955	0.453
	Mean	1.725	1.915	1.08	0.790	0.396
	CV	0.070	0.284	0.026	0.295	0.202
Cluster VI	Chao Phraya	1.15	2.06	0.234	0.239	0.575
	Tana	1.12	1.20	0.120	0.212	0.832
	Mean	1.14	1.63	0.177	0.226	0.704
	CV	0.019	0.373	0.455	0.084	0.258
	Grijalva	1.26	1.91	0.570	0.570	0.483
	Ebro	2.89	0.87	0.710	0.952	0.395
	Overall Mean	1.549	1.04	0.421	0.696	0.437
	Overall CV	0.266	0.552	0.646	0.294	0.232

Table 24

Delta Morphometry Discriminant Analysis--d^2 Values

Cluster	I	II	III	IV	V	VI
I	00.00	25.92	19.65	84.69	199.43	46.69
II	25.92	0.00	19.76	32.07	119.21	76.35
III	19.65	19.76	0.00	99.40	229.12	107.88
IV	84.69	32.07	99.40	0.00	34.12	81.37
V	199.43	119.21	229.12	34.12	0.00	179.56
VI	49.69	76.35	107.88	81.37	179.56	0.00

	Cluster					
Delta	I	II	III	IV	V	VI
Amazon	3.99	35.72	27.19	97.27	227.13	34.87
Senegal	7.40	43.94	36.36	106.76	209.25	66.97
Magdalena	4.76	14.24	11.54	66.18	178.07	54.39
Burdekin	33.20	4.37	12.14	52.34	147.50	110.33
Godavari	33.34	4.30	11.64	53.94	151.89	108.97
Lena	42.17	2.35	32.43	22.59	98.00	89.42
Mississippi	45.76	3.74	28.27	32.88	120.29	98.82
Danube	31.71	1.87	27.98	24.28	104.06	73.70
Mekong	33.27	6.12	32.67	36.08	112.00	73.14
Indus	12.90	3.50	14.53	46.25	146.14	59.91
Yangtze-Kiang	13.70	2.25	16.73	39.70	130.86	62.22
Klang	27.87	8.23	35.50	24.94	103.73	58.41
Po	25.52	3.54	25.94	27.96	107.87	70.91
Hwang Ho	29.86	25.10	1.12	110.22	244.78	127.65
Irrawaddy	32.25	26.20	1.60	112.88	249.17	131.40
Niger	18.65	14.29	1.68	83.25	201.44	102.71
Nile	15.90	22.74	0.66	103.54	234.28	102.52
Orinoco	19.91	5.63	7.23	63.61	172.94	89.28
Red	16.07	20.70	1.56	99.90	226.02	103.31
Sao Francisco	24.00	42.74	5.26	141.52	294.31	117.42
Colville	79.10	26.53	89.39	1.64	35.95	88.87
Shatt-al-Arab	112.74	54.85	128.36	8.26	30.29	102.23
Ganges-Brahmaputra	75.70	31.78	94.67	2.58	43.33	68.72
Ord	91.02	34.92	105.01	7.34	46.74	85.49
Grijalva	46.77	32.10	84.83	14.72	60.47	39.25
Parana	182.45	102.08	205.56	26.47	2.48	170.65
Sagavanirktok	221.36	141.29	257.63	46.73	2.48	193.41
Ebro	176.68	74.89	158.07	41.22	48.51	214.70
Chao Phraya	32.56	58.90	91.22	65.54	150.38	4.84
Tana	70.51	103.50	134.24	106.90	218.42	4.84

Figure 37. ERTS satellite image of the Mississippi Delta.

Figure 38. ERTS satellite image of the Danube Delta.

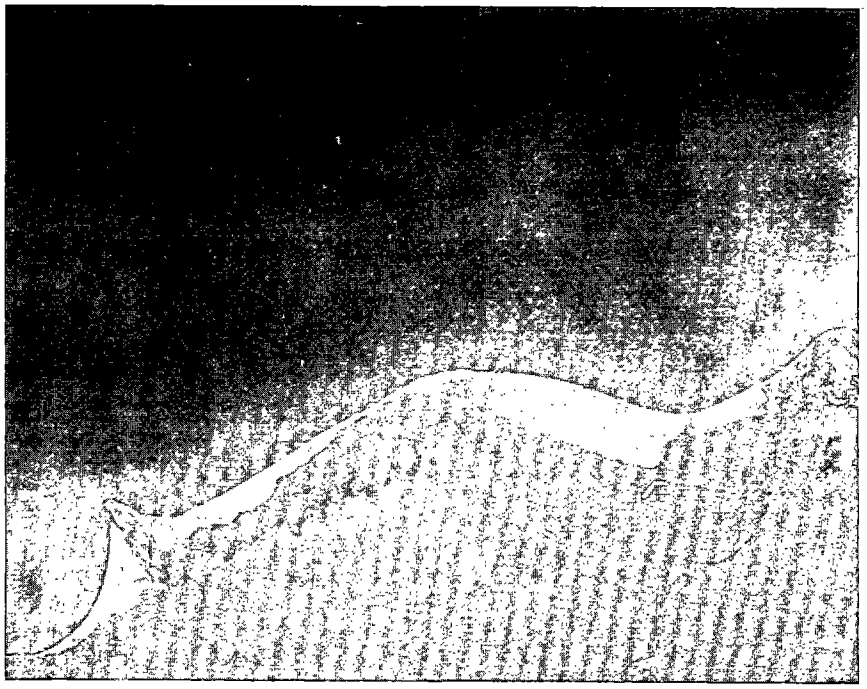

Figure 39. ERTS satellite image of the Nile Delta.

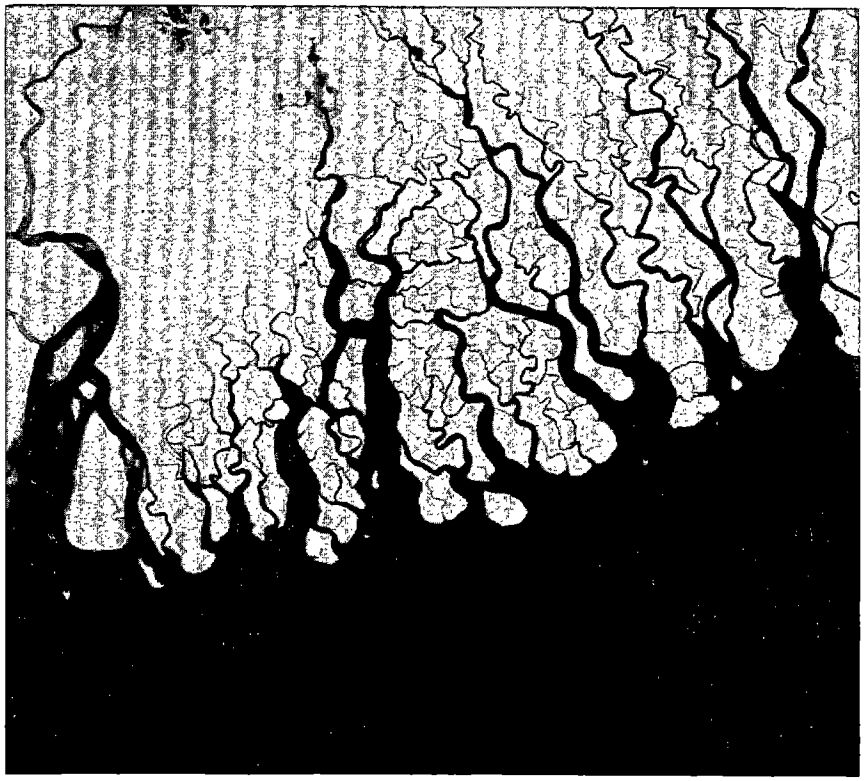

Figure 40. ERTS satellite image of the Ganges-Brahmaputra Delta.

Figure 41. ERTS satellite image of the Chao Phraya Delta.

Abundant active coastline barriers but relatively sparse abandoned beach ridges are the most salient distinguishing features of cluster V. The extensive barrier spits flanking the mouth of the Ebro (Fig. 49) and the relatively continuous beaches, dunes, and barriers fringing the Nile Delta (Fig. 39) are characteristic.

Beaches, beach-ridge plains, and bays and lakes are all common but not abundant in the delta-plain landscape of cluster IV, whereas marshes are the most abundant feature. Owing to the fact that all three of the deltas in this cluster experience negligible tides, tidal flats and tidal creeks are insignificant. The main distinguishing attributes of this landscape type are evident from the high-altitude ERTS infrared image of the Danube Delta shown in Figure 38.

Extremely high wave energy has been responsible for the formation of the extensive coastline barriers and beach-ridge plains characteristic of landscape cluster VII. (The writers have discussed the role of the wave-power climate in Wright and Coleman, 1971b, 1972, 1973.) Because of the overwhelming prevalence of wave-built features and eolian dunes, bays and lakes are absent and tidal features are sparse; however, marshes and swamps are present in swales. The extensive beach-ridge plains and dune sheets of the Sao Francisco (Fig. 50) or the plain of abandoned barrier spits of the Senegal (Fig. 51) characterize this type.

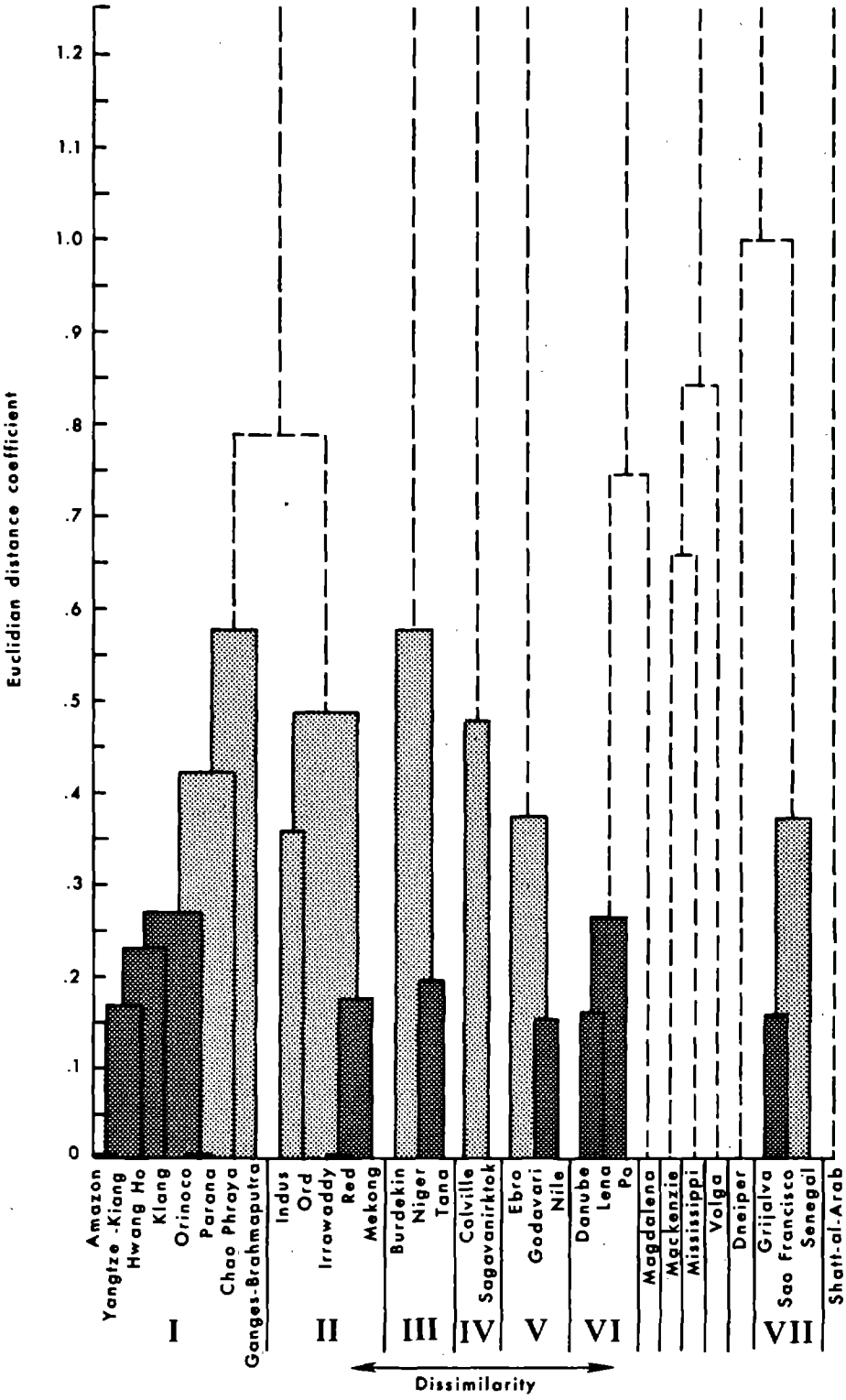

Figure 42. Cluster analysis dendrogram for delta landform suites.

Table 25

Delta Landforms Discriminant Analysis--d^2 Values

Cluster	I	II	III	IV	V	VI	VII
I	0.00	68.22	55.12	65.71	49.79	237.40	39.07
II	68.22	0.00	70.40	54.88	85.98	74.44	15.93
III	55.12	70.40	0.00	25.16	42.38	134.46	43.05
IV	65.71	54.88	25.16	0.00	35.78	115.66	55.37
V	49.79	85.98	42.38	35.78	0.00	189.38	87.50
VI	237.40	74.44	134.46	115.66	189.38	0.00	117.17
VII	39.07	15.93	43.05	55.37	87.50	117.17	0.00

Delta	Cluster I	II	III	IV	V	VI	VII
Amazon	0.71	34.41	63.71	50.90	48.84	61.13	232.88
Yangtze-Kiang	0.71	34.41	63.71	50.90	48.84	61.13	232.88
Hwang Ho	5.56	41.80	63.27	38.42	31.59	38.99	201.84
Klang	5.22	24.58	46.00	64.24	65.64	73.41	203.76
Orinoco	4.21	42.31	86.30	52.42	68.79	75.87	256.34
Parana	4.21	42.31	86.30	52.42	68.79	75.87	256.34
Chao Phraya	6.97	36.26	50.87	59.15	38.64	56.15	219.17
Ganges-Brahmaputra	17.50	101.57	130.72	117.62	72.29	128.21	341.12
Indus	43.93	4.92	12.92	32.43	63.87	44.45	102.21
Ord	54.33	5.40	20.21	49.68	103.02	78.86	98.96
Irrawaddy	33.24	2.22	23.79	42.32	86.99	51.13	140.32
Red	33.24	2.22	23.79	42.32	86.99	51.13	140.32
Mekong	48.40	3.04	16.73	66.31	114.43	74.06	121.25
Burdekin	76.81	18.93	3.92	76.18	92.08	73.52	80.88
Niger	58.81	11.58	2.76	61.36	86.28	46.22	76.39
Tana	77.52	25.75	1.79	82.11	88.03	53.35	74.52
Colville	73.67	67.25	99.20	3.05	46.18	36.74	156.34
Sagavanirktok	42.68	24.96	47.71	3.05	44.69	19.69	118.68
Ebro	56.40	90.97	92.71	40.00	2.53	47.16	188.76
Godavari	38.98	77.03	77.67	44.48	1.95	35.69	199.51
Nile	61.00	101.51	94.56	49.68	2.52	31.51	186.70
Danube	84.00	70.38	62.12	35.27	44.00	3.50	99.19
Lena	55.78	39.70	39.04	23.88	37.23	1.48	105.80
Po	65.83	64.52	71.97	24.83	24.62	3.52	150.50
Magdalena	102.51	163.84	156.28	87.84	27.27	44.95	256.86
Mackenzie	112.22	183.32	221.42	68.99	69.50	82.60	298.26
Mississippi	53.37	121.18	151.05	51.50	33.00	44.83	283.10
Volga	76.87	199.02	243.20	123.21	79.98	130.09	470.00
Dneiper	161.11	70.23	47.59	66.33	114.04	45.28	32.85
Grijalva	226.03	103.00	65.70	127.00	186.70	119.78	2.52
São Francisco	260.30	139.73	94.83	144.44	199.51	127.84	1.95
Senegal	232.90	115.80	69.82	138.94	188.95	106.39	2.53
Shatt-al-Arab	63.14	71.97	96.70	55.81	72.53	113.30	176.89

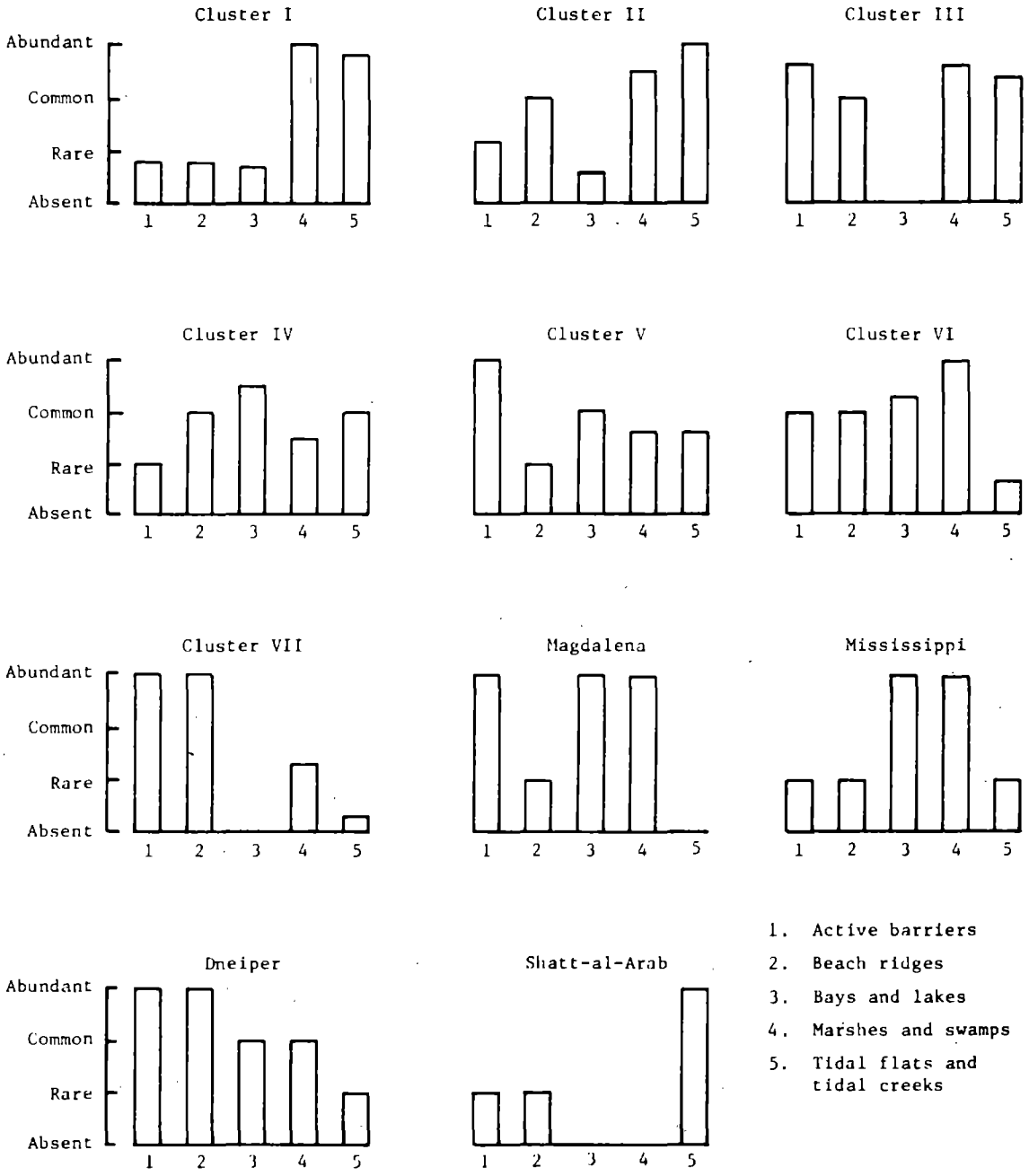

Figure 43. Mean relative abundance of delta-plain landforms in each cluster.

The characteristics of the six unique deltas, the Magdalena, Mackenzie, Mississippi, Volga, Dneiper, and Shatt-al-Arab, are indicated by the histograms in Figure 43. At least three of these deserve special mention owing to the important positions which they occupy in the delta spectrum. The Magdalena (Fig. 52), like the deltas of cluster VII, is fringed by well-developed barrier formations; however, water-filled lagoons and swamps, rather than beach ridges, lie behind the barriers.

Figure 44. Varza forest along the banks of the lower Amazon River.

Figure 45. Barren tidal flats and mangrove-fringed tidal creek in the Ord River delta.

Figure 46. ERTS satellite image of the Mekong Delta.

Figure 47. Beach ridges and barren tidal flats in the Burdekin River delta.

Figure 48. Vertical aerial photograph of the Colville Delta showing thaw lakes, patterned ground, and distributary channels.

As the classic example of a low-energy, river-dominated delta (e.g., Wright and Coleman, 1972, 1973), the interdistributary areas of the Mississippi (Fig. 37) consist largely of marsh and open and closed bays. Wave-deposited barriers and beach ridges are meager and occur primarily in the form of stranded chenier ridges or as narrow, arcuate transgressive barriers in abandoned regions of the delta.

Extensive barren, evaporite-crusted tidal flats are the prevalent form in the delta plain of the Shatt-al-Arab (Fig. 53), reflecting the combination of the high tide range and arid climate. Other features are rare or practically absent altogether.

Delta Distributary Network Patterns

Variations in the patterns of distributary networks are no less conspicuous than differences in landform combination. Several distributary parameters were defined previously (Coleman and Wright, 1971) and were measured for the majority of the deltas considered. However, experience indicates that, at a first-order resolution level, many of the similarities and dissimilarities between distributary patterns can be described in terms of three variables. These are (1) the total number of significant river mouths, (2) the ratio of the total number of distributary rejoinings to the total number of bifurcations (the α ratio discussed by Smart and Moruzzi, 1972), and (3) the distributary density (the total lengths of all distributaries divided by the area of the active delta).

The dendrogram in Figure 54 shows the results of a cluster analysis performed for these three variables on 32 deltas. Seven clusters and five individuals result

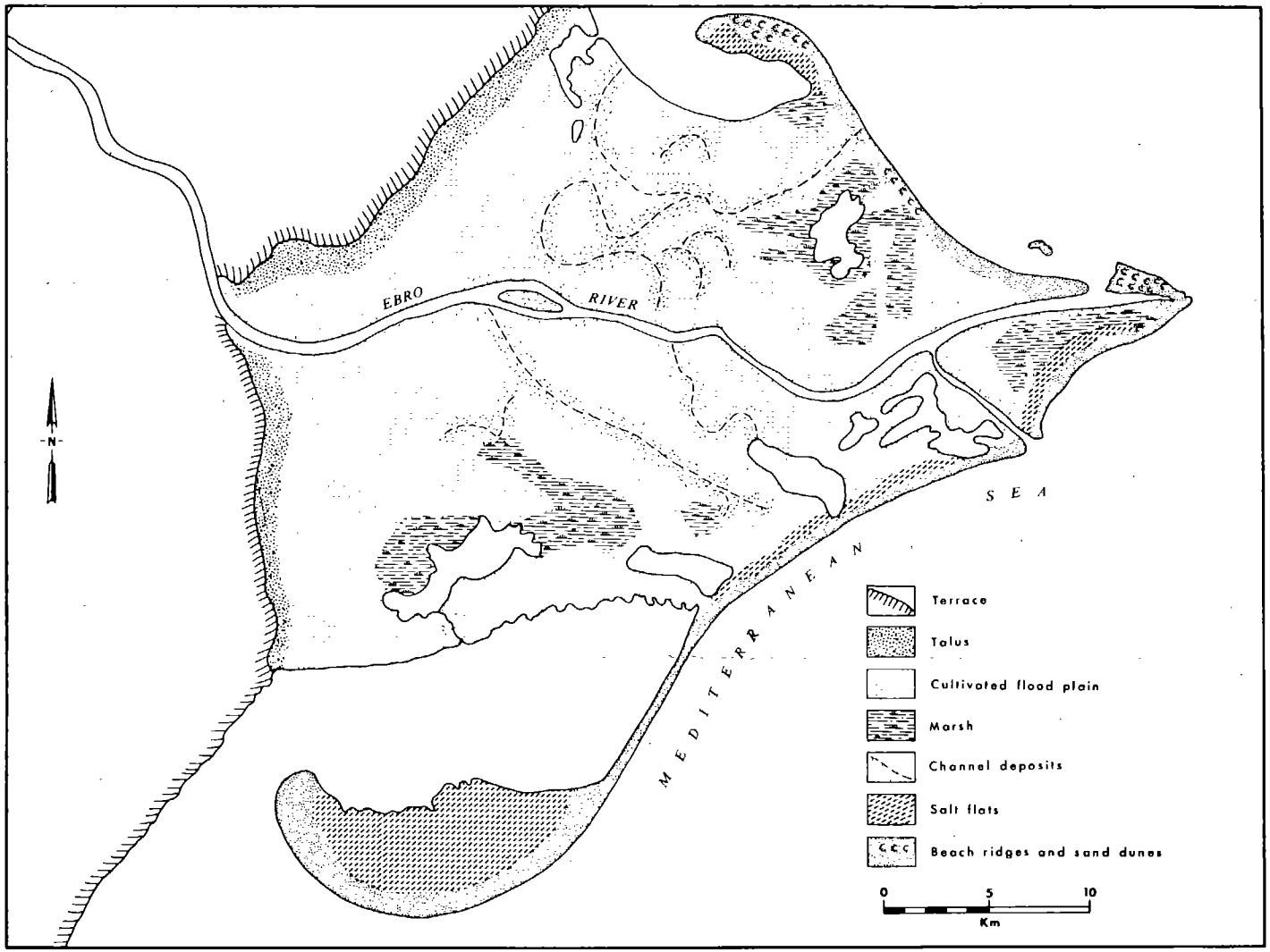

Figure 49. Map of the Ebro Delta showing barrier spits flanking the river mouth.

Figure 50. Dune sheets in the Sao Francisco Delta.

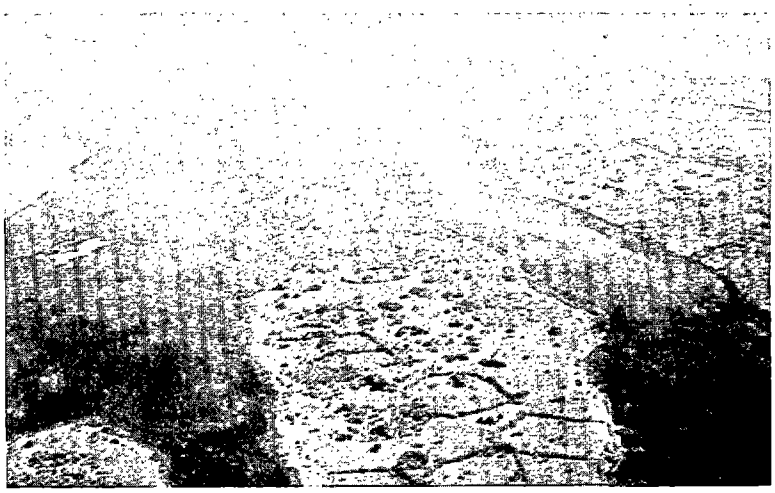

Figure 51. Linear beach ridges and swales in the Senegal Delta.

Figure 52. ERTS satellite image of the Magdalena Delta.

Figure 53. ERTS satellite image of the Shatt-al-Arab Delta.

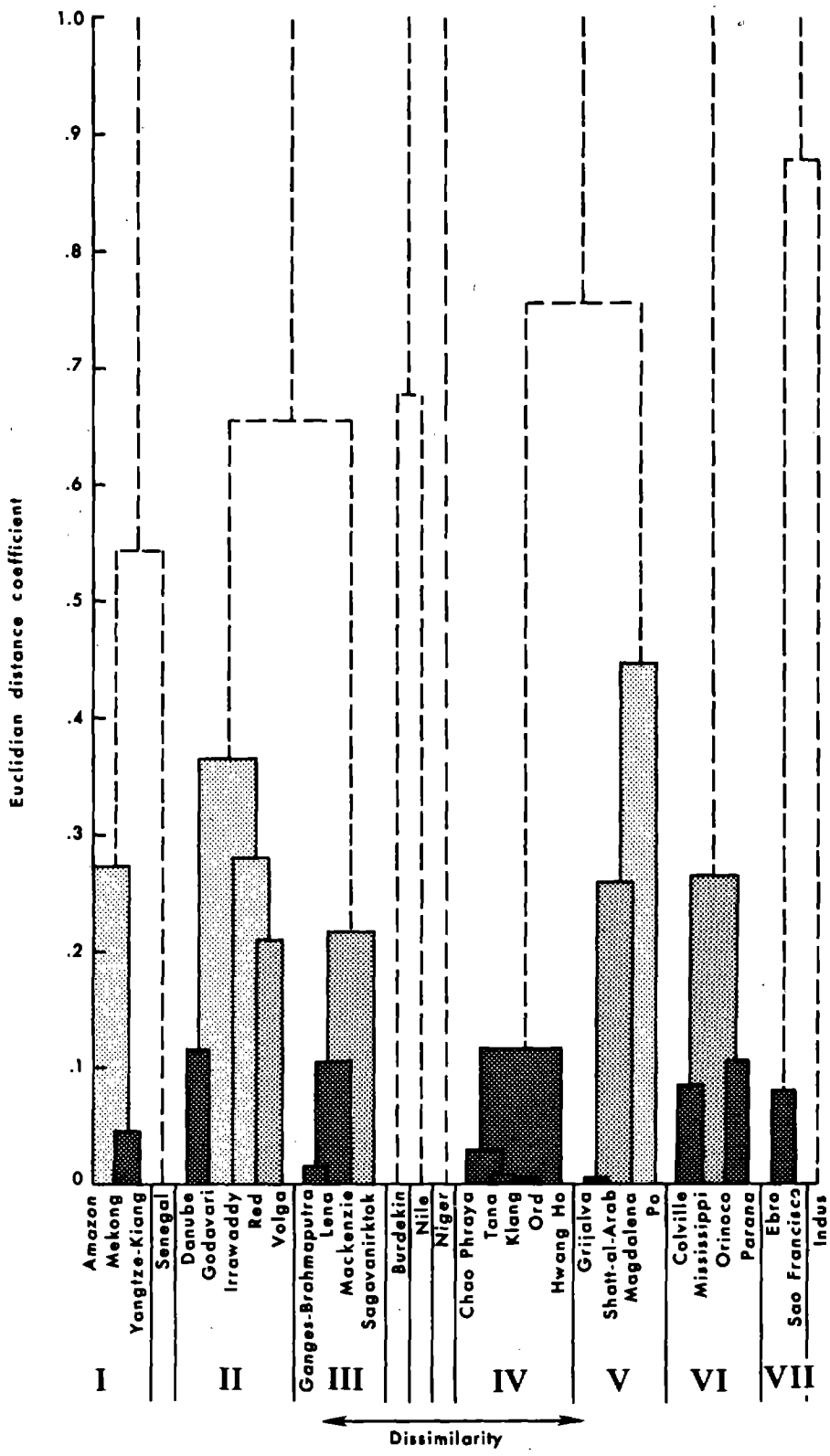

Figure 54. Cluster analysis dendrogram for delta distributary network patterns.

from linkages occurring below a maximum distance coefficient of 0.45. The central tendencies of each cluster are given in Table 26. Discriminant analysis results are presented in Table 27.

Three to six river mouths and high incidence of rejoining, together with low distributary density, are the distinguishing characteristics of the three distributary networks of cluster I. The distributary patterns of the Mekong Delta are representative of this type.

Cluster II differs from cluster I by virtue of a greater number of river mouths, a more moderate percentage of rejoinings, and an eightfold higher mean distributary density. The Danube, as seen in Figure 38, is an example of this type. Cluster III occupies an approximately median position in the distributary network spectrum, as suggested by Table 26, except that distributary density is low.

With one exception (the Hwang Ho), the deltas of cluster IV exhibit only one or two river mouths (the Hwang Ho has five). There are no rejoinings, and distributary density is very low. The single outlet of the Chao Phraya, as seen in Figure 41, is an example. The distributary patterns of cluster V are very similar to those of cluster IV, except that distributary density is high owing to the fact that the channels are more sinuous and are confined to more restricted active deltas. The Magdalena (Fig. 52) and Shatt-al-Arab (Fig. 53) represent the type.

The four deltas of cluster VI exhibit the greatest number of river mouths of any of the clusters. Rejoinings are comparatively infrequent, and distributary densities are substantially higher than those of cluster I or II. The progressively bifurcating network of the Mississippi (Fig. 37) is typical of this group.

The Sao Francisco and Ebro (Fig. 49), the two members of cluster VII, are similar to each other and dissimilar from the other deltas in the sense that they have very high distributary densities but only one distributary. There are no rejoinings. The characteristics of the five remaining individual deltas, the Senegal, Burdekin, Nile, Indus, and Niger, are evident from Table 26 and require no further elaboration.

River-Mouth Morphology

The river mouth is the dynamic dissemination point for sediments which contribute to continued delta progradation and to formation of the subaqueous delta. The river mouth is probably the most fundamental subsystem of a delta; without river mouths there would be no delta. The geometry of the river mouth and the associated bar topography have been found, through the systematic phases of the delta study, to be closely linked with effluent processes, which in turn and degree vary with vertical density stratification, tidal influences, coastal currents, incident wave energy, etc. (Wright, 1970; Wright and Coleman, 1971a and in press; Wright, Coleman, and Thom, 1973). Morphologic variability of river mouths involves several variables. Owing to the limited accuracy and resolution of available map data, only three river-mouth parameters have been included in the cluster comparisons; however, these parameters have been found to be the most significant and apparent morphometric attributes (Wright, Coleman, and Thom, 1973; Wright and Coleman, in press). Cluster analysis results presented in Figure 55 are based on (1) the convergence ratio $b_{(4bo)}/b_o$, where b_o is the river-mouth width and $b_{(4bo)}$ is the channel width at a distance of four river-mouth widths upstream (small values for this ratio indicate funnel-shaped mouths, values of unity indicate straight mouths, and values greater than 1 indicate constricted mouths); (2) the ratio h_o/b_o of mean water depth at the mouth h_o to river-mouth width b_o; and (3) the distance X_{bar}/b_o from the river mouth to the bar crest relative to river-mouth width.

Table 26

Distributary Network Data

	River	No. River Mouths	Rejoinings/ Bifurcations	Distributary Density
Cluster I	Amazon	6.00	0.58	0.00
	Mekong	5.00	0.86	0.06
	Yangtze-Kiang	3.00	0.83	0.03
	Mean	4.67	0.75	0.02
	CV	0.27	0.20	0.71
	Senegal	1.00	1.00	0.16
Cluster II	Danube	14.00	0.46	0.23
	Godavari	11.00	0.50	0.18
	Irrawaddy	10.00	0.83	0.17
	Red	12.00	0.58	0.08
	Volga	15.00	0.77	0.12
	Mean	12.40	0.63	0.16
	CV	0.15	0.23	0.32
Cluster III	Ganges-Brahmaputra	8.00	0.36	0.05
	Lena	7.00	0.40	0.04
	Mackenzie	11.00	0.36	0.04
	Sagavanirktok	11.00	0.17	0.08
	Mean	9.25	0.32	0.05
	CV	0.19	0.28	0.32
	Burdekin	4.00	0.57	0.25
	Nile	2.00	0.96	0.38
	Niger	11.00	0.84	0.48
Cluster IV	Chao Phraya	1.00	0.00	0.04
	Tana	1.00	0.00	0.02
	Klang	2.00	0.00	0.08
	Ord	2.00	0.00	0.07
	Hwang Ho	5.00	0.00	0.03
	Mean	2.20	0.00	0.05
	CV	0.67	0.00	0.45
Cluster V	Grijalva	2.00	0.00	0.22
	Shatt-al-Arab	2.00	0.00	0.21
	Magdalena	1.00	0.00	0.36
	Po	8.00	0.00	0.33
	Mean	3.25	0.00	0.28
	CV	0.85	0.00	0.27
Cluster VI	Colville	19.00	0.25	0.30
	Mississippi	22.00	0.26	0.32
	Orinoco	18.00	0.29	0.15
	Parana	21.00	0.29	0.20
	Mean	20.00	0.27	0.24
	CV	0.08	0.07	0.29
Cluster VII	Ebro	2.00	0.00	0.47
	Sao Francisco	1.00	0.00	0.55
	Mean	1.50	0.00	0.51
	CV	0.33	0.00	0.08
	Indus	4.00	0.40	0.68
	Overall Mean	7.56	0.36	0.20
	Overall CV	0.83	0.92	0.86

Table 27

Distributary-Network Discriminant Analysis - d^2 Values

Cluster	I	II	III	IV	V	VI	VII
I	0.00	18.21	22.78	69.21	53.96	74.06	53.14
II	18.21	0.00	21.36	89.39	55.44	23.54	44.75
III	22.78	21.36	0.00	25.60	13.52	36.53	19.59
IV	69.21	89.39	25.60	0.00	7.97	107.03	25.47
V	53.96	55.44	13.52	7.97	0.00	67.26	5.48
VI	74.06	23.54	36.53	107.03	67.26	0.00	59.35
VII	53.14	44.75	19.59	25.47	5.48	59.35	0.00

River	I	II	III	IV	V	VI	VIII
Amazon	4.03	18.37	8.37	42.13	31.17	59.78	35.16
Mekong	1.73	17.73	34.04	92.32	72.11	78.42	67.36
Yangtze-Kiang	1.00	25.28	32.68	79.94	65.36	90.74	63.67
Senegal	11.16	34.65	63.27	127.66	103.68	114.89	92.59
Danube	31.42	3.18	18.51	84.29	49.90	9.72	41.39
Godavari	16.48	2.13	10.16	65.72	38.34	21.09	33.10
Irrawaddy	13.92	5.54	38.82	118.67	84.49	47.32	72.38
Red	13.84	2.76	11.42	70.10	44.83	24.21	41.90
Volga	27.15	4.99	39.52	127.39	89.90	28.42	79.04
Ganges-Brahmaputra	17.96	21.13	0.43	25.20	14.15	42.62	20.03
Lena	14.56	21.92	1.48	25.43	15.55	48.80	21.53
Mackenzie	22.32	16.26	0.74	34.53	19.46	28.57	24.39
Sagavanirktok	41.80	31.68	2.91	22.80	10.45	31.69	17.96
Burdekin	5.11	9.62	15.78	59.90	36.97	53.75	29.86
Nile	23.27	28.69	74.71	154.75	116.67	100.99	95.10
Niger	52.66	20.68	83.65	190.27	134.98	56.81	106.65
Chao Phraya	72.48	97.04	30.28	0.32	10.55	118.46	28.95
Tana	74.62	100.58	32.02	0.54	12.07	122.24	31.52
Klang	67.08	86.04	24.28	0.08	6.60	103.98	22.78
Ord	67.69	87.12	24.75	0.04	7.00	105.13	23.53
Hwang Ho	66.52	78.50	18.99	1.34	5.97	87.64	22.90
Grijalva	57.47	67.15	17.42	3.36	1.16	83.53	10.33
Shatt-al-Arab	58.05	68.46	17.78	2.93	1.41	84.96	11.13
Magdalena	53.37	56.85	17.43	10.50	0.91	74.73	3.39
Po	56.40	38.73	10.87	24.55	5.97	35.26	6.54
Colville	73.57	22.55	36.51	105.97	64.87	0.25	55.18
Mississippi	96.30	33.77	56.36	137.83	90.39	2.22	77.87
Orinoco	55.23	17.58	20.39	79.48	48.01	2.54	45.21
Parana	76.34	25.44	38.07	110.01	70.95	0.19	64.34
Ebro	52.52	45.10	17.54	22.17	3.89	58.60	0.15
Sao Francisco	54.66	44.68	21.93	29.06	7.38	60.39	0.15
Indus	39.87	14.83	43.18	103.61	58.66	43.88	34.10

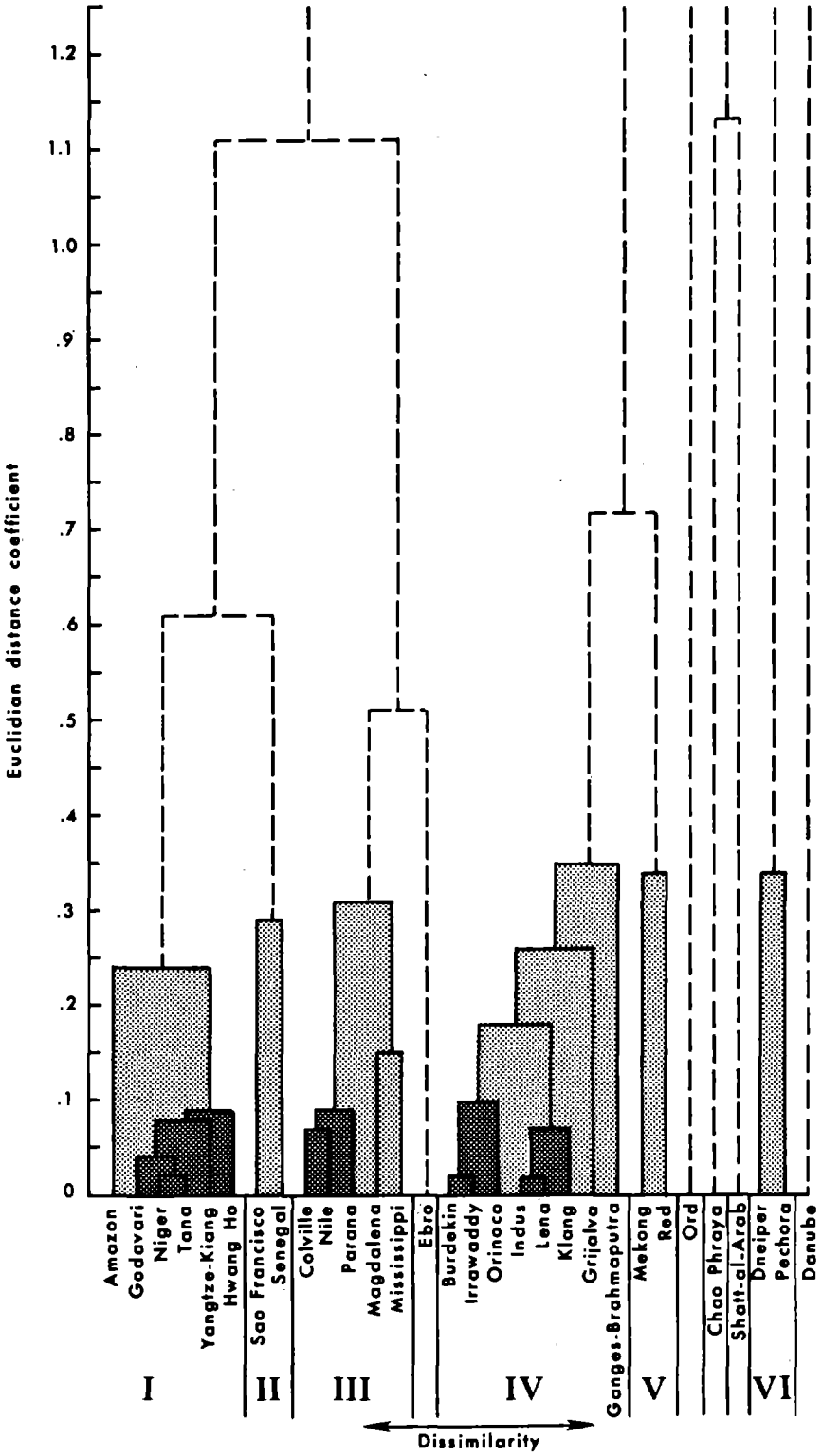

Figure 55. Cluster analysis dendrogram for river-mouth morphometry.

Linkages below d_{jk} levels of 0.4 yield six clusters of mutually similar river mouths. Five rivers remain separate at the accepted cluster cutoff distance. The central tendencies of each cluster and each of the five nonclustered rivers are presented in Table 28. Discriminant analysis (Table 29) suggests that these clusters are relatively homogeneous internally.

The river mouths of cluster I converge slightly upstream and have typically low depth/width ratios and bar crests situated comparatively near the outlets. The mouths of the Niger, some of which are shown in Figure 56, are representative of this type.

Powerful wave action causes the Sao Francisco (Fig. 57) and Senegal, the two rivers of cluster II, to have constricted river mouths. This constriction is very likely responsible for the moderately high mean depth/width ratio. Mean relative distance to the bar crest is only slightly greater than in cluster I.

Straight to very gently funnelling river mouths with high depth/width ratios and a strong tendency for the crests of the distributary-mouth bars to be situated at four river-mouth widths seaward of the mouths are the distinguishing characteristics of cluster III. The mouths of the prograding distributaries of the Mississippi River (Fig. 58) offer ideal examples of this type. The mouths of both the Ebro and the Danube are similar to the mouths in cluster III in the sense that they are relatively straight and have high depth/width ratios; however, the bar crest of the Ebro is situated immediately seaward of the mouth, whereas those of the Danube average 9.6 channel widths seaward of the mouth. Also, the depth/width ratios at the mouths of both these rivers are higher than in cluster III.

The eight rivers of cluster IV have shallow, funnel-shaped mouths and low depth/width ratios. Mean distance from the mouths to the bar crest is 2.95 b_o. Examples of this type of river mouth include the mouths of the Irrawaddy (Fig. 59) and Ganges-Brahmaputra (Fig. 60). Although the mouths of the Mekong (Fig. 61) and Red Rivers are roughly similar to the river-mouth type of cluster IV, they compose a fifth cluster because of somewhat greater depth/width ratios and greater distances to their bar crests. The mouths of the Mekong are also apparent in the satellite imagery shown in Figure 46.

The Dneiper and Pechora are the sole members of cluster VI, which is set apart primarily by extreme distances to the bar crests.

The mouths of the Chao Phraya (Fig. 62), Ord (Fig. 63), and Shatt-al-Arab (Fig. 53) all exhibit pronounced funnel shapes; however, in terms of depth/width ratio and distance to the bar crest they are mutually distinct.

Composite Delta Morphologies

The overall morphologic patterns exhibited by the entire delta as a unit reflect the combination of all 21 of the delta morphology variables just discussed. Hence the degree to which the similarities between deltas in terms of delta component ratios, dimensionless delta morphometry, delta landform suites, distributary patterns, and river-mouth forms intersect determines the composite morphology of the delta. In order to evaluate the similarities and dissimilarities between composite delta morphologies, an attempt was made to incorporate all salient morphologic properties into a single cluster analysis. To do this, it was necessary to reduce the initial 21 variables to a fewer number of factors by factor analysis and to use the resultant factor scores for each delta as input to the cluster analysis. Three separate factor analyses were performed on the following data subsets: (1) the delta component ratios

Table 28

River-Mouth Morphology Data

	River	$b(4b_o)/b_o$	d/W	Distance to Bar (Channel Width)
Cluster I	Amazon	0.90	0.15	6.00
	Godavari	0.90	0.43	2.00
	Niger	0.95	0.31	2.50
	Tana	0.90	0.19	2.50
	Yangtze-Kiang	0.83	0.12	3.20
	Hwang Ho	0.90	0.02	1.00
	Mean	0.89	0.20	2.86
	CV	0.83	0.64	0.54
Cluster II	Sao Francisco	1.20	0.87	1.50
	Senegal	1.10	0.50	4.70
	Mean	1.15	0.68	3.10
	CV	0.04	0.27	0.51
Cluster III	Colville	0.85	1.28	4.80
	Nile	0.90	1.15	3.00
	Parana	0.90	0.90	4.50
	Magdalena	1.00	1.80	3.00
	Mississippi	0.96	1.49	5.30
	Mean	0.92	1.32	4.12
	CV	0.05	0.22	0.23
	Ebro	0.90	1.90	0.47
Cluster IV	Burdekin	0.68	0.22	3.60
	Irrawaddy	0.69	0.08	3.40
	Orinoco	0.60	0.44	4.10
	Indus	0.55	0.07	2.10
	Lena	0.57	0.02	3.00
	Klang	0.45	0.05	2.06
	Grijalva	0.48	0.49	1.00
	Ganges-Brahmaputra	0.36	0.17	4.40
	Mean	0.54	0.19	2.95
	CV	0.19	0.87	0.36
Cluster V	Mekong	0.63	0.12	7.70
	Red	0.50	0.60	10.30
	Mean	0.56	0.36	9.00
	CV	0.11	0.80	0.14
	Ord	0.20	1.50	1.40
	Chao Phraya	0.15	0.07	10.50
	Shatt-al-Arab	0.43	0.28	17.50
Cluster VI	Dneiper	0.86	0.82	16.70
	Pechora	0.90	0.17	18.50
	Mean	0.88	0.49	17.60
	CV	0.02	0.64	0.05
	Danube	0.90	3.00	9.60
	Overall Mean	0.74	0.64	5.34
	Overall CV	0.34	1.09	0.90

Table 29

River-Mouth Morphology Discriminant Analysis--d^2 Values

Cluster	I	II	III	IV	V	VI
I	0.00	22.76	18.73	116.01	34.35	12.92
II	22.76	0.00	41.93	93.24	37.11	16.76
III	18.73	41.93	0.00	140.03	20.29	57.74
IV	116.01	93.24	140.03	0.00	58.88	109.70
V	34.35	37.11	20.29	58.88	0.00	63.01
VI	12.92	16.76	57.74	109.70	63.01	0.00

	Cluster					
Delta	I	II	III	IV	V	VI
Amazon	4.94	14.90	22.50	25.84	22.06	74.20
Godavari	1.04	11.52	17.25	19.07	37.73	125.04
Niger	0.58	8.43	20.08	24.56	40.58	118.75
Tana	0.08	13.37	24.29	19.01	37.09	122.00
Yangtze-Kiang	0.75	19.46	26.03	12.72	28.11	114.84
Hwang Ho	2.59	19.80	36.43	21.15	50.52	151.20
Sao Francisco	19.27	1.78	19.75	68.08	80.82	135.32
Senegal	10.16	1.78	17.34	50.95	48.76	87.63
Colville	23.59	22.80	0.93	35.49	27.85	85.96
Nile	14.88	14.21	1.41	31.54	36.07	106.95
Parana	10.51	11.58	2.83	28.62	26.23	85.27
Magdalena	42.60	25.41	4.37	68.31	64.36	117.85
Mississippi	33.38	20.94	1.58	56.83	42.16	81.30
Ebro	49.92	37.67	5.60	65.14	55.20	109.35
Burdekin	7.30	35.27	27.71	3.07	16.96	115.52
Irrawaddy	6.53	36.03	33.00	3.66	20.26	121.04
Orinoco	15.48	45.86	26.61	2.35	11.90	112.54
Indus	19.31	60.82	49.23	0.72	27.74	156.46
Lena	6.44	56.18	46.21	0.62	22.17	140.64
Klang	31.76	81.00	62.43	2.40	31.64	172.52
Grijalva	31.78	73.86	48.32	3.98	34.47	177.31
Ganges-Brahmaputra	44.03	95.68	64.72	5.97	19.93	146.98
Mekong	20.23	48.85	35.11	13.10	2.74	69.04
Red	53.94	82.65	44.57	32.96	2.74	54.20
Ord	111.40	159.80	88.96	51.05	72.16	232.52
Chao Phraya	104.46	166.35	114.75	47.34	26.60	120.09
Shatt-al-Arab	132.61	163.00	118.64	108.78	37.18	31.31
Dneiper	111.39	103.05	78.42	131.92	53.31	2.04
Pechora	124.70	120.42	112.13	152.20	68.53	2.04
Danube	169.49	135.66	70.26	184.80	127.30	117.76

A_u/A_l, $A_{subaerial}/A_{subaqueous}$, and $A_{abandoned}/A_{active}$; the morphometric parameters L_s/W, L_x/W; the protrusion index L_b/W_b; the bulge skewness $|V_r/V_l|$; the bulge volume distribution $\bar{\beta}$; and the subaqueous hypsometric integral H_s; (2) the relative abundance of active shoreline barriers, stranded beach ridges, bays and lakes, marshes and swamps, and tidal flats and tidal creeks; and (3) number of river mouths, ratio of distributary rejoinings to bifurcations, distributary density, the river-mouth

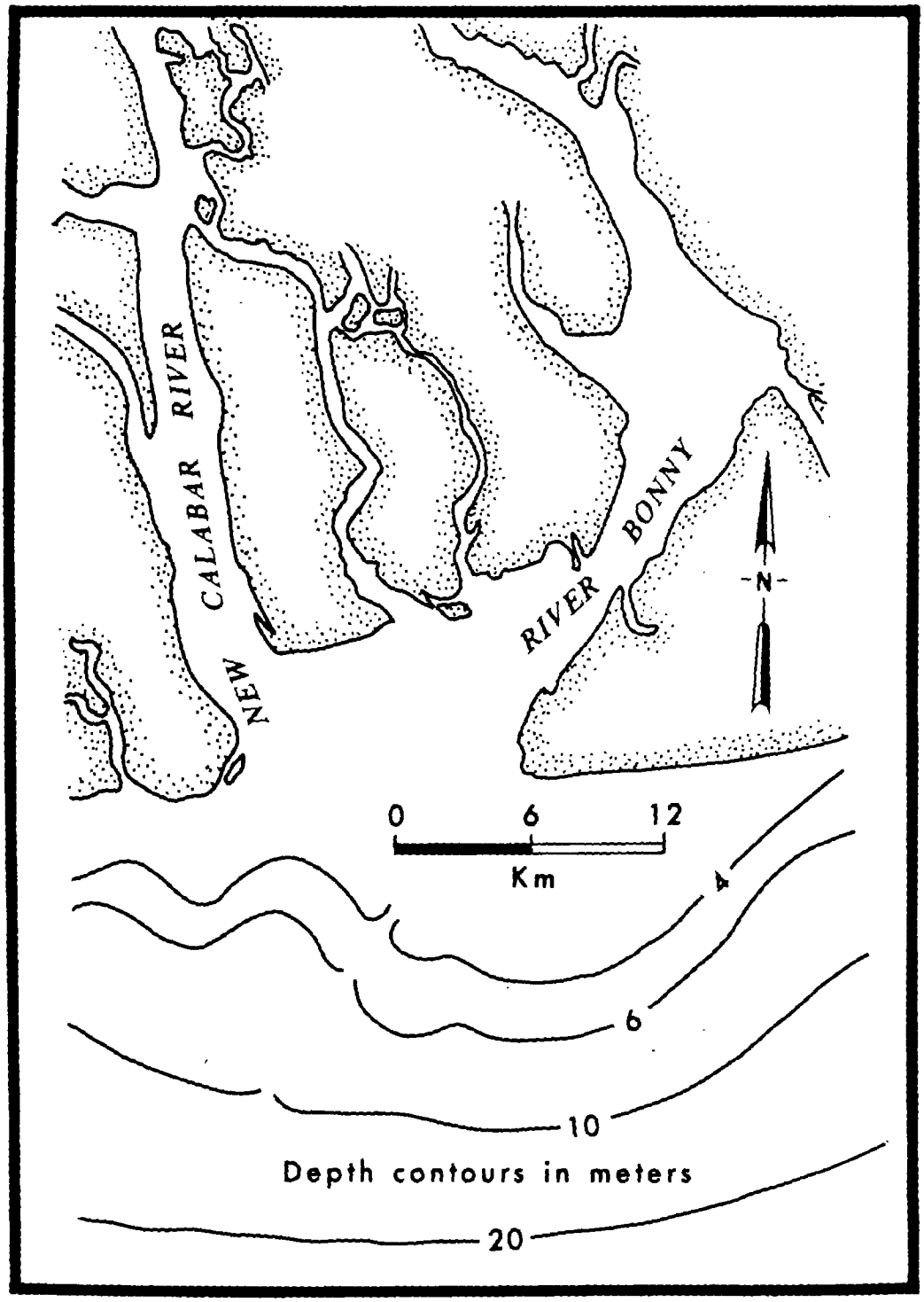

Figure 56. Mouths of two distributaries of the Niger River.

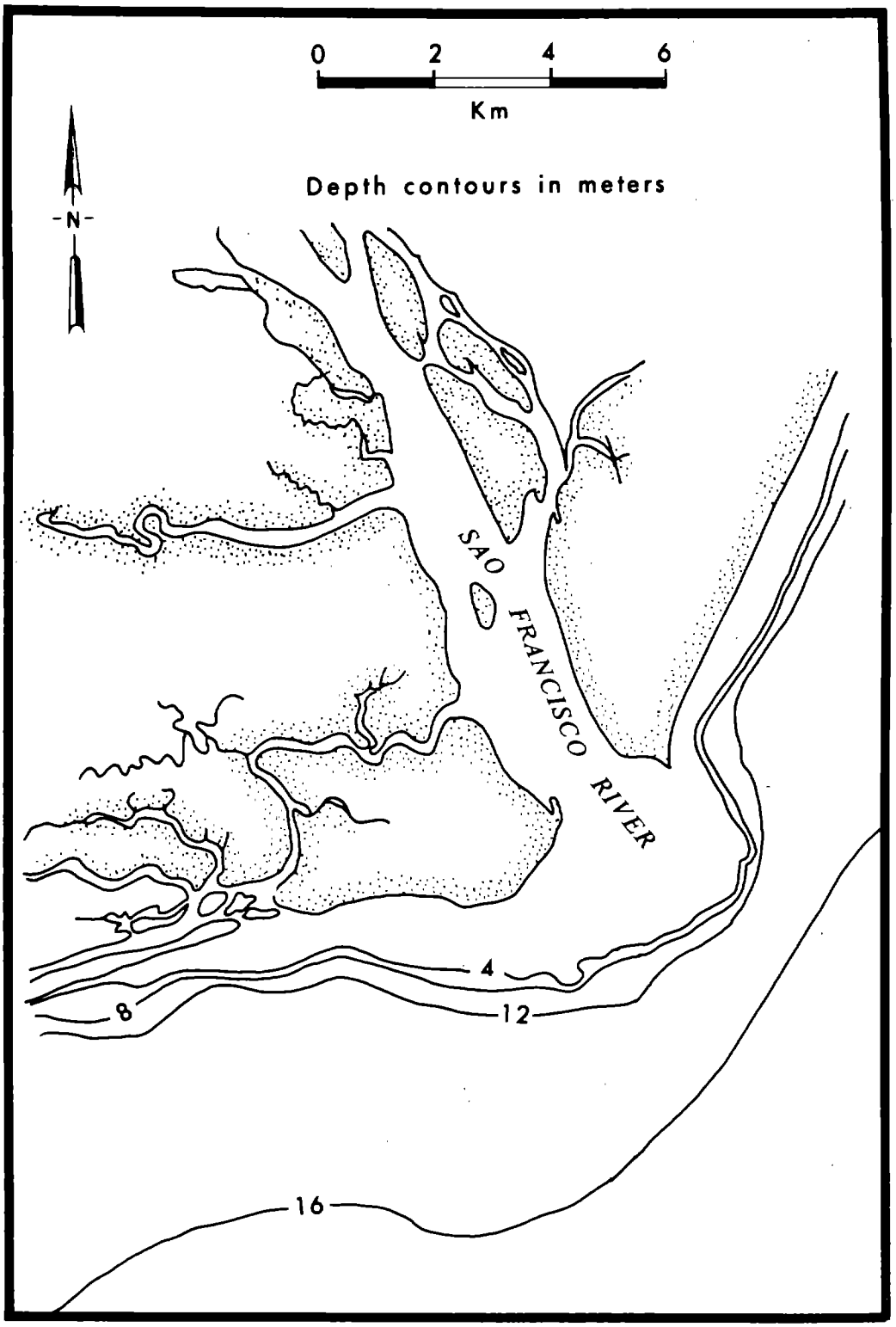

Figure 57. Constricted mouth of the Sao Francisco River.

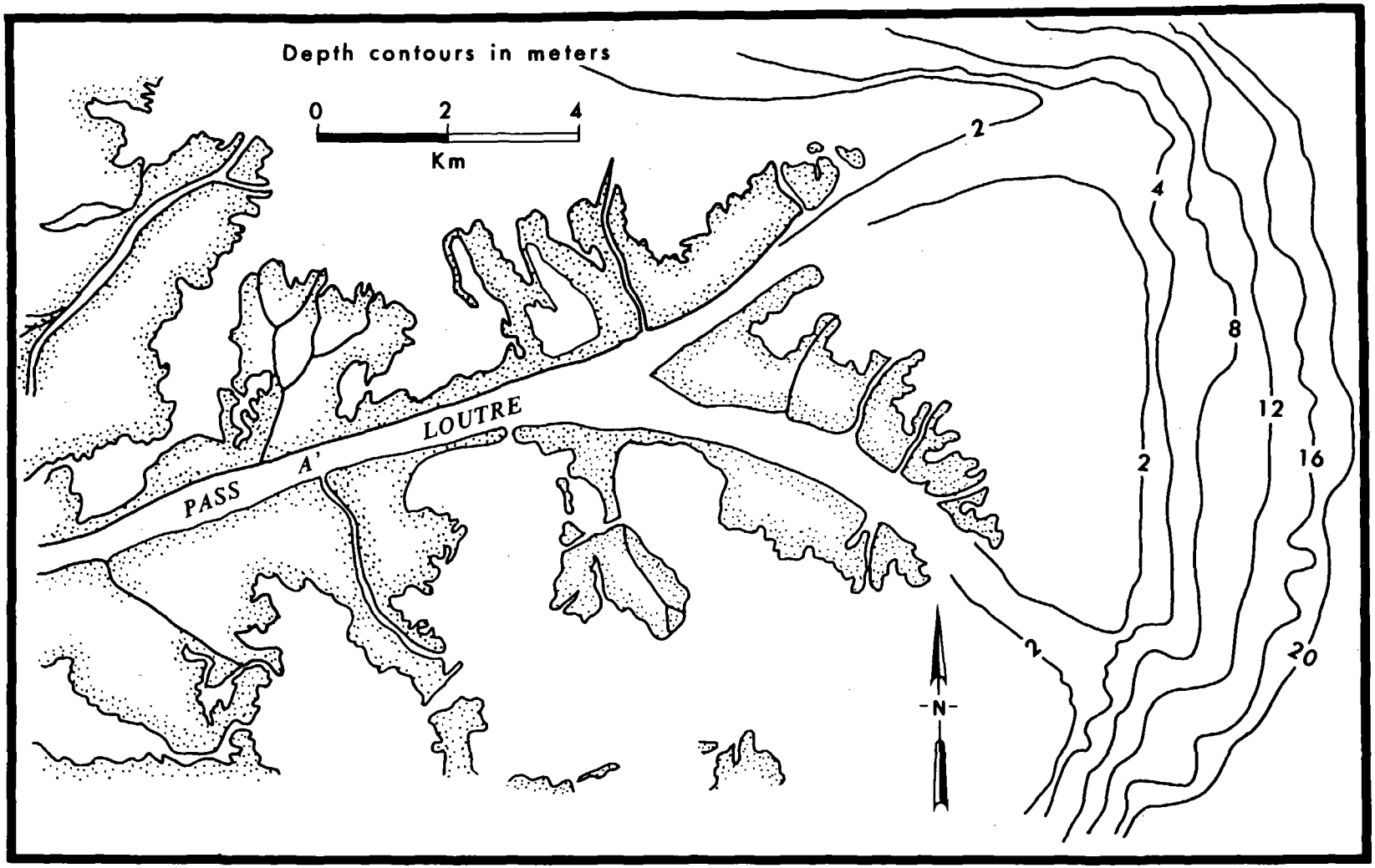

Figure 58. Mouths of Pass a Loutre, a distributary of the Mississippi River.

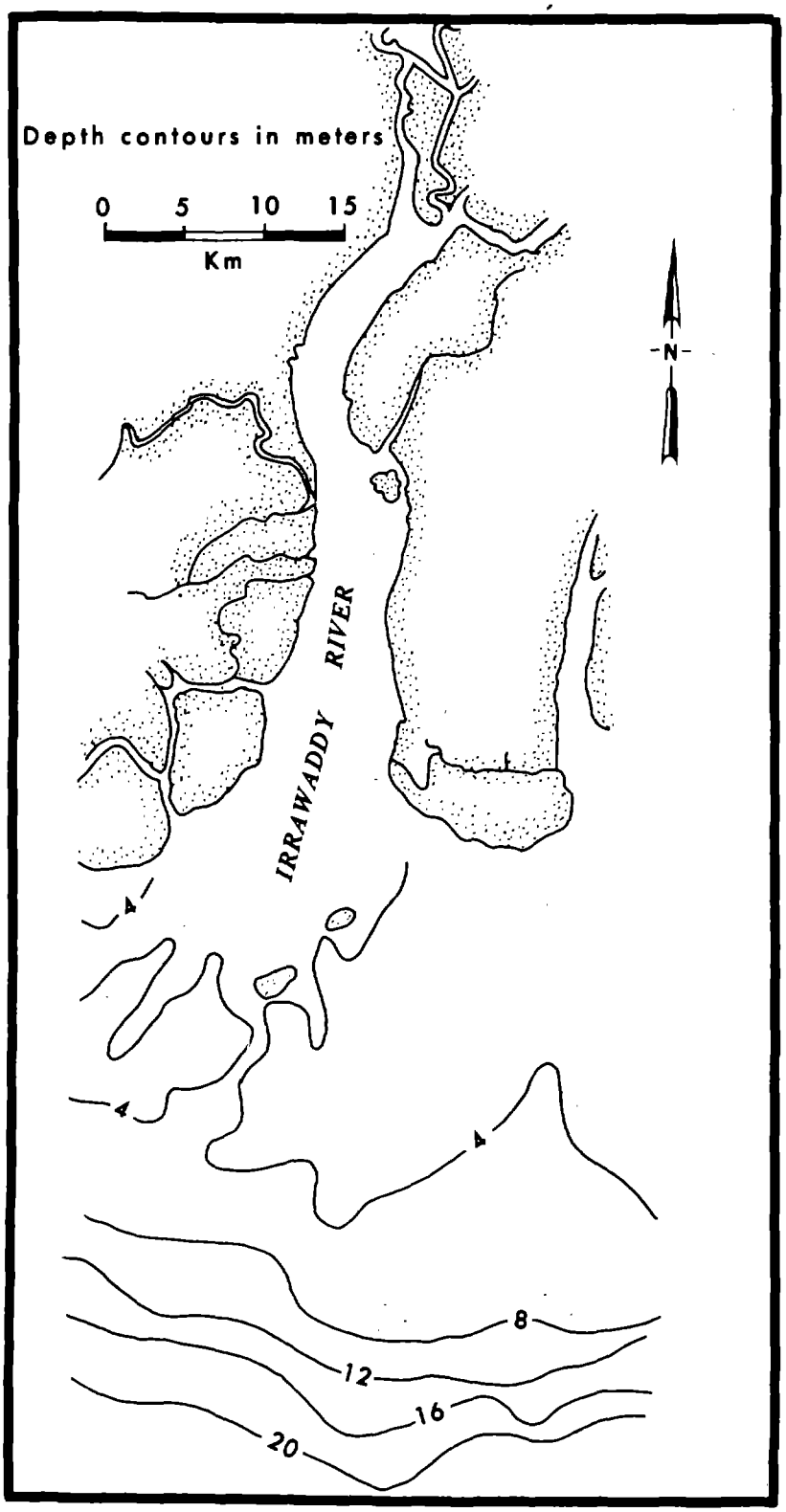

Figure 59. Mouth of the Irrawaddy River.

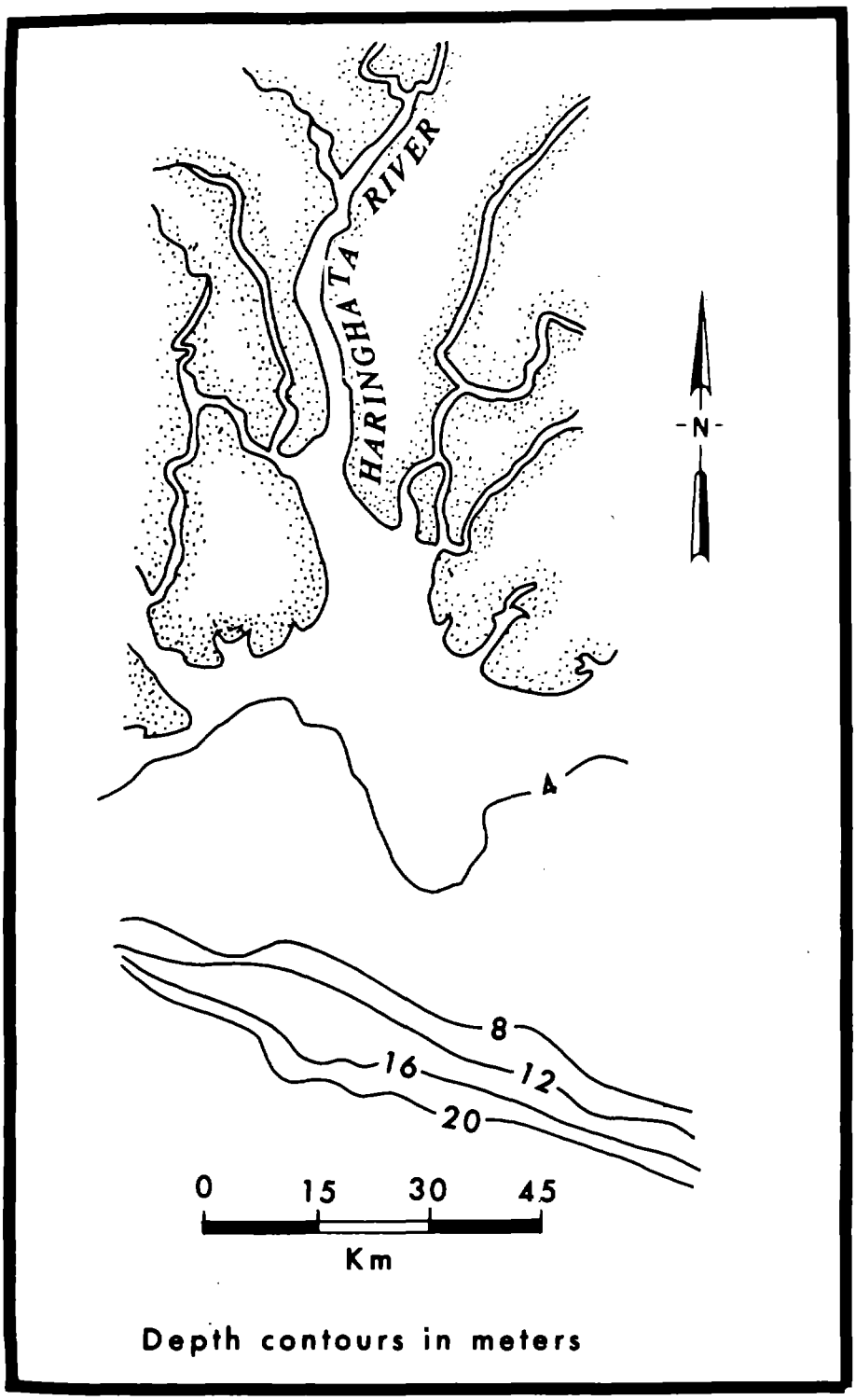

Figure 60. Mouth of a distributary of the Ganges-Brahmaputra River.

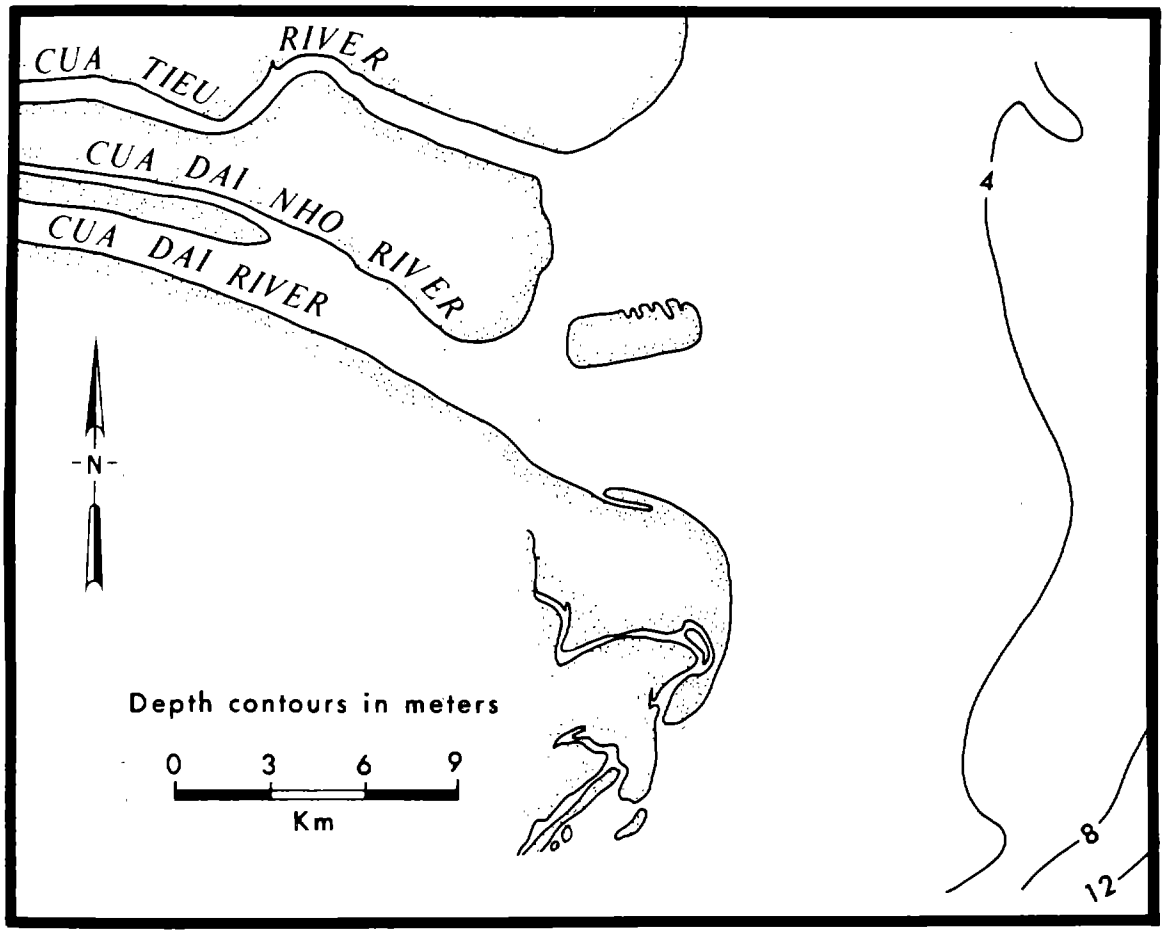

Figure 61. Mouths of the Mekong River.

depth/width ratio h_o/b_o, and the bar distance X_{bar}/b_o.

The results of factor analyses are presented in Tables 30-32. In these tables the eigenvalues corresponding to each significant factor and the unrotated and rotated factor matrices are given. As before, only those factors with eigenvalues greater than 1.0 are accepted as accounting for a significant proportion of the overall variability. The factor loadings presented in the factor matrix tables are equivalent to the square roots of the fraction of the variance of each variable that is accounted for by each factor. Correlation matrices are not presented because correlation coefficients for all pairs of variables within each of the three subsets were nonsignificant, indicating relative mutual independence among the variables examined. Through factor analysis the total number of variables in each variable subset was reduced to three significant factors, or a combined total of nine factors, resulting from the 20 input variables.

Cluster analysis results based on the factor scores of the nine factors are shown as a dendrogram in Figure 64. Although several linkages occur at relatively low distance coefficients, the dendrogram suggests that there are no well-defined clusters but rather a progressive hierarchy of dissimilarities, as indicated by the

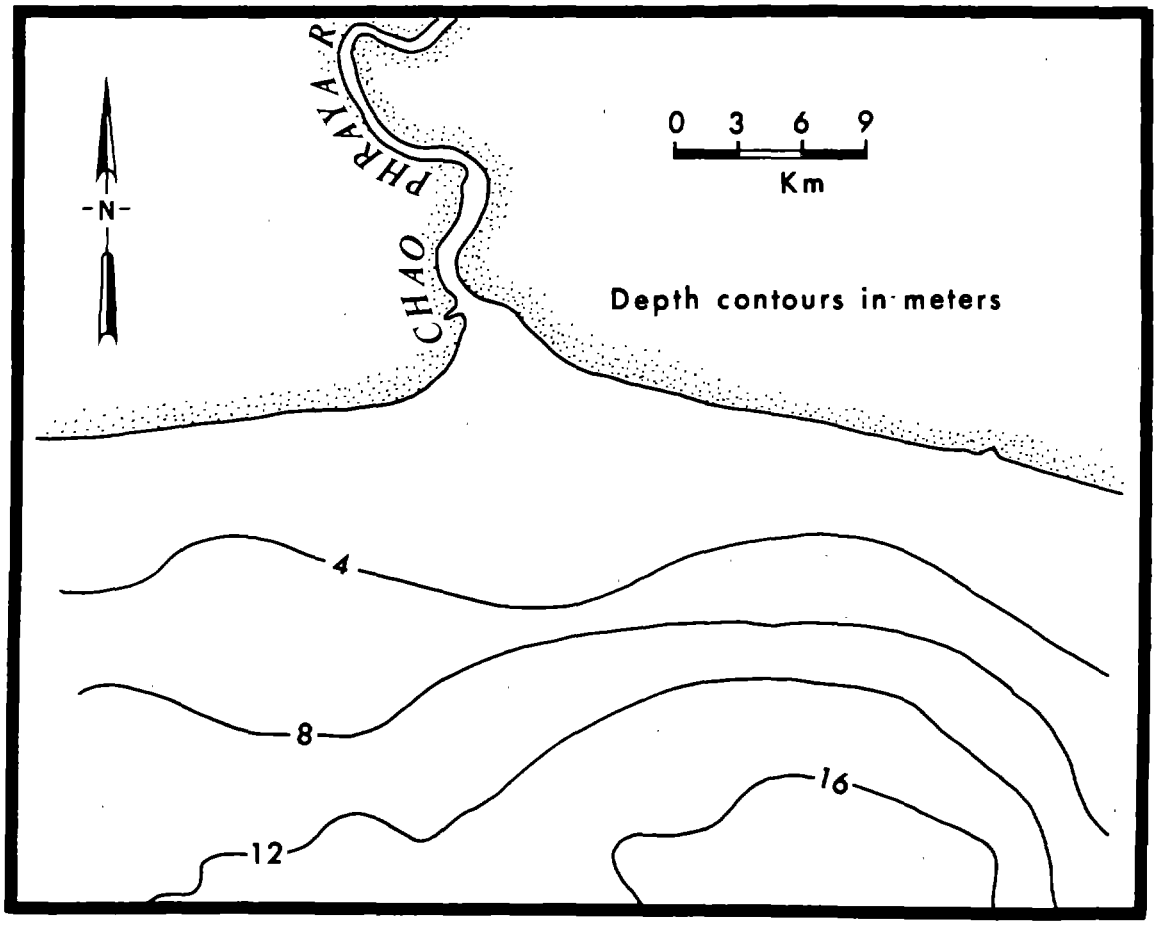

Figure 62. Mouth of the Chao Phraya.

absence of an objectively identifiable cluster cutoff distance. This situation points to the conclusion that, in terms of the composite delta morphology, individual deltas tend to be relatively unique with respect to one another. Thus, although deltas fall into reasonably homogeneous types as far as particular morphologic characteristics such as river-mouth form or landform suites are concerned, they comprise a semicontinuous morphologic spectrum when all morphologic characteristics are considered together.

As in the cases previously discussed, however, the dendrogram shows individual deltas arranged according to their mutual similarities, with each delta situated adjacent to its nearest analogue. A similarity matrix indicating the mutual similarities and dissimilarities between all pairs of deltas is presented in Table 33.

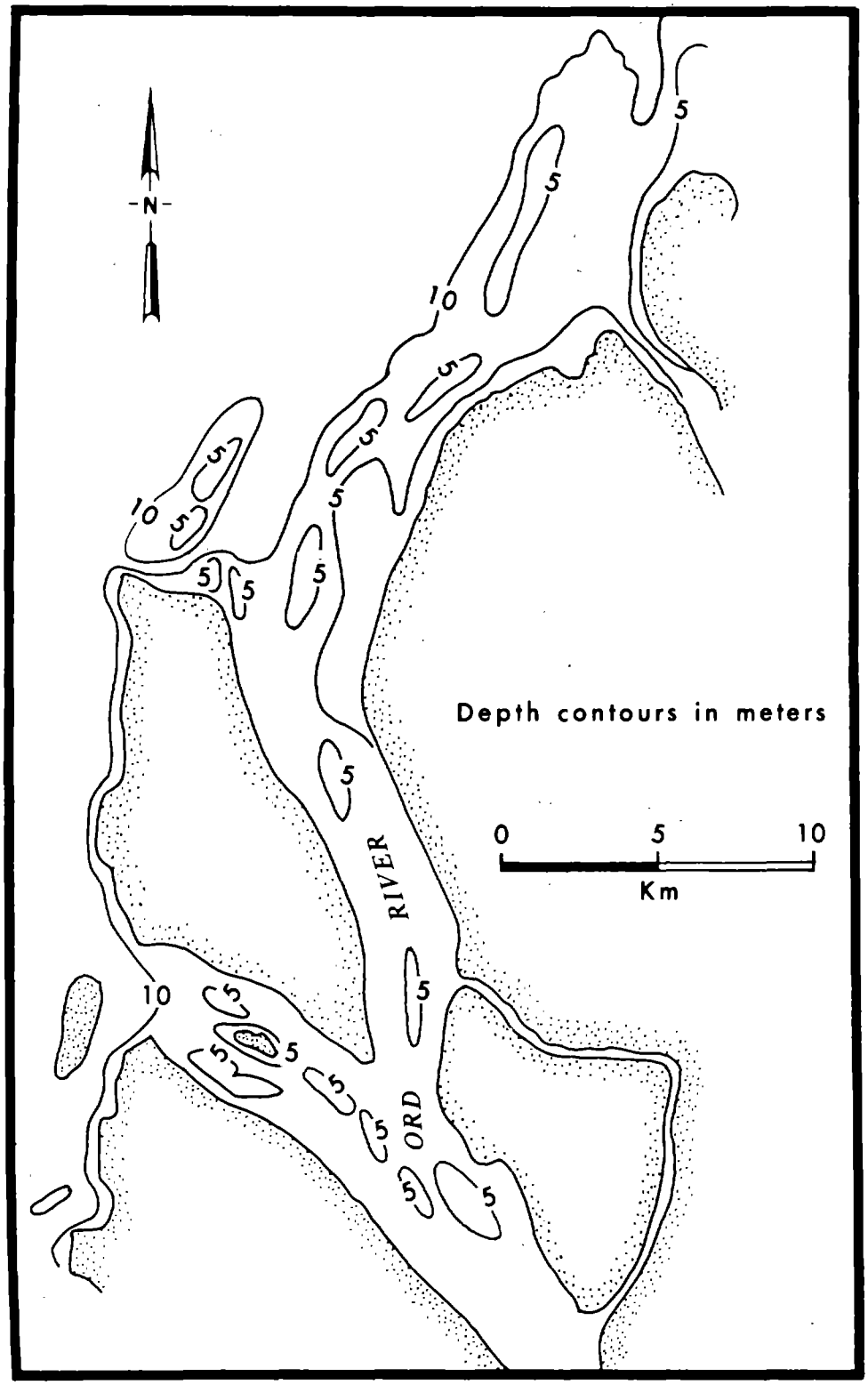

Figure 63. Mouth of the Ord River.

Table 30

Factor Analysis of Delta Morphometry and Delta Components

Variable No.	Variable	Mean	Standard Deviation	Factor Matrices: Unrotated Factor 1	Unrotated Factor 2	Unrotated Factor 3	Rotated Factor 1	Rotated Factor 2	Rotated Factor 3
1.	Upper Area/Lower Area	3.64	5.93	0.41	-0.63	-0.39	0.05	-0.84	-0.09
2.	Subaerial/Subaqueous	4.92	4.56	0.71	0.24	-0.44	0.78	-0.30	-0.26
3.	Abandoned/Active Delta	7.18	24.65	0.37	-0.71	-0.22	-0.05	-0.83	0.07
4.	Hypsometric Integral	0.47	0.10	-0.65	-0.44	0.12	-0.79	-0.01	0.03
5.	Shoreline Length/Maximum Width of Delta	1.55	0.42	-0.75	-0.13	-0.14	-0.67	0.19	-0.32
6.	Delta Plain - Length/Width	1.04	0.58	0.47	-0.44	0.10	0.13	-0.54	0.34
7.	Protrusion Index	0.42	0.28	-0.47	-0.53	-0.17	-0.66	-0.26	-0.17
8.	Bulge (Protrusion) Vol. - Right/Left	0.70	0.21	-0.49	0.05	-0.61	-0.30	0.06	-0.72
9.	Mean Vol. Distribution Parameter of Bulge	0.44	0.10	0.13	-0.33	0.80	-0.18	-0.05	0.86

Correlation Matrix

Variable No.	Variable	Variable No. 1	2	3	4	5	6	7	8	9
1.	Upper Area/Lower Area	1.00	0.27	0.60	-0.00	-0.17	0.20	0.09	-0.03	0.03
2.	Subaerial/Subaqueous	0.27	1.00	0.10	-0.51	-0.34	0.29	-0.38	-0.08	-0.27
3.	Abandoned/Active Delta	0.60	0.10	1.00	0.02	-0.14	0.27	0.08	-0.10	0.09
4.	Hypsometric Integral	-0.00	-0.51	0.24	1.00	0.44	-0.10	0.29	0.22	0.12
5.	Shoreline Length/Maximum Width of Delta	-0.17	-0.34	-0.14	0.44	1.00	-0.24	0.36	0.32	-0.12
6.	Delta Plain - Length/Width	0.20	0.29	0.27	-0.10	-0.24	1.00	0.15	-0.22	0.24
7.	Protrusion Index	0.09	-0.38	0.08	0.29	0.36	0.15	1.00	0.19	-0.10
8.	Bulge (Protrusion) Vol. - Right/Left	-0.03	-0.08	-0.10	0.22	0.32	-0.22	0.19	1.00	-0.36
9.	Mean Vol. Distribution Parameter of Bulge	0.03	-0.27	0.09	0.12	-0.12	0.24	-0.10	-0.36	1.00

	Factor 1	2	3	4	5	6	7	8	9
Eigenvalue	2.49	1.77	1.48	0.93	0.67	0.58	0.47	0.42	0.20

Table 31

Factor Analysis of Delta Landforms

Variable	Mean	Std. Deviation	Correlation Matrix: Active Barriers	Beach Ridges	Bays and Lakes	Marshes and Swamps	Tidal Flats	Factor Matrices: Unrotated Factor 1	Unrotated Factor 2	Unrotated Factor 3	Rotated Factor 1	Rotated Factor 2	Rotated Factor 3
Active Barriers	0.55	0.34	1.00	0.03	0.03	0.31	0.23	0.54	0.10	0.74	0.13	-0.08	0.91
Beach Ridges	0.52	0.26	0.03	1.00	-0.22	-0.31	-0.29	-0.54	-0.47	0.63	0.95	0.01	0.00
Bays and Lakes	0.40	0.34	0.03	-0.22	1.00	0.08	-0.47	-0.27	0.88	0.04	0.26	0.87	0.09
Marshes and Swamps	0.80	0.27	0.31	-0.31	-0.08	1.00	0.14	0.65	0.44	0.18	0.46	0.04	0.65
Tidal Flats	0.63	0.37	0.23	-0.29	-0.47	0.14	1.00	0.76	-0.46	-0.22	0.33	-0.83	0.19

Factor	1	2	3	4	5
Eigenvalue	1.66	1.41	1.03	0.63	0.27

As before, the values in this table are Euclidian distance coefficients, so that small values indicate similarity and large values indicate dissimilarity. The deltas are listed in order of their positions in the dendrogram.

Despite the overall heterogeneity which appears to characterize the delta population, the cluster analysis reveals some interesting but not unexpected patterns, including the existence of a few closely analogous pairs or triads of deltas. Particularly notable are the similarities between the Amazon and Yangtze-Kiang; the Irrawaddy, Mekong, and Red; the Ganges-Brahmaputra and Klang; the Orinoco and Parana; the Godavari and Nile; and the Indus and Niger. These similarities are attributable to corresponding similarities in process environments; some of their causes will be discussed in the next section. In addition to these close similarities, there are several other important associations. For example, the Ord and Shatt-al-Arab Deltas, which experience high tide ranges and arid climates, are similar at the 0.7 level. The Colville, Mississippi, Danube, Ebro, and Magdalena, though exhibiting significant differences, tend to fall together at distances below 2.0, as do the high-energy Sao Francisco and Senegal Deltas.

Because of the innumerable complex analogies and dissimilarities between deltas in terms of the variables and variable combinations just described, it is not feasible to discuss all of the possible similarities and mutual associations present; the interested reader may discern from the dendrographs, tables, and data presented many more relationships than have been discussed. In the discussion that follows, some of the most important process-form relationships responsible for the observed similarities and contrasts will be considered.

DELTAIC PROCESS-FORM VARIABILITY: A BRIEF SUMMARY

The morphologic contrasts, similarities, and groupings of deltas just described can be attributed to corresponding differences and similarities in forcing environments. However, it is typical of morphodynamic systems that the cause-effect relationships are bidirectional, so that the behavior of the dynamic forces in the immediate vicinity of the various deltaic forms can differ substantially from the incident, unmodified conditions. Furthermore, with a few possible exceptions, no single process subsystem (such as alluvial-valley discharge regime or receiving-basin energy regimes) can be invoked to explain deltaic patterns because all factors interact to produce the observed morphology. Hence, the associations between the

Table 32

Factor Analysis of River-Mouth and Distributary-Network Morphology

Variable Number	Variable	Mean	Standard Deviation	Factor Matrices: Unrotated Factor 1	Unrotated Factor 2	Unrotated Factor 3	Rotated Factor 1	Rotated Factor 2	Rotated Factor 3
1.	River Mouth Type	0.74	0.26	0.77	-0.15	-0.34	0.73	-0.05	-0.43
2.	Number of Active River Mouths	7.56	6.27	0.41	-0.56	0.37	0.24	-0.74	-0.13
3.	No. Rejoinings/No. Bifurcations	0.36	0.33	0.14	-0.69	-0.60	0.02	-0.15	-0.91
4.	River Mouth - Depth/Width	0.64	0.70	0.69	0.16	0.52	0.67	-0.37	0.43
5.	Distributary Density	0.20	0.17	0.72	0.33	-0.12	0.79	0.16	0.45
6.	Distance to Bar/River Mouth Width	5.34	4.82	-0.15	-0.63	0.49	0.32	-0.74	-0.03

Correlation Matrix

Variable Number	Variable	Variable Number	1	2	3	4	5	6
1.	River Mouth Type		1.00	0.18	0.28	0.30	0.39	-0.11
2.	Number of Active River Mouths		0.18	1.00	0.16	0.24	0.03	0.17
3.	No. Rejoinings/No. Bifurcations		0.28	0.16	1.00	-0.19	-0.02	0.12
4.	River Mouth - Depth/Width		0.30	0.24	-0.19	1.00	0.35	0.02
5.	Distributary Density		0.39	0.03	-0.02	0.35	1.00	-0.19
6.	Distance to Bar/River Mouth Width		-0.11	0.17	0.12	0.02	-0.19	1.00

	Factor	1	2	3	4	5	6
Eigenvalue		1.80	1.35	1.12	0.74	0.54	0.44

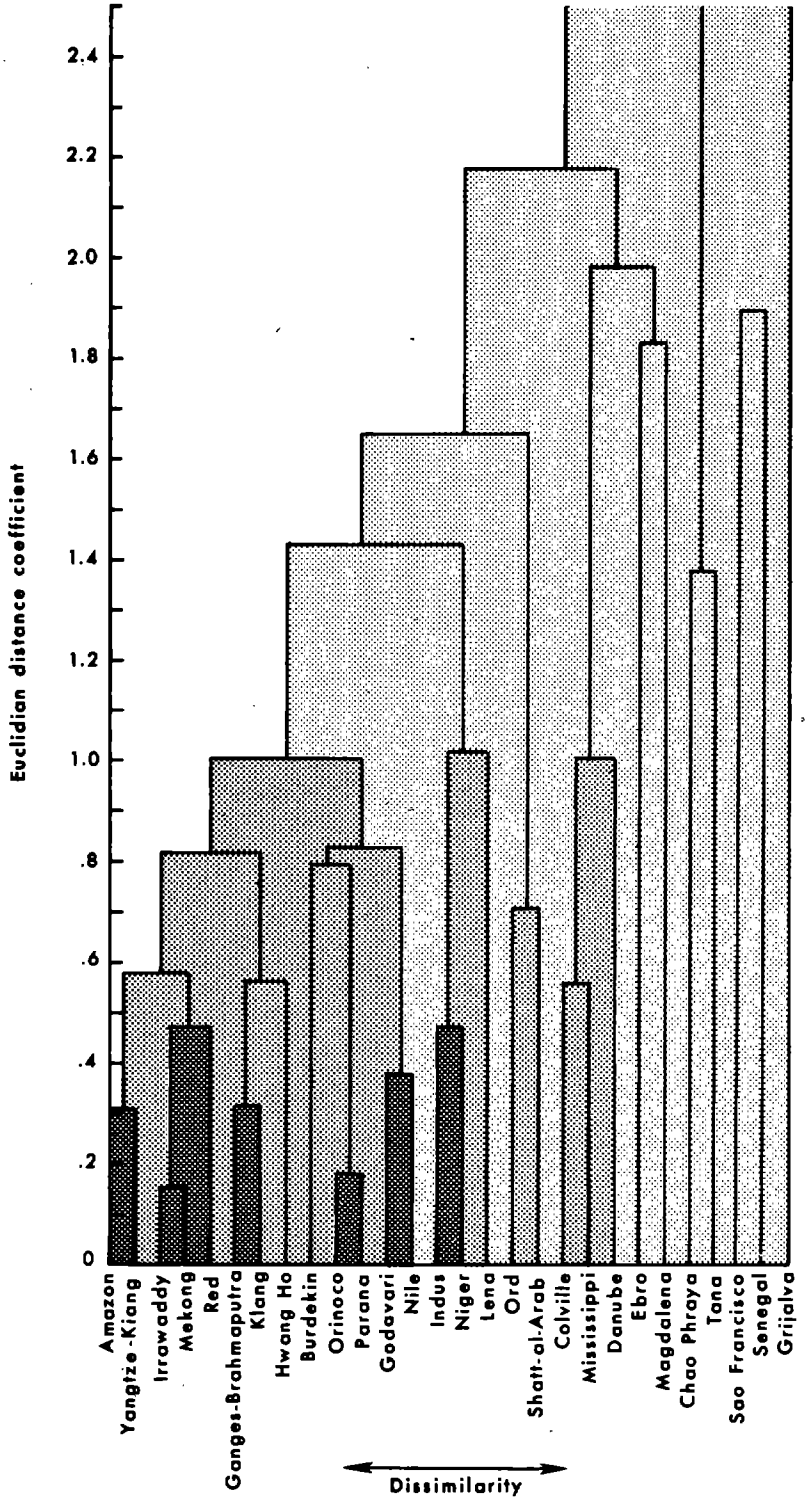

Figure 64. Cluster analysis dendrogram for deltas based on combined factor scores.

form and process groupings just described are highly complex and elude direct statistical correlation. Moreover, attempts to demonstrate process-form relationships by inferential statistics were precluded by the small sample size, large number of important variables, and consequent insufficient degrees of freedom. Nevertheless, the comparisons just presented reveal many interesting process-form relationships. An exhaustive discussion of these relationships would require a very lengthy report. The purpose of this section is simply to summarize some of the more prominent relationships; the reader may identify many other process-form associations from further analysis of the data presented in this report.

The Drainage Basin and the Discharge Regime

In accordance with logical expectations, the data indicate direct correspondence between drainage-basin climate and size and the discharge regime of the alluvial valley: the largest and wettest basins yield the greatest discharge volume, and arid basins or basins with pronounced seasonal variations in precipitation are associated with erratic or seasonally variable discharge regimes. The actual roles of basin geomorphic factors are less obvious. Although basin morphology must certainly influence sediment discharge, the general lack of sediment data did not allow demonstration of the relationship.

A comparison of Tables 2 and 19 suggests a rough tendency for the largest deltas to derive from the largest basins. However, because factors such as the geologic framework of the delta and energy conditions in the receiving basin also affect the area of the delta, there is by no means direct correspondence between basin area, or even total discharge, and delta area.

More important are the roles that the total discharge and discharge concentration per unit width of river mouth play in determining the degrees to which delta morphologies are river dominated or the products of marine forces. The writers have demonstrated previously, however, that discharge regime alone is insufficient to explain deltaic morphologic patterns; it must be considered in terms of its ability to prevail over marine forces (Wright and Coleman, 1971b, 1972, 1973). It is not simply the strength of the river that matters, but the strength of the river relative to the strength of the opposing waves or tides of the receiving basin. Hence, before river discharge effects can be further evaluated, the nearshore marine energy regimes with which river discharge interacts must be considered.

Nearshore Marine Energy Climate and Discharge Effectiveness

Overall, the morphologic likenesses and contrasts of deltas, as discussed earlier, exhibit only weak correspondence to the deepwater wave regimes of the receiving basins. This apparent lack of cause-effect association arises largely from the fact that the wave climate in the nearshore region often differs substantially from the deepwater wave climate owing to wave modification by the subaqueous topography of the delta front and offshore regions. These modifications result largely from wave refraction and attenuation by bottom friction; the significance of these effects on wave climates and resulting morphologies of deltas has been discussed in Wright and Coleman (1971b, 1972, 1973).

A computer program was developed to take into account the effects of refraction, shoaling, and frictional attenuation. This program was applied to seven deltas in previous reports to permit a more accurate estimate of the nearshore wave climate. Unfortunately, it was not possible to subject data from all 34 deltas to this type of analysis because the large amounts of detailed input data required by the procedure were in many cases unavailable. However, the procedures were successfully

Table 33

Similarity Matrix from Factor Scores for Composite Delta Morphology--Euclidian Distance Coefficients d_{jk}

Delta	Amazon	Yangtze-Kiang	Irrawaddy	Mekong	Red	Ganges-Brahmaputra	Klang	Hwang Ho	Burdekin	Orinoco	Parana	Godavari	Nile	Indus
Amazon	0.0													
Yangtze-Kiang	0.313	0.0												
Irrawaddy	0.460	0.188	0.0											
Mekong	0.869	0.453	0.155	0.0										
Red	0.763	0.714	0.456	0.500	0.0									
Ganges-Brahmaputra	0.651	0.568	0.781	0.791	0.783	0.0								
Klang	1.047	0.829	0.899	0.930	1.062	0.316	0.0							
Hwang Ho	0.872	0.506	0.698	1.064	0.774	0.671	0.464	0.0						
Burdekin	1.200	0.682	0.683	0.756	0.932	1.013	0.860	0.631	0.0					
Orinoco	0.818	0.695	0.810	0.984	0.480	0.424	0.847	0.564	0.657	0.0				
Parana	1.157	1.020	1.015	1.218	0.716	0.808	1.338	0.969	0.934	0.176	0.0			
Godavari	1.081	0.666	0.876	1.293	1.001	1.082	1.337	0.524	0.552	0.372	0.528	0.0		
Nile	1.327	1.113	1.460	2.250	1.814	2.086	2.289	1.006	1.144	1.168	1.210	0.378	0.0	
Indus	1.523	1.170	1.117	1.642	1.382	1.967	1.288	0.580	0.980	1.653	1.962	1.423	1.460	0.0
Niger	1.309	1.060	0.890	2.439	1.231	2.439	2.259	1.208	1.400	1.891	1.986	1.624	1.468	0.472
Lena	1.396	1.016	0.728	1.014	0.820	1.610	1.280	0.714	1.650	1.593	1.991	1.494	2.061	1.091
Ord	1.905	1.862	1.536	1.491	1.325	1.086	0.460	1.019	1.157	1.306	1.729	1.956	3.026	1.488
Shatt-al-Arab	1.886	1.849	1.519	1.180	1.013	0.942	0.968	1.596	1.000	0.854	1.099	1.639	2.927	2.701
Colville	1.849	1.698	1.160	1.450	0.993	1.812	1.804	1.311	1.441	0.987	0.753	0.965	1.589	1.954
Mississippi	1.966	1.884	1.670	2.288	1.272	2.094	2.444	1.378	2.334	1.086	0.897	1.067	1.552	2.236
Danube	3.226	3.355	2.662	3.195	1.891	3.677	3.686	2.609	3.605	2.591	2.058	2.781	2.918	2.691
Ebro	3.371	2.661	2.660	3.000	2.560	2.375	2.008	1.441	1.452	1.394	1.250	1.070	1.732	2.240
Magdalena	2.359	2.632	2.955	4.094	2.848	2.905	2.712	1.467	2.757	2.007	2.132	1.449	1.022	2.045
Chao Phraya	1.133	1.898	1.841	2.041	1.590	1.161	1.103	1.751	2.854	2.050	2.634	3.068	3.697	2.634
Tana	1.361	2.046	1.846	2.188	2.673	1.781	1.511	2.385	2.448	2.512	2.932	2.858	3.297	3.064
Sao Francisco	3.005	2.923	2.587	3.313	3.027	3.815	2.821	2.055	1.612	2.791	2.978	1.999	1.742	1.330
Senegal	2.217	2.439	2.410	3.171	2.714	4.139	4.018	2.676	2.172	3.157	3.326	2.313	1.335	1.988
Grijalva	5.059	5.073	4.673	4.688	4.818	4.865	4.096	4.436	3.880	4.840	4.461	4.736	4.501	4.592

Table 33 continued

Delta	Niger	Lena	Ord	Shatt-al-Arab	Colville	Mississippi	Danube	Ebro	Magdalena	Chao Phraya	Tana	Sao Francisco	Senegal	Grijalva
Amazon														
Yangtze-Kiang														
Irrawaddy														
Mekong														
Red														
Ganges-Brahmaputra														
Klang														
Hwang Ho														
Burdekin														
Orinoco														
Parana														
Godavari														
Nile														
Indus														
Niger	0.0													
Lena	1.276	0.0												
Ord	2.734	1.674	0.0											
Shatt-al-Arab	3.421	2.377	0.702	0.0										
Colville	2.080	1.278	1.585	1.424	0.0									
Mississippi	2.122	1.469	2.681	2.741	0.558	0.0								
Danube	2.416	1.912	3.339	3.578	1.067	0.998	0.0							
Ebro	3.406	2.887	1.860	2.046	1.223	1.723	3.083	0.0						
Magdalena	2.802	2.502	2.962	3.851	1.917	1.398	2.563	1.834	0.0					
Chao Phraya	3.225	1.854	1.445	2.059	2.878	3.277	3.678	4.731	3.339	0.0				
Tana	3.674	2.896	1.691	2.223	2.707	3.906	5.204	4.215	3.493	1.377	0.0			
Sao Francisco	2.117	2.865	2.190	3.164	2.072	3.158	3.843	2.041	2.038	4.547	2.985	0.0		
Senegal	1.535	3.052	4.273	4.180	3.243	3.973	3.966	4.586	3.004	4.432	4.103	1.886	0.0	
Grijalva	5.661	4.962	3.615	3.452	3.868	6.214	4.662	4.263	5.195	4.701	4.582	4.265	4.220	0.0

Table 34

Mean Annual Wave Power

Delta	Nearshore Wave Power x 10^7 Ergs Sec^{-1}	10-m Wave Power x 10^7 Ergs Sec^{-1}	Attenuation Ratio
Shatt-al-Arab	0.014	5.35	976.77
Danube	0.033	49.08	1,598.63
Mississippi	0.034	181.83	5,302.78
Yangtze-Kiang	0.127	54.68	430.55
Ebro	0.155	180.25	1,162.90
Amazon	0.193	204.42	1,052.00
Irrawaddy	0.193	245.50	2,028.83
Hwang Ho	0.218	83.50	310.00
Ganges-Brahmaputra	0.585	732.30	914.00
Chao Phraya	0.736	220.58	1,052.00
Ord	1.000	19.60	20.11
Niger	2.000	174.50	70.76
Burdekin	6.410	98.83	16.43
Nile	10.250	128.16	12.65
Indus	14.150	914.30	64.61
Sao Francisco	30.420	594.90	20.35
Senegal	112.420	284.92	2.60
Magdalena	206.250	916.60	4.44

applied to 18 delta coastlines. The results of the analyses of these 18 delta wave climates and associated morphologies remain in agreement with the writers' previous conclusions (Wright and Coleman, 1971b, 1972, 1973). In Table 34 these 18 deltas are listed in order of increasing nearshore wave power, together with the mean annual wave power at the 10-meter contour and the mean annual attenuation ratio indexing the wave power at the 10-meter contour to the nearshore wave power. Monthly variations in average wave power per meter of wave crest at the 10-meter contour and at the shoreline and in the longshore component of wave power are illustrated by the graphs in Figure 65. From Table 34 and the graphs it is apparent that nearshore wave power by no means directly reflects deepwater wave power but is to a greater extent a function of the attenuation ratio. The latter is in turn dependent on the offshore slope fronting the delta and on the height of the incident waves; the flatter the slope and the greater the original wave height, the greater is the amount of attenuation. Hence, the lowest nearshore wave-power values tend to occur along delta coasts which are fronted by the flattest offshore profiles.

The morphologic similarities and contrasts among deltas, as discussed earlier, show some gross tendencies to parallel the nearshore wave climate spectrum. In general, coastal barriers and interdistributary beach ridges become more abundant, delta shorelines become straighter, and deltaic protrusions become more subdued as nearshore wave power increases and as offshore slopes steepen.

Delta morphology cannot be attributed solely to nearshore wave climate, however, inasmuch as deltas result from fluvial as well as marine forces. The actual delta form depends on the degree to which the river is able to play the dominant role as a morphologic control. In order to index the relative delta-molding ability of river discharge, a ratio referred to as the "discharge effectiveness index" was

devised (Coleman and Wright, 1971; Wright and Coleman, 1971b, 1972, 1973). This quantity is the ratio of the discharge per unit width of river mouth of the nearshore wave power per unit width of wave crest. Although the absolute value of this ratio probably has little or no physical meaning, the relative values and ordering provide a highly significant means of comparing the degree of riverine dominance between deltas.

Table 35 lists 16 deltas in order of decreasing discharge effectiveness with index values normalized relative to the maximum. The Mississippi Delta has the largest discharge effectiveness (normalized value of 1.0) and is consequently the one most dominated by the river, whereas the Senegal Delta exhibits the lowest value (normalized value of 5.99×10^{-5}) and is thus the one most dominated by waves. In accordance with the conclusions presented by Wright and Coleman (1973), delta morphologies define a broad range of patterns between the two extremes. At the river-dominated (high discharge effectiveness) end of the spectrum, deltas are highly indented and have extended distributaries and marshes, bays, or tidal flats in interdistributary regions. With increasing nearshore wave power and decreasing discharge effectiveness, delta shorelines tend to become more regular, and gentle, arcuate protrusions and beach ridges become more common. The highest nearshore wave-power values and lowest discharge-effectiveness indices are associated with deltas which exhibit wave-straightened shorelines and abundant beach ridges.

Despite the generalities just discussed, wave and discharge regimes alone do not explain the entire range of deltaic landscapes, particularly under extreme conditions of climate, tide range, or subsidence rate. Deltas in macrotidal environments are characterized by abundant tidal flats and tidal creek networks in their interdistributary areas. Climatic effects are equally significant: those deltas with abundant swamps or other interdistributary vegetation tend to occur in humid environments, whereas arid delta climates are associated with barren evaporite flats. Numerous thaw lakes are common in arctic deltas.

River-Mouth Process-Form Variability

The forms of river mouths and lower river courses also exhibit a broad range of variability. Studies of river-mouth processes conducted by the writers in connection with the Coastal Information Program have revealed some of the physical reasons for this variability (Wright, 1970, 1971; Wright and Coleman, 1971a and in press; Wright, Coleman, and Thom, 1973). The reader is referred to these reports for detailed discussions. In brief, the systematic investigations suggest that river-mouth morphology reflects differences in the relative importance of the mechanisms of effluent buoyancy, inertia, bottom friction, and bidirectional bottom shear. The intensities of these effects are, in turn, dependent on the sharpness of water-density contrasts at the river mouth, the depth and slope of the bottom fronting the river mouth, and the tidal range and strength of tidal currents. Investigations at the mouths of the Mississippi River have suggested that flow tendencies associated with the expansion of buoyant effluents may be responsible for maintaining straight, parallel distributary levees and high depth-width ratios. These buoyant effects are dominant when the tidal prism is minor relative to river discharge, allowing salt wedges to intrude into channels wihout appreciable tidal mixing. This type of river-mouth system characterizes the Mississippi, Danube, Po, and Magdalena Rivers. The effects of bottom friction play a major role in controlling effluent expansion and deceleration when outflow velocities are high relative to water depths in and immediately beyond the outlet. Under these conditions, the river-mouth effluents expand and decelerate more rapidly, producing distributary levees which diverge downstream and middle-ground-type bars. River mouths in macrotidal environments tend to experience strong bidirectional flow and appreciable tidal mixing,

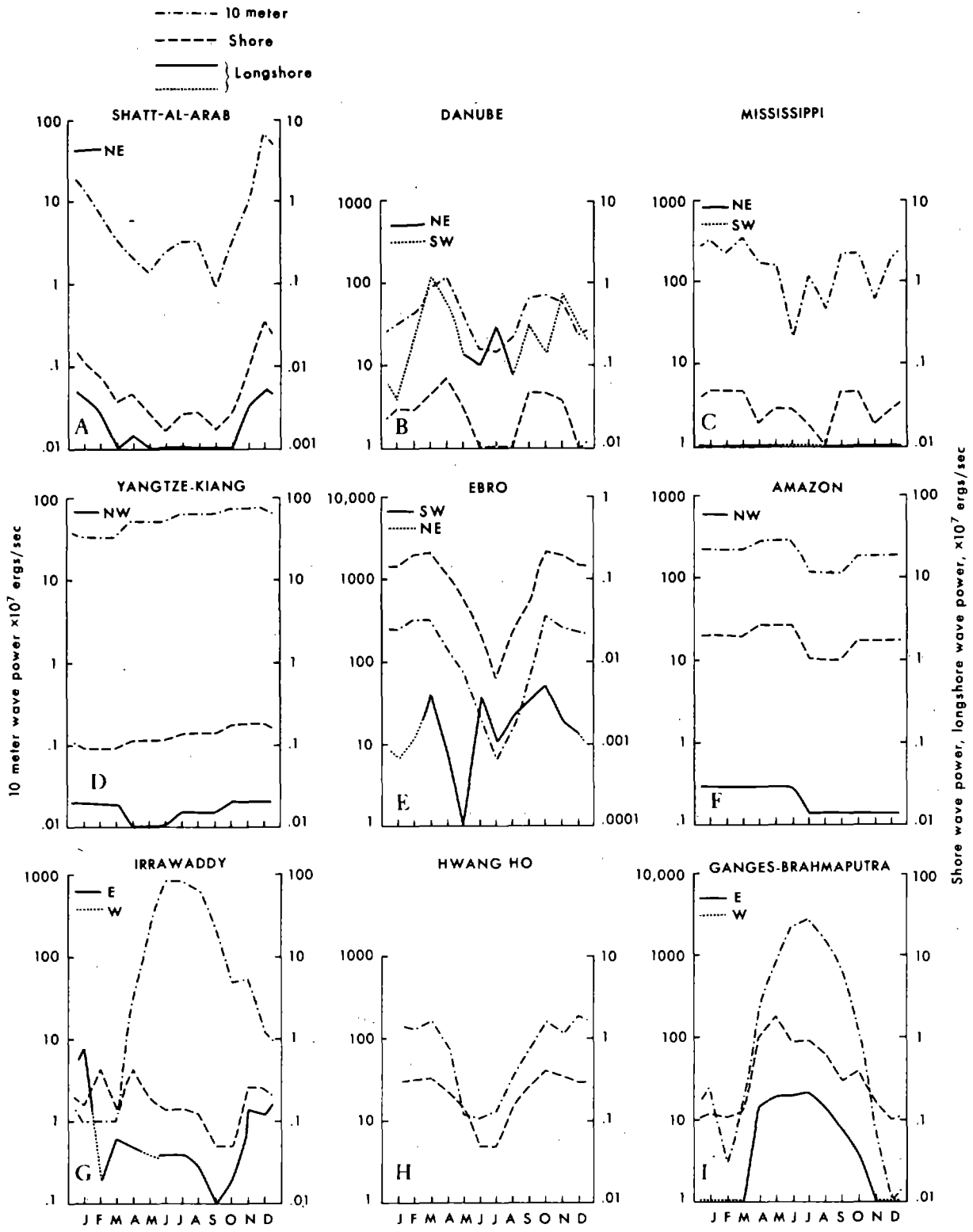

Figure 65. Monthly mean wave power at the 10-meter contour and shoreline and monthly mean longshore power of 18 deltas.

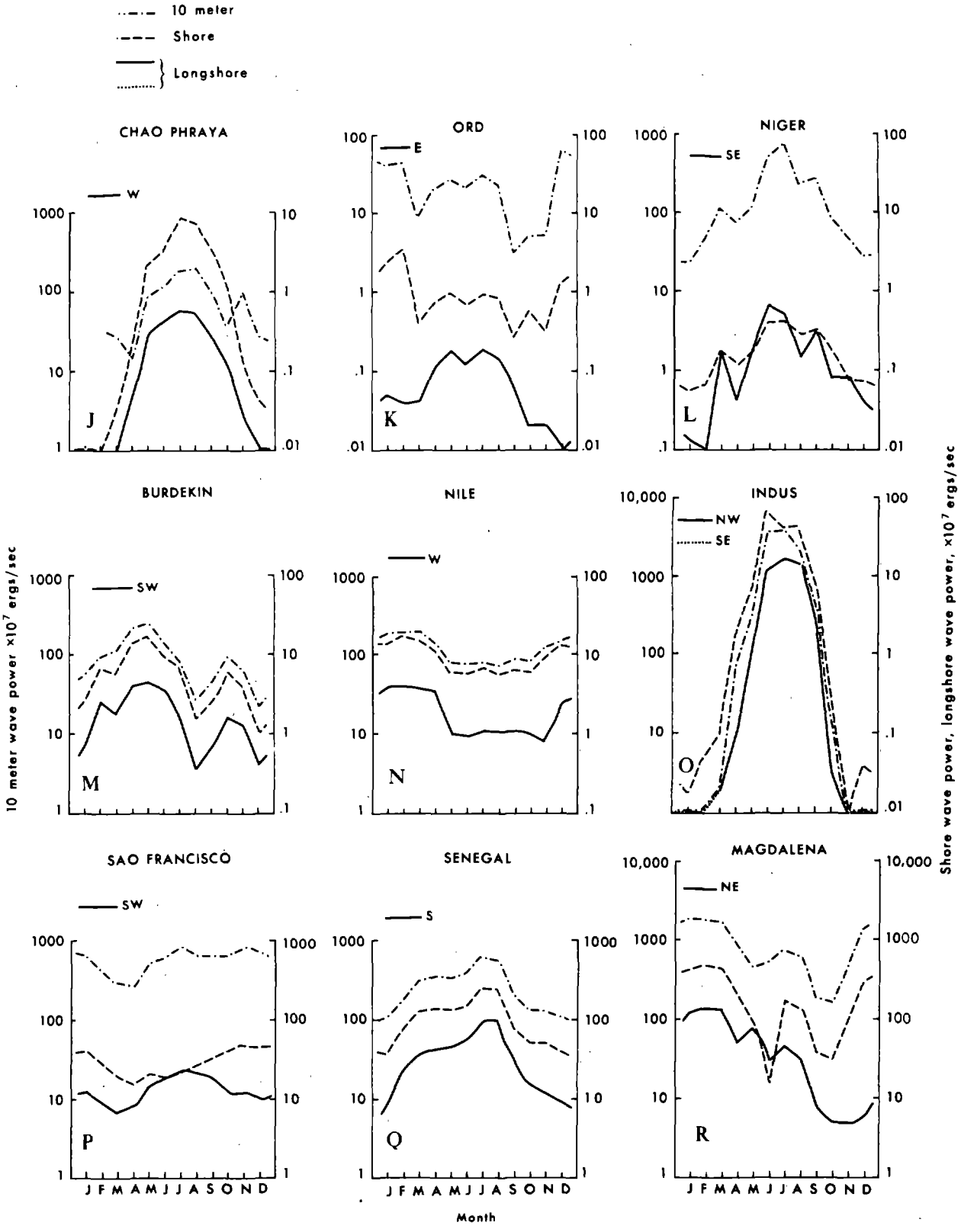

Figure 65 continued.

Table 35

Discharge Effectiveness of Sixteen Rivers

River	Discharge Effectiveness Index (Relative to Maximum)	River	Discharge Effectiveness Index (Relative to Maximum)
Mississippi	1.00	Indus	1.1×10^{-2}
Shatt-al-Arab	6.98×10^{-1}	Ord	3.66×10^{-3}
Danube	2.14×10^{-1}	Burdekin	2.08×10^{-3}
Amazon	1.17×10^{-1}	Chao Phraya	1.77×10^{-3}
Ebro	4.87×10^{-2}	Niger	8.03×10^{-4}
Hwang Ho	4.16×10^{-2}	Nile	5.86×10^{-4}
Irrawaddy	1.7×10^{-2}	Sao Francisco	2.37×10^{-4}
Ganges-Brahmaputra	1.12×10^{-2}	Senegal	5.99×10^{-5}

which obliterates vertical density gradients. These river mouths characteristically exhibit downstream bank divergence at exponential rates and linear tidal ridges in and seaward of the mouths (Wright, Coleman, and Thom, 1973 and in press). The mouths of the Ord, Shatt-al-Arab, Chao Phraya, and Irrawaddy Rivers fall into this general category.

CONCLUSIONS

The Coastal Information Program on deltas was designed to systematically describe and explain the variability displayed by modern river systems. The project consisted of collecting available data on river systems and developing techniques for generating and structuring information and comparing river systems in terms of their similarities and dissimilarities. Concurrently with this study, specific cause-effect relationships were identified and were studied systematically in greater detail; they provided input to the overall information program. The results of these studies have been presented in various reports, and only the conclusions arising from the comparison of river system information are included.

The most salient conclusions are as follows:

1. Attempts to classify deltas on the basis of single parameters are not meaningful. Classifications such as those based on subjective delta shape, climate, energy, etc., communicate minimal information.

2. Deltas represent responses to forcing functions which are active not only within the delta but within other component parts of a river system.

3. Deltas cluster into relatively discrete groups on the basis of sets of related morphologic or process variables but display a continuous spectrum of dissimilarities when combinations of mutually unrelated variables are considered. This indicates that the individual response to specific processes must be understood before the composite delta landscape can be explained.

4. Among drainage basins, 65 percent fall into one or two groups in terms of absolute dimensions. Dimensionless morphometric parameters, such as

relief ratios and hypsometric integrals, account for the greatest morphologic variability and are responsible for the existence of four discrete clusters which exhibit very little coincidence with the clusters based on absolute dimensions.

5. A broad range of variability is displayed by drainage-basin climates, and nine discrete clusters result. Mean annual precipitation and the difference between precipitation and actual evapotranspiration account for most of the variability.

6. Alluvial-valley landform suites are highly variable and fall into seven clusters. There are five very discrete alluvial-valley discharge regimes; most of the variability is exhibited by mean annual discharge and discharge range, but all variables contribute significantly.

7. The largest amount of variability displayed by the receiving basin can be explained in terms of offshore slope (to either the 10- and 20-meter contours) spring tide range, and relative strength of alongshore winds. Deepwater wave height and period are of minor importance because of the control imposed by offshore slope.

8. The deltas examined showed a broad spectrum of sizes, ranging from a maximum of 467,000 km^2 to a minimum of 620 km^2, and there is a continuous progression between the extremes.

9. In terms of the delta components, i.e., ratio of subaerial to subaqueous areas, etc., deltas fall into four very tight and discrete clusters, and all three variables play significant roles.

10. With respect to dimensionless morphometry, deltas display appreciable variability and fall into six clusters. All variables make significant contributions to the variability and can be considered to contain significant information for the description of deltas.

11. Distributary network patterns fall into seven small clusters and five unique systems. The ratio of rejoining to bifurcation, distributary density, and number of active river mouths contain significant information for describing delta distributary network patterns.

12. River-mouth morphometric variables, convergence rate, depth-width ratio, and distance to bar crests were responsible for describing the variability of river-mouth form and resulted in six discrete clusters.

13. Combining all sets of delta morphologic variables failed to yield discrete clusters but indicated a progressive spectrum of delta dissimilarities because of causal independence among the individual morphologic parameters. Thus the total delta landscape results from multiple process-form relationships, and each of these must be understood individually.

14. The most conspicuous morphologic variations can be accounted for in terms of a few processes; notably, these are river discharge regime, tide range, effluent mechanisms, wave-energy regime, coastal currents, tectonics of receiving basin, and climate.

15. Results from the study point to several critical areas for future research, including:

a. The relationship between river discharge regime and sediment transport in delta distributaries.

b. Tidal transport phenomena in delta distributaries and the interactions between tidal currents and river flow.

c. The effluent mechanisms affecting dissemination of sediment at river mouths.

d. Field assessment of relationships between riverine supply of sediment and wave redistribution of sediment.

e. Influence of coastal currents on deltaic sedimentation.

f. Development of methodology for quantifying tectonic factors and their effect on delta sedimentation.

g. The processes of temporal evolution of delta landscapes and the role of equilibrium adjustment.

h. Utilization of information generated by this project to determine in more detail the cause-effect relationship in deltas.

REFERENCES

Biscoe, C., Jr., B. Hayden, and R. Dolan, 1973, Classification of the coastal environments of the world. The climatic regimes of western South America: a case study. Univ. of Virginia, Dept. of Environmental Sciences Tech. Rept. 6, 33 pp.

Coleman, J. M., and L. D. Wright, 1971, Analysis of major river systems and their deltas: procedures and rationale, with two examples. Louisiana State Univ., Coastal Studies Inst. Tech. Rept. 95, 125 pp.

Cooley, W. W., and P. R. Lohnes, 1971, Multivariate data analysis. New York (John Wiley), 364 pp.

Dooley, J. A., 1970, Information compilation and comparison system: what the user needs to know. Wright-Patterson A.F.B., Ohio, Foreign Technology Div., 61 pp.

Kendall, M. G., 1966, Discrimination and classification. In (P. R. Krishnaiah, ed.) Multivariate analysis. New York (Academic Press), pp. 165-185.

Mather, P. M., 1972, Areal classification in geomorphology. In (R. J. Chorley, ed.) Spatial analysis in geomorphology. New York (Harper & Row), pp. 305-322.

McCammon, R. B., 1968a, Multiple components analysis and its application in classification of environments. Am. Assoc. Petrol. Geologists Bull., 52(11):2178-2196.

_____, 1968b, The dendrograph: a new tool for correlation. Bull. Geol. Soc. Am., 79(11):1663-1670.

_____, and G. Wenninger, 1970, The dendrograph. Univ. of Kansas, State Geol. Surv. Computer Contribution 48, 28 pp.

Melton, M. A., 1957, An analysis of the relations among elements of climate, surface properties and geomorphology. Columbia Univ., Dept. of Geology, Tech. Rept. 11, 102 pp.

Resio, D., L. Vincent, J. Fisher, B. Hayden, and R. Dolan, 1973, Classification of coastal environments. Analysis across the coast barrier island interfaces. Univ. of Virginia, Dept. of Environmental Sciences Tech. Rept. 5, 31 pp.

Shumm, S. A., 1956, Evolution of drainage systems and slopes in badlands at Perth Amboy, New Jersey. Bull. Geol. Soc. Am., 67:597-646.

Smart, J. S., and U. L. Moruzzi, 1972, Quantitative properties of delta channel networks. Zeitschrift für Geomorphologie, 16(3):268-282.

Sokal, R. R., and P. H. A. Sneath, 1963, Principles of numerical taxonomy. San Francisco (W. H. Freeman), 359 pp.

Strahler, A. N., 1952, Hypsometric (area-altitude) analysis of erosional topography. Bull. Geol. Soc. Am., 63:1117-1142.

Waldrop, W. R., and R. C. Farmer, 1973, Three-dimensional flow and sediment transport at river mouths. Louisiana State Univ., Coastal Studies Inst. Tech. Rept. 150, 137 pp.

Wishart, David, 1969, FORTRAN II programs for 8 methods of cluster analysis (CLUSTAN I). State Geol. Survey, Univ. of Kansas, Computer Contribution 38, 111 pp.

Wright, L. D., 1970, Circulation, effluent diffusion, and sediment transport, mouth of South Pass, Mississippi River delta. Louisiana State Univ., Coastal Studies Inst. Tech. Rept. 84, 56 pp.

_____, 1971, Hydrography of South Pass, Mississippi River delta. Am. Soc. Civil Engrs. Proc., J. Waterways, Harbors and Coastal Engr. Div., 97:491-504.

_____, and J. M. Coleman, 1971a, Effluent expansion and interfacial mixing in the presence of a salt wedge, Mississippi River delta. J. Geophys. Res., 76: 8649-8661.

_____, 1971b, The discharge/wave-power climate and the morphology of delta coasts. Proc. Assoc. Am. Geographers, 3:186-189.

_____, 1972, River delta morphology: wave climate and the role of the subaqueous profile. Science, 176:282-284.

_____, 1973, Variations in morphology of major river deltas as functions of ocean wave and river discharge regimes. Bull. Am. Assoc. Petrol. Geologists, 57:370-398.

_____, in press, Mississippi river mouth processes: effluent dynamics and morphologic development. J. Geol.

_____, and J. N. Suhayda, 1973, Periodicities in interfacial mixing. Louisiana State Univ., Coastal Studies Inst. Bull. 7, pp. 127-135.

Wright, L. D., J. M. Coleman, and B. G. Thom, 1972, Emerged tidal flats in the Ord River estuary, Western Australia. Search, 3(9):339-341.

_____, 1973, Processes of channel development in a high-tide-range environment: Cambridge Gulf - Ord River delta, Western Australia. J. Geol., 81:15-41.

_____, in press, Sediment transport and deposition in a macrotidal river channel: Ord River, Western Australia. Recent Advances in Estuarine Research, Proceedings volume of Estuarine Research Federation Symposium, October 15-18, 1973, Myrtle Beach, South Carolina.